European Spatial Data Research

December 2009

Detection of Unregistered Buildings for Updating 2D Databases

by Nicolas Champion

NEWPLATFORMS - Unconventional Platforms (Unmanned Aircraft Systems) for Remote Sensing

by Jurgen Everaerts

Official Publication Nº 56

Published by EuroSDR

Printed by Gopher, Amsterdam, The Netherlands

EUROPEAN SPATIAL DATA RESEARCH

PRESIDENT 2008 – 2010:
Antonio Arozarena, Spain

VICE-PRESIDENT PRESIDENT 2009 – 2011:
Dieter Fritsch, Germany

SECRETARY-GENERAL:
Kevin Mooney, Ireland

DELEGATES BY MEMBER COUNTRY:

Austria: Michael Franzen
Belgium: Ingrid Vanden Berghe; Jean Theatre
Croatia: Željko Hećimović; Ivan Landek
Cyprus: Christos Zenonos; Michael Savvides
Denmark: Thorben Hansen; Lars Bodum
Finland: Risto Kuittinen; Juha Vilhomaa
France: Jean-Philippe Lagrange; Xavier Briottet
Germany: Dietmar Grünreich; Klement Aringer; Dieter Fritsch
Iceland: Magnús Guðmundsson; Eydís Líndal Finnbogadóttir
Ireland: Colin Bray, Ned Dwyer
Italy: Carlo Cannafoglia
Netherlands: Jantien Stoter; Aart-jan Klijnjan
Norway: Jon Arne Trollvik; Ivar Maalen-Johansen
Spain: Antonio Arozarena, Francisco Papí Montanel
Sweden: Anders Olsson; Anders Östman
Switzerland: Francois Golay; André Streilein-Hurni
United Kingdom: Malcolm Havercroft; Jeremy Morley

COMMISSION CHAIRPERSONS:

Sensors, Primary Data Acquisition and Georeferencing: Michael Cramer, Germany
Image Analysis and Information Extraction: Juha Hyyppä, Finland
Production Systems and Processes: André Streilein-Hurni, Switzerland
Data Specifications: Ulf Sandgren, Sweden
Network Services: Mike Jackson, United Kingdom

OFFICE OF PUBLICATIONS:

Bundesamt für Kartographie und Geodäsie (BKG)
Publications Officer: Andreas Busch
Richard-Strauss-Allee 11
60598 Frankfurt
Germany
Tel.: + 49 69 6333 312
Fax: + 49 69 6333 441

CONTACT DETAILS:

Web: www.eurosdr.net
President: president@eurosdr.net
Secretary-General: secretary@eurosdr.net
Secretariat: admin@eurosdr.net

EuroSDR Secretariat
Faculty of the Built Environment
Dublin Institute of Technology
Bolton Street
Dublin 1
Ireland

Tel.: +353 1 4023933

The official publications of EuroSDR are peer-reviewed.

EuroSDR Project

Commission 2 "Image Analysis and Information Content"

Detection of Unregistered Buildings for Updating 2D Databases

Final Report

Report by Nicolas Champion
MATIS – Institut Géographique National (French Mapping Agency)
Nicolas.Champion@ign.fr

Abstract

In the past few years, the production of 2D topographic databases has been completed in most industrialised countries. Presently, most efforts in the National Mapping and Cadastral Agencies (NMCAs) are devoted to the update of such databases. Because the update process is generally carried out manually by visual inspection of orthophotos, it is time-consuming and expensive. The development of semi-automatic systems is, thus, of high interest for NMCAs. The current deficits in automation and the lack of expertise within NMCAs have driven the EuroSDR (European Spatial Data Research - http://www.eurosdr.net) to launch a project in this topic. The aim of the project "Detection of unregistered buildings for updating 2D databases" is to evaluate the feasibility of semi-automatically detecting changes in a 2D building vector database from optical imagery or LIDAR. Three specific sub-topics are investigated in detail: firstly, the impact of methodology; secondly, the impact of the type and spatial resolution of input data; lastly, the impact of the complexity of the scene, especially with respect to topography and land use. A comparison of algorithms representative of the current state-of-the-art in the field of change detection is performed. In this report, we describe the three test areas used in the project, the methodology used for assessing and comparing the methods, and the results that have been obtained with the four different approaches. The results are thoroughly analysed and a discussion enables to bring out conclusions and promising directions to follow for building an optimal operational system in the future.

1 Introduction

Traditionally, the mapping process is carried out in National Mapping and Cadastre Agencies (NMCAs) and consists of a linear workflow. As stated in (Heipke, 2008), a typical mapping process is composed of four separate stages. In the first stage, we define the specifications of the future database, in particular those concerning the type of objects to include (e.g. road, buildings, rivers, etc.), their representation in the map (e.g. in the form of a point, a line, a polygon or a surface), other semantic information (tourist information such as refuge hut, camp site, other place of interest, etc.) and the accuracy of the database (the scale for paper map). In the second stage, source data (aerial images, alternatively LIDAR data) are acquired and/or a field survey is carried out. Cartographic products (e.g. vector databases and raster maps) are then generated (Stage 3) and delivered (Stage 4). At the end of the project, the question that immediately arises concerns the update of the database, more specifically the strategy to use for that purpose. This question is a very topical issue in NMCAs, as the production of 2D topographic databases has been completed in the most European countries in the last decade.

As shown in (Heipke, 2008), two strategies can be considered for the update: the participatory and centralised approaches. The first update strategy (participatory approach) consists in collecting the information about changes from other public agencies (e.g. town councils and cadastre) and other contracted bodies (e.g. real estate agencies). Even general public's service can be called upon, which is considered in an increasing number of Web 2.0 applications, such as OpenStreetMap[1], Google Map Maker[2], WikiMapia[3], or other applications developed by private companies, in particular Map Insight[4]

[1] http://www.openstreetmap.org/. Last visited: 04-08-09
[2] http://www.google.com/mapmaker/. Last visited: 04-08-09
[3] http://wikimapia.org/. Last visited: 04-08-09
[4] http://mapinsight.teleatlas.com/. Last Visited: 04-08-09

by TeleAtlas. The second update strategy (centralised approach) consists in collecting the information about changes by field surveying or from external data, particularly airborne and spaceborne images, alternatively LIDAR data. This strategy also consists of a comparison of the existing database to more recent image data (considered ground truth) in order to detect *new*, *demolished* or *modified* objects in the initial database. If the participatory approach – in particular the collaborative approach – could lead to promising applications, some limitations appear and are related to the inevitable remaining errors in the database that require an ultimate ground truth in order to be eliminated. The centralised approach produces this required ground truth and also appears to be the only possible way to update specific databases, especially those that have a legal purpose (e.g. for land valuation, taxation, etc.), i.e. those that can not be built by private partners (using the participatory way) or individuals (using the collaborative way) but have to be compulsorily edited by public authorities.

From a practical point of view, the update strategy involved in the centralised way consists of a visual inspection of images and their comparison to the database to update. Such a work is no surprisingly tedious, time-consuming and expensive. In (Steinnocher, 2006) manual updating purposes are estimated to require up to 40% of the costs that are involved in the case where maps are generated from scratch. In addition, update cycles tend nowadays to be shorter (e.g. from 10 to 3 years). These two observations show the necessity to speed up the update procedures, i.e. to increase their degree of automation and, as a consequence, to develop expert systems that are able to send an alarm to an operator when a change is detected between the database and more recent data. The general trend, observed in the literature concerns the specialisation of update procedures with respect to the kind of objects to update (Baltsavias, 2004); the methodologies used to update the roads are also different from those used to update buildings. This specialisation is obviously due to the fact that knowledge is required to develop an updating process. Moreover, update procedures can generally be split into two steps: the *change detection* step, in which the outdated database is compared to recently collected sensor data in order to detect changes, and the *vectorization* step, i.e. the digitization of the correct geometry of the changed objects. Given the state-of-the-art in automatic object detection (Mayer, 2008), only the automation of the *change detection* step seems to be possible at this time. The key idea here is to focus the operator's attention on the areas that may have changed. Work is saved because the operator needs not inspect areas classified as *unchanged* by the automatic procedure.

This EuroSDR project focused on the update of the building layer of a 2D topographic database, such as cadastral maps or city maps. The buildings are here represented by their 2D footprints (i.e. outlines). Although buildings are very important GIS components and have received much attention for the last 15 years, especially for automatic or assisted 2D/3D reconstruction (see (Ortner, 2008) and (Lafarge, 2008) for one example), only a few solutions have been proposed for *change detection* purposes, both in academia and private companies. Therefore, many questions that have arisen remain unanswered, e.g. those regarding the most efficient methodology, the type of primary data to use (LIDAR / imagery) or the most appropriate spatial resolution to choose. These considerations have driven EuroSDR to set up a change detection project. This project is in line with previous EuroSDR projects, e.g. the projects on "Automated Extraction, Refinement, and Update of Road Databases" (Mayer et al., 2006) and on "Change Detection" (Steinnocher and Kressler, 2006).

The aim and highlights of this EuroSDR project are described in more details in the next section.

2 Description of the project

This project also aims at evaluating the feasibility of semi-automatically detecting changes in a 2D building vector database from imagery or LIDAR. Three specific sub-topics are investigated more thoroughly:

- the impact of the methodology on the change detection performance
- the impact of the type and the spatial resolution of input data
- the impact of the complexity of the scene, especially with respect to topography and land use

The methodology of the project consists of comparing four different algorithms representative of the current state-of-the-art in the field of change detection. These four algorithms are described in details in (Olsen and Knudsen, 2005), (Champion, 2007), (Matikainen et al., 2007) and (Rottensteiner, 2008), respectively. We also give a brief description of them in Section 3.

2.1 Description of datasets

Three test areas were used in this study: Marseille (France), Lyngby (Denmark) and Toulouse (France). The test areas differ considerably regarding topography, land use, urban configuration and roofing material.

2.1.1 The Marseille Test Area

The first test area has an area of about 0.9 x 0.4 km2 and contains about 1300 buildings. The area corresponds to a very dense urban settlement and features a complicated urban configuration (lower buildings connected to higher buildings). The test area is hilly (with height differences of 150m) and vegetated, especially along streets. Regarding primary data, colour infrared (CIR) aerial images with a Ground Sample Distance (GSD) of 20cm and multiple overlap (a forward and a side lap of minimum 60%) are available. A Digital Surface Model (DSM) was computed using a stereo-matching algorithm based on the 2D minimization of discontinuities and radiometric similarities (Pierrot-Deseilligny and Paparoditis, 2006). The GSD of the DSM is equal to the GSD of the aerial images. CIR orthophotos were also computed from input DSM and images (Figure 1).

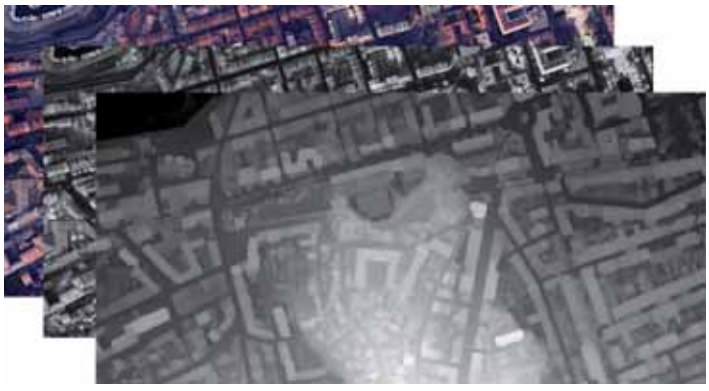

Figure 1. Input data used in Marseille (aerial context) for updating. From the back to the front, RGB Orthophoto, Infrared (IR) Orthophoto and Correlation DSM. The GSD is 20cm for all the input data.

2.1.2 The Lyngby Test Area

The second test area is situated in Lyngby (Denmark). It has an area of about 2.0 x 2.0 km^2 and contains about 500 buildings. It features a mixed area that contains both industrial and residential buildings. These buildings are very different to each other with respect to the size and roofing material. The terrain is flat (with a height difference smaller than 10m). A DSM is also available and here corresponds to a grid derived from first pulse LIDAR data. Digital CIR orthophotos are also provided. They were generated from scanned aerial images. Both data have a GSD of 1m (Figure 2).

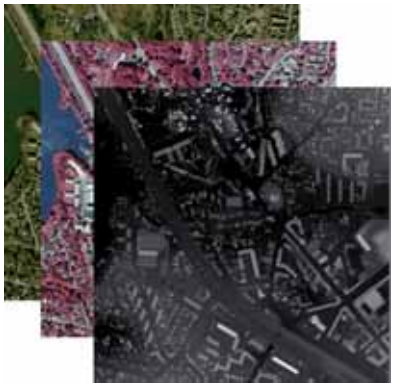

Figure 2. Input data used in Lyngby (LIDAR context) for updating. From the back to the front, RGB Orthophoto, Infrared (IR) Orthophoto and LIDAR DSM. The GSD is 1m for all the input data.

2.1.3 The Toulouse Test Area

The third test area is situated in Toulouse (France). It has an area of about 1.1 x 1.1 km2 and contains about 200 buildings. It features a suburban area and is composed of detached buildings that are very different to each other with respect to the size, height, shape and roofing material. The terrain is also undulating (with height differences of 100m) and vegetated. Pléiades tri-stereoscopic Satellite CIR images are used for Toulouse, with a GSD equal to 50cm. The same stereo-matching algorithm, by Pierrot-Deseilligny and Paparoditis (2006) is used to compute a correlation DSM (with the same GSD) and CIR orthophotos are generated (Figure 3).

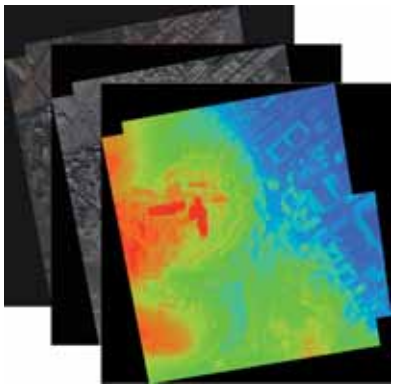

Figure 3. Input data used in Toulouse (satellite context) for updating. From the back to the front, RGB Orthophoto, Infrared (IR) Orthophoto and Correlation DSM. The GSD is 50cm for all the input data.

2.1.4 The Reference Building Database

Reference (up-to-date) building databases, representing the 2D outlines of buildings were created manually and served as a reference in the test. In order to achieve an objective evaluation, the outdated databases were simulated by manually adding or removing buildings some of the existing buildings. 102 *changes* were simulated (84 *new* and 18 *demolished* buildings) in Marseille (Figure 4-bottom); 70 *changes* (49 *new* and 21 *demolished* buildings) were simulated in Lyngby (Figure 5-right); eventually, 38 *changes* (23 *new* and 15 *demolished* buildings) were simulated in Toulouse (Figure 6-right). The outdated databases were converted to binary image files (building vs. no building) having the same GSD as the input data, and distributed to the participants along with the CIR orthophotos and the DSM.

Figure 4. (Top) Initial database to update and (Bottom) ground truth (initial reference database), superimposed on the Orthophoto in Marseille. Cyan: *unchanged*; Magenta: *demolished*; Green: *new*.

Figure 5. (Left) Initial database to update and (Right) ground truth (initial reference database), superimposed on the RGB Orthophoto in Toulouse (with the same colour code as in Figure 4).


Figure 6. (Left) Initial database to update and (Right) ground truth (initial reference database) superimposed on the RGB Orthophoto in Toulouse (with the same colour code as in Figure 4).

2.2 Evaluation Procedure

Each group participating in the test was asked to deliver a change map in which each building of the vector database is labelled either as *unchanged*, *demolished* or *new*. Because the methods have been developed in different contexts, their designs noticeably differ, for instance regarding the definitions of the classes considered in the final change map – e.g. four classes for (Champion, 2007) and six classes for (Rottensteiner, 2008) – and the format of the input data – e.g. vector for (Champion, 2007) and raster for (Matikainen et al., 2007). As a work-around, it was decided to use the building label image representing the updated version of the building map (cf. Section 3) for the evaluation of those methods that do not deliver the required change map in the way described above. Only the method by (Champion, 2007) delivered such a change map, which was also directly used in the evaluation.

In order to evaluate the results achieved by the four algorithms, they are compared to the reference database, and the *completeness* and the *correctness* of the results, described for instance in (Heipke et al., 1997), are derived as quality measures.

$$Completeness = \frac{TP}{TP + FN} \in [0,1]$$
$$Correctness = \frac{TP}{TP + FP} \in [0,1] \qquad (1)$$

In Equation 1, *TP*, *FP*, and *FN* are the numbers of *True Positives*, *False Positives*, and *False Negatives*, respectively. They refer to the update status of the vector objects in the automatically-generated change map, compared to their real update status given by the reference. In the case where the final change map is directly used for the evaluation, i.e. with (Champion, 2007), a *TP* is an object of the database reported as changed (demolished or new) that is actually changed in the reference. A *FP* is an object reported as changed by the algorithm that has not changed in the reference. A *FN* is an object that was reported as unchanged by the algorithm, but is changed in the reference. In the three other cases, where a building label image representing the updated map is used for the evaluation, the rules for defining an entity as a *TP*, a *FP*, a *FN* had to be adapted. In these cases, any unchanged

building in the reference database is considered a *TN* if a predefined percentage (T_h) of its area is covered with buildings in the new label image. Otherwise, it is considered a *FP*, because the absence of any correspondence in the new label image indicates a change. A demolished building in the reference database is considered a *TP* if the percentage of its area covered by any building in the new label image is smaller than T_h. Otherwise, it is considered to be a *FN*, because the fact that it corresponds to buildings in the new label image indicates that the change has remained undetected. A new building in the reference is considered a *TP* if the cover percentage is greater than T_h. Otherwise, it is considered a *FN*. The remaining areas in the new label image that do not match any of the previous cases correspond to objects wrongly alerted as new by the algorithm and thus constitute *FP*s.

The quality measures are presented in the evaluation on a per-building then per-pixel basis. Note that only the quality metrics based on a per-building analysis are meaningful because the effectiveness of a change detection approach is limited by the number of changed buildings that is missed or over-detected, and not by the area covered by these buildings. As shown in Section 4, these quality measures are also computed separately for each change class.

3 Methods description

The four methods tested in this study are concisely presented, ordered alphabetically according to the corresponding author.

3.1 Method of Champion, 2007

The input of the method is given by a DSM, CIR orthophotos and the outdated vector database. Optionally, the original multiple images can be used. The outcome of the method is a modified version of the input vector database, in which *demolished* and *unchanged* buildings are labelled and vector objects assumed to be *new* are created.

The methodology proposed in this work consists of a twofold recursive approach. The change detection procedure is also split into 2 subtasks, easier to handle: on the one hand, the automatic *verification of the database* in order to detect *demolished* buildings and, on the other hand, the *detection of new buildings*.

In the first stage, geometric primitives, e.g. 2D contours extracted from the DSM (Deriche, 87) or 3D segments reconstructed from input multi-view images (Taillandier, 2002), are collected for each building and matched with primitives derived from the existing vector map. A final decision about acceptance or rejection is then achieved per building, using predefined threshold-based rules. This first step leads to a partially updated database, in which buildings are labelled *unchanged* or *demolished*. In the second stage, the results of the first step are re-used in an incremental way to extract the *new* constructions from the scene. The main idea of this stage consists in extracting the blobs of the DSM that only correspond to *new* buildings, namely those that correspond neither to a tree nor to a building already present in the partially updated database. The input of this second step consists of a vegetation mask, derived from RGB and IR orthophotos through NDVI – Normalized Difference Vegetation Index – criterion and a building mask, easily derived from the partially updated database. A DTM is then automatically computed from the DSM and input masks with (Champion, 2006) and a normalized DSM (nDSM), defined as the difference between the DSM and the DTM is then easily

calculated. A new above-ground mask is computed by thresholding and is then compared to the initial vegetation and building masks to extract *new* structures, through appropriate morphological tools.

3.2 Method of Matikainen et al., 2007

The building detection method of the Finnish Geodetic Institute (FGI) was originally developed to use laser scanning data as primary data. In this study, it is directly applied to the input DSM and CIR orthophotos. A raster version of the database (for part of the study area) is used for training. The method includes the following stages:

- The pre-classification of DSM points to separate *ground* points from *above-ground* points, using (TerraScan software; Terrasolid, 2008) – **Stage 1**.
- The region-based segmentation of the DSM into homogeneous regions and the calculation of various attributes for each segment using (Definiens, 2008) – **Stage 2**.
- The classification of the segments into *ground* and *above-ground* classes by using the pre-classification, obtained at the end of Stage 1 – **Stage 3**.
- The definition of training segments for *buildings* and *trees* on the basis of training data sets – **Stage 4**.
- The construction of a classification tree by using the attributes of the training segments (Breiman et al., 1984) – **Stage 5**.
- The classification of *above-ground* segments into *buildings* and *trees* on the basis of their attributes and the classification tree – **Stage 6**.
- A post-processing step in order to correct small, misclassified areas by investigating the size and neighbourhood of the areas – **Stage 7**, which results in the building label image used in this study for evaluation (Figure 7).

Additional remarks related to practical aspects

Here, we want to give some practical details about the processing of input data, regarding the several stages (from 1 to 7) previously described.

Firstly, the parameters used in the *ground*/*above-ground* classification step (Stage 1 - Stage 3) are selected by testing different values and evaluating the results visually. It should be noticed here that the process remains fully automatic and that there is no manual edition, even if it is a normal practice when using TerraScan software in an operational context.

Secondly, the parameters used in the segmentation step (Stage 2) for the Marseille test area is the same as the one used for the test area (located in Finland), for which the method was originally built and validated. On the contrary, those used for the Lyngby test area were manually selected by an operator.

Thirdly, regarding the *building*/*tree* classification, more specifically the corresponding training step, a subarea i.e. a part of the study area (of respectively 165 m x 330 m for Marseille and 320 m x 300 m for Lyngby) is used as a training area. Thus, training segments are constructed from the outdated database, and defined under the following rule "*If over 80% of a building or tree segment belong to building in the map, the segment is labelled as building. If less than 20% belong to building, the*

segment is labelled as tree". Due to inaccuracies in the database, a visual check of the training segments is needed to exclude erroneous training segments.

Regarding the attributes used to perform the *building*/*tree* classification, they differ from one test area to another one. In Marseille, a total of 43 attributes are provided as input data for the classification tree method to distinguish *buildings* from *trees*. These attributes include mean values of the segments in the different image channels and in slope images, derived from the DSM, standard deviations and texture features calculated from the DSM and image channels. They also include various shape attributes and the Normalised Difference Vegetation Index (NDVI) calculated from the mean values in the near-infrared and red channels. Only one attribute, NDVI, is selected in the tree by the algorithm for the Marseille test area. As a consequence, the classification of the segments into *buildings* and *trees* is simply based on thresholding NDVI data. Note that tests were also carried out by using only DSM derived attributes and shape attributes as input data in the classification, but the quality of these results was clearly lower. In Lyngby, the total number of attributes available for the *building*/*tree* classification is 49 (similar attributes as in the Marseille area, but there are two additional image channels available in the infrared ortho image). Two alternative classification results are produced, corresponding to two different pruning levels of the classification tree. The pruning level determines the size of the tree, i.e. the number of classification rules used. The first tree includes two NDVI rules and one rule based on a shape attribute (average length of edges). The second tree includes only one NDVI rule. Here again, tests were carried by using only DSM derived attributes and shape attributes as input data in the classification, but the quality of these results was lower. Note that the result corresponding to the first option (first tree, two NDVI rules, one shape rule) is used for this study.

Figure 7. Results of automatic building detection, produced with (Matikainen et al., 2007) in Marseille (Left) and Lyngby (Right).

3.3 Method of Olsen and Knudsen, 2005

The input data of this method consist of a DSM, CIR data and a map database. The method is based on three high level processing steps: a preparation step, a classification step and a change detection step:

- The ***preparation step*** is composed of two separate steps. Firstly, input data are geo-referenced in the same cartographic frame. Secondly, they are used to generate additional data that are used as primary data by the algorithm. Thus, a DTM is estimated from the DSM through a grey scale image opening procedure. A normalized DSM (nDSM), defined as the difference between the DSM and the DTM, is also produced, along with a so-called Object Above Terrain (OAT) mask. Finally, a NDVI mask (Normalized Difference Vegetation In-

dex) is generated from input CIR orthophotos and a so-called *existing building mask* is easily extracted from the outdated database.

- The ***classification step*** consists in classifying the object space into two classes, namely *buildings* and *non buildings*. For that purpose, the OAT mask and the NDVI mask are combined and objects that stand above the terrain are separated into two classes: *vegetation* and *man-made objects*. An initial *building* mask is then easily created and refined, by selecting the objects contained in the *man-made* mask and fulfilling the criteria that best characterise buildings, with respect to the size and form. This results in the *building label image* (Figure 8) that is used for the evaluation in this study

- The ***change detection step*** consists in comparing (on a per-pixel basis) the *building label image* to the initial *existing building mask*. The outcomes of this comparison are then post-processed (through morphological methods) in order to eliminate the noise that may correspond to classical geometric differences between the input data and the initial outdated database, related for instance to registration specifications.

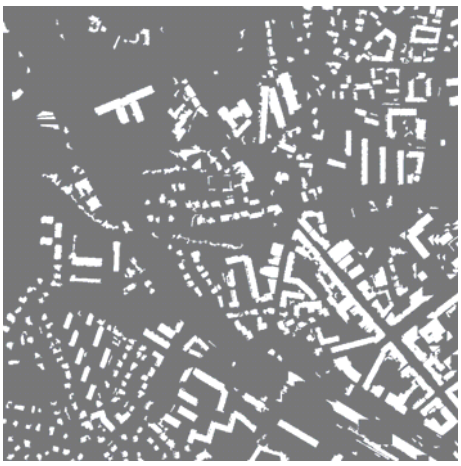

Figure 8. Results of automatic building detection, produced with (Olsen and Knudsen, 2005) in the Lyngby test area.

3.4 Method of Rottensteiner, 2008

The input data of this method consist of a DSM obtained by LIDAR or stereo-matching techniques. A geocoded NDVI image, the initial building data base, and a Digital Terrain Model (DTM) can optionally be used. If no DTM is available, it is derived from the DSM by hierarchic morphologic filtering. If the initial database is available, it can be used to introduce a bias that favours a classification consistent with the initial data base, because in most scenes only a small percentage of buildings will actually have changed. The workflow of the method consists of three stages. First, a Dempster-Shafer fusion process is carried out on a per-pixel basis and results in a classification of the input data into one of four predefined classes: *buildings*, *trees*, *grass* land, and *bare soil*. Connected components of building pixels are grouped to constitute initial building regions. A second Dempster-Shafer fusion

process is then carried out on a per-region basis to eliminate regions corresponding to trees. The third stage of the work flow is the actual change detection process, in which the detected buildings are compared to the existing map. A very detailed change map is generated in this process. The output of the method consists of a building label image representing the *new* state of the data base and in change maps describing the change status both on a per-pixel and a per-building level (Refer to (Rottensteiner, 2007 and 2008) for more details). Since the definition of the classes in the change map does not match those required in Section 2.2, the building label image (Figure 9) is used for evaluation in this study.

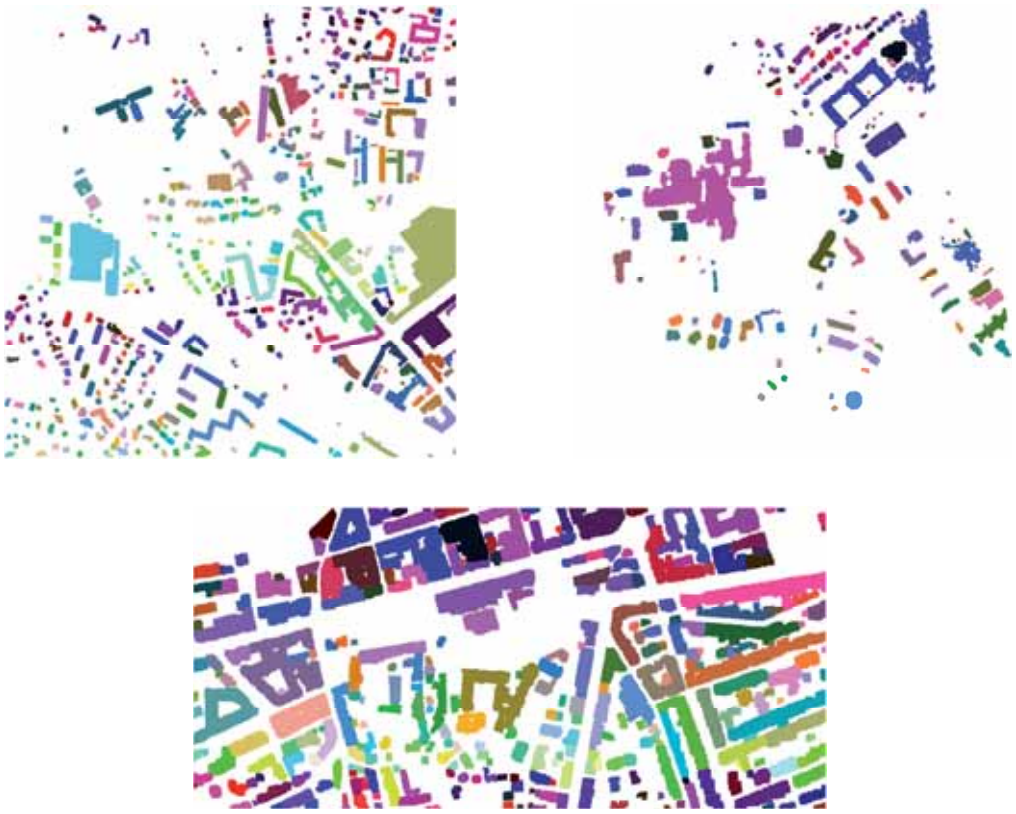

Figure 9. Results of automatic building detection, produced with (Rottensteiner, 2008) in Lyngby (Top Left), Toulouse (Top Right) and Marseille (Bottom).

4 Results, Evaluation and Discussion

In an *ideal* situation, the quality measures, presented in Section 2, namely the completeness and correctness of the results are equal to 1. That corresponds to the *optimal* change detection system that delivers no *FN* object (no under-detection) and no *FP* object (no over-detection). In our opinion, in an *operational* context, the effectiveness of a change detection system is mostly related to its capacity to guide the operator's attention only to objects that have changed so that *unchanged* buildings do not need to be investigated unnecessarily. These considerations result in the evaluation criteria used in this project to analyze the change detection performance.

On the one hand, to support the generation of a map that is really up-to-date, i.e. **to be effective qualitatively**, the *completeness* of the system for buildings classified as *demolished* and the *correctness* for *unchanged* buildings are required to be high. The *completeness* of *new* buildings also has to be high if the operator is assumed not to look for any *new* building except for those which are suggested by the system. (Note that this also holds true for *modified* buildings, a case not considered in this study because the simulated changes only consisted in *new* and *demolished* buildings).

On the other hand, to reduce the amount of manual work required by the operator i.e. **to be effective economically**, the *correctness* of the changes highlighted by the system and the *completeness* of *unchanged* buildings must be high. However, if a low *completeness* of *unchanged* buildings implies that many buildings are checked uselessly, this is not necessarily critical for the application itself, because the updated database is still correct. Moreover, the economical efficiency that could then appear to be low has to be put into perspective according to the size of the building database to update. For instance, if a change detection system reports 60% of a *national* database as changed, we cannot necessarily conclude about the inefficiency of this system because it still means that 40% of the buildings need not be checked, which here amounts to millions of buildings.

The evaluation outputs are summarized in Table 1. The completeness and correctness are given for each test area and approach, on a per-building basis and on a per-pixel basis. Values in bold indicates for which methods the best results are achieved. The completeness of detected changes is high for all the methods, especially in the aerial (Marseille) and LIDAR (Lyngby) contexts. By contrast, the correctness observed in our experiments is relatively poor, which indicates that many FP changes are reported by the systems. In this respect, only the results obtained in the Lyngby test area with (Rottensteiner, 2008) seem to achieve a relatively acceptable standard.

Method	Completeness [%]		Correctness [%]	
	Per building	Per pixel	Per building	Per pixel
Marseille Test area				
(Champion,2007)	94.1	94.1	45.1	71.1
(Matikainen,2004)	**98.8**	**98.8**	54.3	79.1
(Rottensteiner,2007)	95.1	97.8	**59.1**	**83.6**
Toulouse Test Area				
(Champion,2007)	78.9	**95.0**	**54.5**	**83.3**
(Rottensteiner,2007)	**84.2**	89.2	47.1	50.0
Lyngby Test Area				
(Matikainen,2004)	94.3	98.0	48.8	87.9
(Olsen and Knudsen,2005)	**95.7**	**98.3**	53.6	85.3
(Rottensteiner,2007)	91.4	97.6	**76.1**	**96.5**

Table 1. Completeness and Correctness, achieved by the four algorithms for the three data sets.

We focus now the analysis on the outcomes of the methods, for each test area, i.e. Marseille (Section 1), Lyngby (Section 2) and Toulouse (Section 3).

4.1 The Marseille Test Area

Table 2 presents the per-building confusion matrix for the change detection results obtained in the Marseille data set. The completeness and correctness, computed for each change class (namely *demolished*, *new* and *unchanged*) are shown in Table 3, on a per-building basis. These two tables are used in the following paragraphs in order to analyze the outcomes of each method, firstly those of (Champion, 2007), secondly those of (Matikainen et al., 2007) and lastly those of (Rottensteiner, 2008).

Algorithm Reference	*Unchanged* (A)	*Demolished* (A)	*New* (A)	Background (A)
(Champion, 2007)				
Unchanged (R)	1018	71	-	-
Demolished (R)	2	16	-	-
New (R)	-	-	80	4
Background (R)	-	-	46	1
(Matikainen, 2004)				
Unchanged (R)	1031	58	-	-
Demolished (R)	0	18	-	-
New (R)	-	-	82	2
Background (R)	-	-	26	1
(Rottensteiner, 2008)				
Unchanged (R)	1025	64	-	-
Demolished (R)	0	18	-	-
New (R)	-	-	79	5
Background (R)	-	-	3	1

Table 2. [per-building] Confusion matrix for Marseille with (Champion, 2007), (Matikainen et al., 2004) and (Rottensteiner, 2008). A: Automatic. *R*: Reference.

	Unchanged	*Demolished*	*New*	Background
(Champion, 2007)				
Completeness [%]	93.3	88.9	95.2	2.1
Correctness [%]	99.8	18.4	63.5	20.0
(Matikainen, 2004)				
Completeness [%]	94.7	100	97.6	03.7
Correctness [%]	100	23.7	75.9	33.3
(Rottensteiner, 2008)				
Completeness [%]	94.1	100	94.0	25.0
Correctness [%]	100	22.0	96.3	16.7

Table 3. [per-building] Completeness and correctness for Marseille with (Champion, 2007), (Matikainen, 2004) and (Rottensteiner, 2008), derived from the confusion matrix (Table 2).

(a) Champion

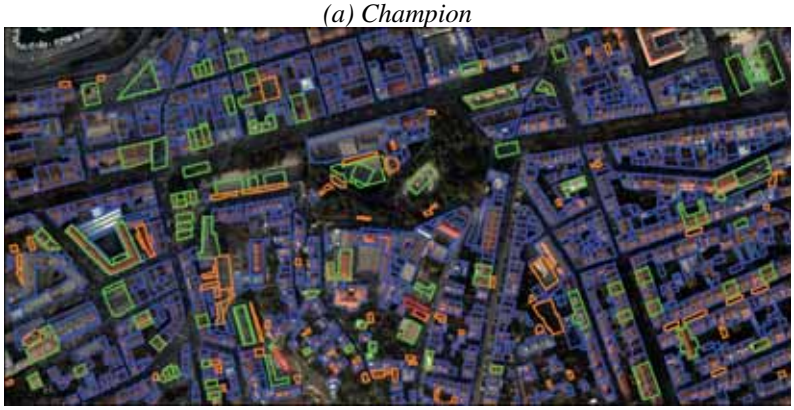

(b) Matikainen et al.

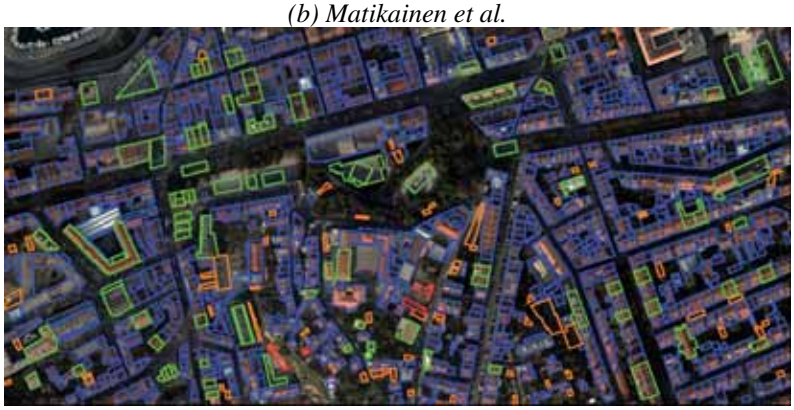

(c) Rottensteiner

Figure 10. Evaluation of change detection in Marseille.
Green: *TP*; Red: *FN*; Orange: *FP*; Blue: *TN*.

4.1.1 Method of Champion (2007)

The evaluation of this method is illustrated in Figure 10-a.

The overall completeness of the system is high, both for *demolished* buildings (88.9%) and *new* buildings (95.2%). Five *FN*s appear with the method. Two of them concern *demolished* cases and occur during the *verification step* of the method, in the north-western corner of the scene and are caused by extracted primitives that are wrongly used to validate *demolished* buildings (as illustrated in Figures 11a and 11b). *FN new* cases are related to DTM inaccuracies, especially in the parts of the

study areas, where the terrain is topographically difficult (presence of a cliff) and for which the height is overestimated in the DTM, automatically generated with (Champion and Boldo, 2006).

Regarding the false alarms (*FP* cases), many of them are related to *demolished* buildings, for which the system achieves a correctness rate of only 18.4%. The situation is a bit better with *new* buildings, for which the correctness rate rises to 63.5%. In our experiments, one can see that most *FP new* buildings are related to building-like structures e.g. walls, wrongly reported as *new* buildings (Figure 11c), errors in the vegetation mask (omitted trees, Figure 11d), inaccuracies in the correlation DSM (e.g. large overestimated areas in narrow streets, Figure 11e) and overestimated areas in the DTM (here again related to a poor modeling of a difficult terrain configuration, Figure 11f).

In spite of such limitations, the method appears to be efficient in classifying *unchanged* buildings, for which the completeness rate is 93.5%, which indicates that only 6.5% of *unchanged* buildings are wrongly given to the operator for verification.

4.1.2 Method of Matikainen et al. (2007)

The evaluation of this method is illustrated in Figure 10b.

The method appears to best operate in terms of completeness (98.8), especially for *demolished* buildings (100%). The two changes that are missed by the algorithm also correspond to *new* buildings and are related to errors in the *ground* / *above-ground* classification i.e. to objects, wrongly considered *ground* in the classification.

Regarding the false alarms, many of them are here again related to *demolished* buildings, for which the system achieves a correctness rate of only 23.7% and are caused by similar errors in the *ground* / *above-ground* classification. Thus, the building shown in Figures 11g and 11h, is lower than its surroundings, wrongly classified as *ground* and at the end reported as *demolished* by the system. *FP new* cases also occur with the method but the situation is here better, as indicated by a correctness rate rising to an acceptable standard (75.3%). The main reason of these *FP new* cases is the presence of errors in the correlation DSM that occur e.g. along the building edges (not sharp enough) and the areas between some buildings (generally over-estimated). These errors cause misclassification of some street areas as buildings (Figures 11i and 11j) – similar to those generated with (Champion, 2007) – and results in over-detections in the final change map.

However, similarly to what is observed with (Champion, 2007), the system features a high completeness rate for *unchanged* buildings (94.7%) and also appears to be efficient in reducing the amount of useless work, given to an operator.

4.1.3 Method of Rottensteiner (2007 and 2008)

The evaluation of this method is illustrated in Figure 10c.

The completeness of the system is optimal for *demolished* buildings (100%) and high for *new* buildings (94.0%). The five *new* buildings, missed by the algorithm (Figures 11k and 11l) are related to inaccuracies in the DTM, more specifically to the poor modeling of complicated topographic features (cliffs), which predictably limits the extraction of new buildings that is partly based on the normalized DSM and also the DTM.

However, the correctness of the system achieves an acceptable standard. If the correctness of this system for *demolished* buildings is similar to those obtained with (Champion, 2007) and (Matikainen et al., 2007), the correctness for *new* buildings is largely higher (96.3%), which means that the *FP new*

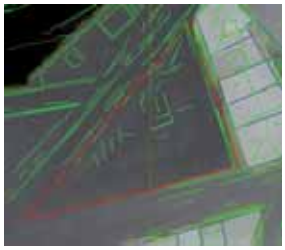

(a) Champion: *FN* case – building wrongly validated with non-filtered primitives (in green).

(b) Champion: *FN* case - same as case (a) - superimposed on the RGB othophoto.

(c) Champion: *FP* case (retaining wall).

(d) Champion: *FP* case (omitted tree in the vegetation mask), superimposed on the RGB orthophoto.

(e) Champion: *FP* case (narrow overestimated street), superimposed on the DSM.

(f) Champion: *FP* case (topography - cliff).

(g) Matikainen et al.: *FP* case (low building), superimposed on the RGB orthophoto.

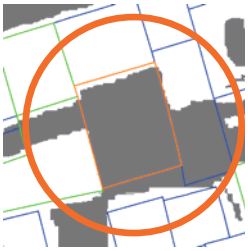

(h) Matikainen et al.: *FP* case (low building), superimposed on the building label image.

(i) Matikainen et al.: *FP* case (narrow overestimated street), superimposed on the DSM.

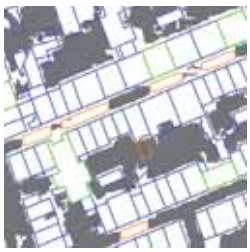

(j) Matikainen et al.: *FP* case (narrow overestimated street), superimposed on the building label image.

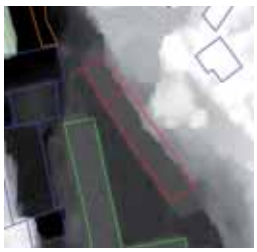

(k) Rottensteiner: *FN* case (topography - cliff), superimposed on the DSM.

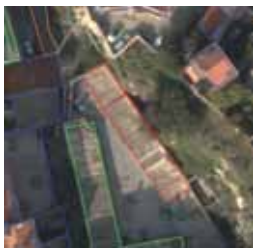

(l) Rottensteiner: *FN* case (topography), superimposed on the RGB orthophoto.

Figure 11. Evaluation details in Marseille (the same colour code as Figure 10).

cases that occurred with the previous methods and were related e.g. to a confusion between buildings and other objects (walls, trees, etc.) do not occur here. This may be related to the use of the initial description of the database as a priori information for producing and improving the building label image.

In addition, the completeness for *unchanged* buildings appears to be high, which demonstrates the high economic effectiveness of the method.

4.1.4 Summary

In the context of aerial imagery, there is not a visible predominance of one approach over another one. The three of them perform well in terms of completeness. The main difference mostly concerns the correctness for *new* buildings. In this respect, the method by Rottensteiner (2008) seems to be more efficient than (Champion, 2007) - to a lesser extent, (Matikainen et al., 2007) - and also delivers fewer *FP new* buildings. Our experiments show that the main limitation of this context is the correctness rate, achieved for *demolished* buildings, that ranges from 18.4% to 23.7% only. However, all the methods presented here are very efficient in classifying *unchanged* buildings. Here, the completeness rates are higher than 93%, which indicates that a considerable amount of manual work is saved and also demonstrates the economical efficiency of these approaches, in the aerial context. This outcome is particularly noteworthy for the method by Rottensteiner (2008) and Matikainen et al. (2007), as they were not originally designed to deal with such a context. In this respect, the outcomes presented here demonstrate the high transferability of these methods.

4.2 The Lyngby Area

Table 4 presents the per-building confusion matrix for the change detection results obtained for the Lyngby data set. The completeness and correctness of the results on a per-building basis are shown in Table 5. These two tables are used in the following paragraphs to analyse the outcomes of each method, firstly those of (Matikainen et al., 2007), secondly those of (Olsen and Knudsen, 2005) and lastly those of (Rottensteiner, 2008).

4.2.1 Method of Matikainen et al., 2007

The evaluation of this method is illustrated in Figure 12a.

Here again, the method performs well, in terms of completeness, especially for *demolished* buildings (100%). Compared to the outcomes obtained in the Marseille test area, the main difference concerns the *new* buildings, which appear to be more difficult to extract. Thus, 8.2% of the *new* buildings present in the reference are missed by the system. The corresponding *FN new* cases (Figure 13a) actually correspond to three houses, present in the reference database, but for which only the ground-works are visible in images. As the building detection system is based on the assumption that build-ings have a positive height in the normalized DSM, these three houses are missed by the system.

The correctness of the system here again appears to be relatively poor, especially for *demolished* buildings, for which the system achieves a correctness of only 22.6%, which means that a lot of *unchanged* buildings are wrongly reported as *changed* (*demolished*) by the system, as illustrated e.g. in Figures 13b, 13c and 13d. By contrast, the correctness for *new* buildings is optimal (100%), which means that no object in the study area is wrongly alerted as *new*. This outcome is most certainly

related to the absence in the LIDAR DSM of the errors that occurred in the correlation DSM in the Marseille test area.

In addition, the system appears to be effective in reducing the amount of work, given to an operator, as indicated by the relatively high completeness (81.7%), achieved for *unchanged* buildings.

Algorithm Reference	*Unchanged* (A)	*Demolished* (A)	*New* (A)	Background (A)
(Matikainen, 2004)				
Unchanged (R)	323	72	-	-
Demolished (R)	0	21	-	-
New (R)	-	-	45	4
Background (R)	-	-	0	1
(Olsen and Knudsen, 2005)				
Unchanged (R)	347	48	-	-
Demolished (R)	0	21	-	-
New (R)	-	-	46	3
Background (R)	-	-	10	1
(Rottensteiner, 2008)				
Unchanged (R)	379	16	-	-
Demolished (R)	0	21	-	-
New (R)	-	-	43	6
Background (R)	-	-	4	1

Table 4. Confusion matrix for Lyngby [buildings] with (Matikainen, 2004), (Olsen and Knudsen, 2005) and (Rottensteiner, 2008). A: Automatic. *R*: Reference.

	Unchanged	*Demolished*	*New*	Background
(Matikainen, 2004)				
Completeness [%]	81.7	100	91.8	100
Correctness [%]	100	22.6	100	20.0
(Olsen and Knudsen, 2005)				
Completeness [%]	87.8	100	93.9	9.1
Correctness [%]	100	30.4	82.1	25.0
(Rottensteiner, 2008)				
Completeness [%]	95.9	100	87.8	20.0
Correctness [%]	100	56.8	91.5	14.3

Table 5. Completeness and correctness for Marseille [buildings] with (Matikainen, 2004), (Olsen and Knudsen, 2005) and (Rottensteiner, 2008), derived from the confusion matrix (Table 4).

4.2.2 Method of Olsen and Knudsen, 2005

The evaluation of this method is illustrated in Figure 12b.

Based on the quality measures given in Tables 4 and 5, the outcomes of this system are very similar to those obtained with (Matikainen et al., 2007). Compared to (Matikainen et al., 2007), three *FPs* occur in the south-eastern part of the scene and correspond to bridges or elevated roads, wrongly reported as *new* buildings by the algorithm. In addition, five *FPs* are located in the sea, and three *FP*s in a lake

(Figures 13e and 13f). In such areas, single points were not eliminated from the original LIDAR points, but used in an interpolation process based on a triangulation of the LIDAR points, which there produced essentially meaningless data and ultimately led to errors in the final change map. Note that the *FP* cases that occur here in the sea did not occur with (Matikainen et al., 2007) because the sea was excluded manually from the study area (which is a normal practice in an operational context).

Comparatively to (Matikainen et al., 2007), the completeness for *unchanged* buildings is higher (87.8%): that means that only 12.2% of *unchanged* buildings are wrongly given to the operator for verification.

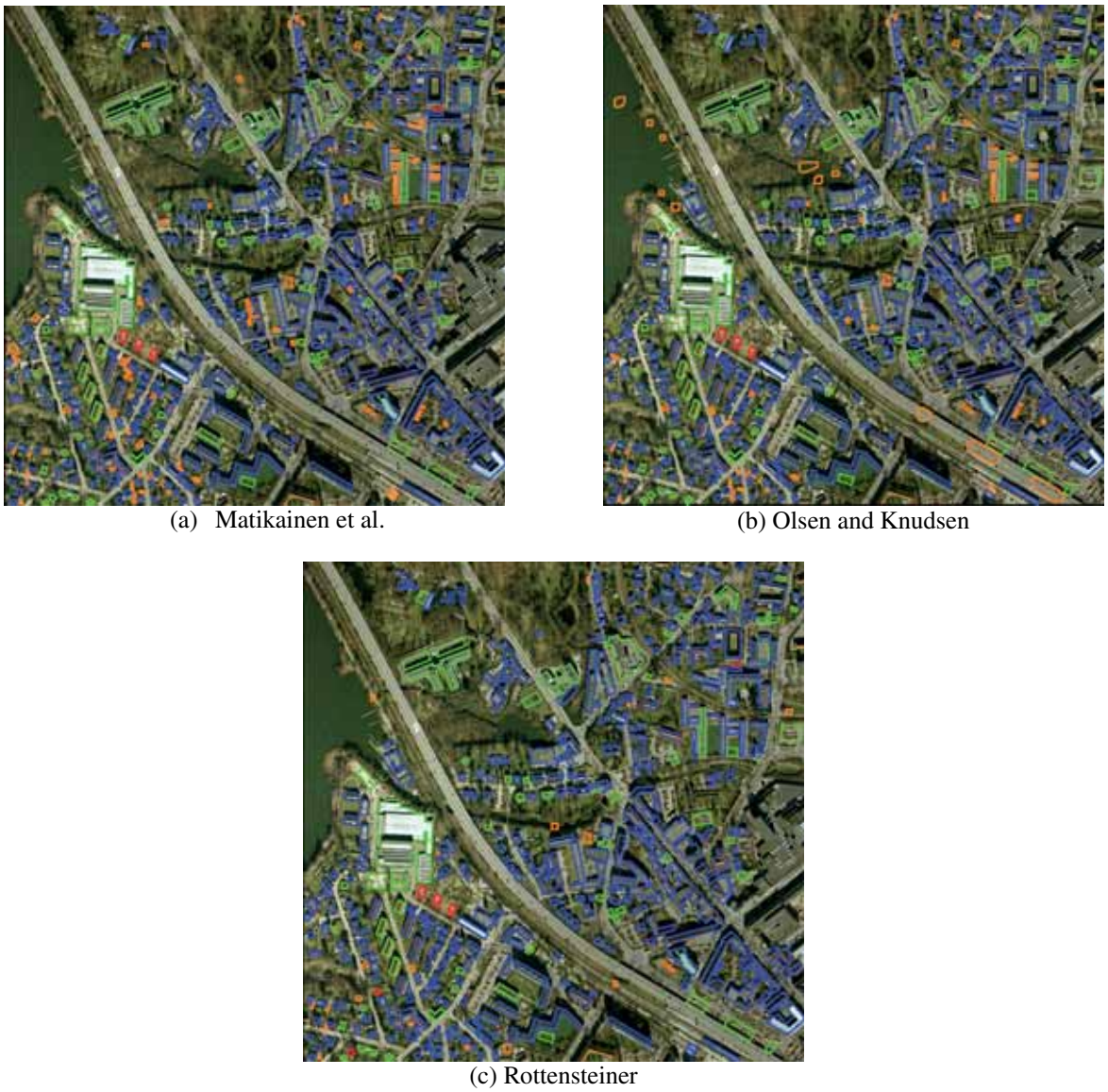

(a) Matikainen et al.

(b) Olsen and Knudsen

(c) Rottensteiner

Figure 12. Evaluation of change detection in Lyngby. Green: *TP*; Red: *FN*; Orange: *FP*; Blue: *TN*.

4.2.3 Method of Rottensteiner, 2008

The evaluation of this method is illustrated in Figure 12c.

Compared to the two previous methods, this system clearly delivers fewer false alarms, especially concerning *demolished* buildings, for which the system achieves here less than 50% false positives (the correctness for *new* buildings is 56.8%). In addition, the completeness for *unchanged* buildings is the highest one of the three methods. Here, only 4.1% of *unchanged* buildings are wrongly given to an operator for a useless verification.

These good results are achieved at the expense of a slightly lower completeness rate for *new* buildings, related to two *FN* cases that occur in the south-western part of the study area and are not present in the change maps, produced by Matikainen et al. (2007) and Olsen and Knudsen (2005)

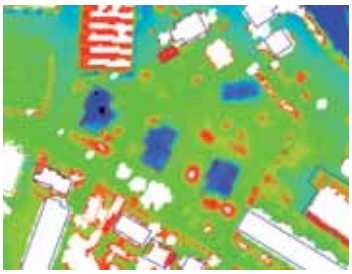

(a) **Matikainen et al.**: *FN* case (*new* building - groundwork)

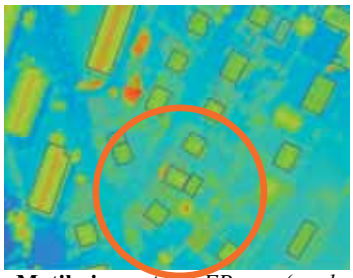

(b) **Matikainen et al.**: *FP* case (*unchanged* **small** buildings)

(c) **Matikainen et al.**: *FP* cases (*unchanged* **small** buildings), superimposed on the RGB orthophoto

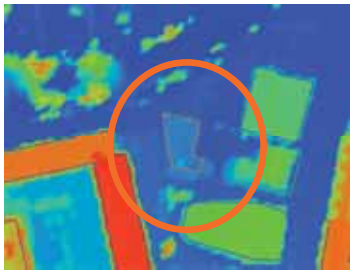

(d) **Matikainen et al.**: *FP* case (*unchanged* **small** buildings)

(e) **Olsen and Knudsen**: *FP* case (water areas), superimposed on the RGB orthophoto.

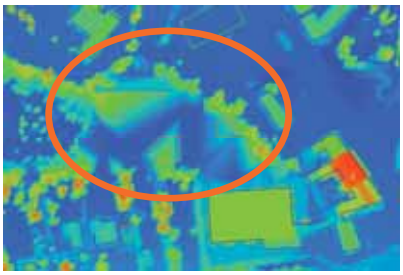

(f) **Olsen and Knudsen**: *FP* case (water areas), superimposed on the DSM.

Figure 13. Evaluation details in Lyngby (the same colour code as Figure 12).

4.2.4 Summary

In summary, the problems observed in the LIDAR context are similar to those observed in the imagery context and are mainly related to the generation of a high number of false alarms, in particular *FP demolished* buildings. However, it should be noted here that the LIDAR dataset used in this study was not ideal and contained many errors, which, in our opinion, must be considered to explain this relative outperformance of the methods. Firstly, the ground resolution of LIDAR data (1m) is relatively low, especially compared to the ground resolution of the input data, used in the Marseille test area (20cm). Secondly, the original LIDAR point clouds were re-sampled on a regular raster grid, which entails a loss in the data quality, especially along the building outlines. Thirdly, orthophotos were computed from a Digital Terrain Model: some façades are visible in orthophotos, which also limits the quality of the building label image, ultimately, of the change map. Lastly, no Last Pulse data was available for this dataset, which limits the efficiency in separating buildings from trees, as explained e.g. in (Rottensteiner, 2008). If the limited quality of input data prevented us from verifying the superiority of LIDAR data in the change detection topic, the results presented here have shown the good behaviour of these systems in the presence of (unusual) errors in the LIDAR data set. More specifically, the capability of these systems to rightly detect a large part of *unchanged* buildings, which, according to the preliminary discussion of this section, shows their economical effectiveness.

4.3 The Toulouse Area

Table 6 presents the per-building confusion matrix for the change detection results obtained in the Toulouse test area. The completeness and correctness of the results on a per-building basis are shown in Table 7. These two tables are used in the following paragraphs to analyse the outcomes of each method, firstly those of (Champion, 2007) and then those of (Rottensteiner, 2008).

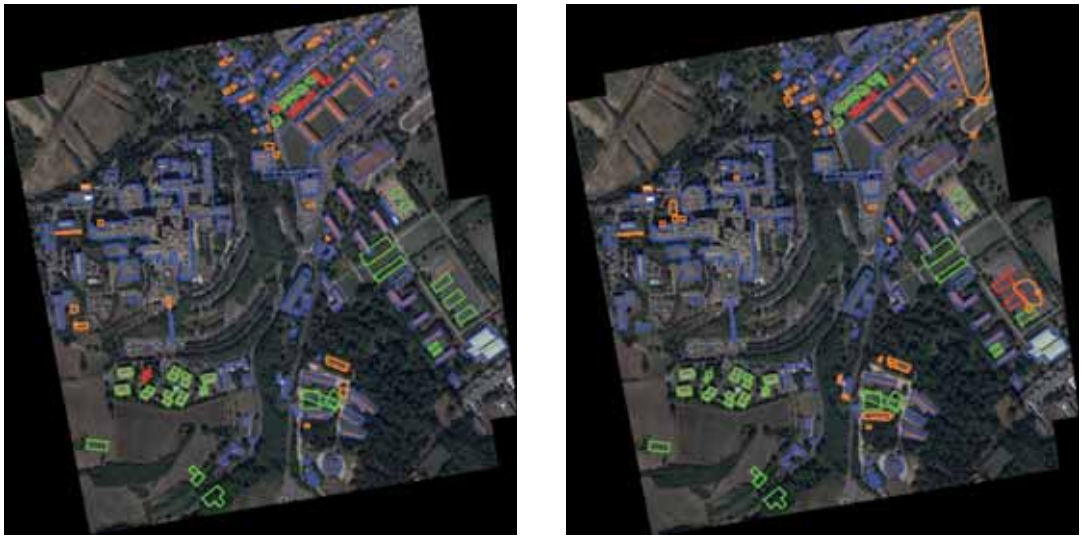

(a) Champion (b) Rottensteiner

Figure 14. Evaluation of change detection in Toulouse.
Green: *TP*; red: *FN*; orange: *FP*; blue: *TN*.

Algorithm Reference	*Unchanged* (A)	*Demolished* (A)	*New* (A)	Background (A)
(Champion, 2007)				
Unchanged (R)	96	20	-	-
Demolished (R)	0	15	-	-
New (R)	-	-	15	8
Background (R)	-	-	5	1
(Rottensteiner, 2008)				
Unchanged (R)	93	23	-	-
Demolished (R)	2	13	-	-
New (R)	-	-	19	4
Background (R)	-	-	13	1

Table 6. Confusion matrix for Toulouse [buildings] with (Rottensteiner, 2008) and (Champion, 2007). A: Automatic. *R*: Reference.

	Unchanged	*Demolished*	*New*	Background
(Champion, 2007)				
Completeness [%]	82.8	100	65.2	16.7
Correctness [%]	100	42.9	75.0	11.1
(Rottensteiner, 2008)				
Completeness [%]	80.2	86.7	82.6	07.1
Correctness [%]	97.9	36.1	59.4	20.0

Table 7. Completeness and correctness for Marseille [buildings] with (Rottensteiner, 2008) and (Champion, 2007) derived from the confusion matrix (Table 6).

4.3.1 Method of Champion, 2007

The evaluation of this method is illustrated in Figure 14a.

The method by (Champion, 2007) is very effective in detecting *demolished* buildings (100%), but this is achieved at the expense of a low correctness rate (42.9%). Our experiments show that the *FP demolished* cases, generated by the method are mostly related to the building size and topology. Thus, the northern part of the scene corresponds to housing estate i.e. a pool of small buildings with small recesses and overhangs. In such a configuration, the DSM is not accurate enough to allow a correct extraction of 2D contours. Small 3D segments could overcome the problem but the pruning procedure (used at the end of the 3D reconstruction) intrinsically gives the priority to longest segments. As a result, no primitive is extracted and an alert is wrongly sent to the operator, as illustrated in Figure 15a. The main limitation of the system appears to be the extraction of *new* buildings, which is featured by a completeness rate of only 75%, which means that 25% of the *new* buildings (in the reference) is missed by the algorithm (Figure 15b), which is clearly not sufficient to provide a full update of the database.

4.3.2 Method of Rottensteiner, 2008

The evaluation of this method is illustrated in Figure 14b.

On the whole, the same analysis can be carried out with (Rottensteiner, 2008).

Compared to (Champion, 2007), the method by Rottensteiner (2008) misses quite a few *demolished* buildings (the completeness rate for *demolished* buildings is 86.7%) but appears to be better at extracting new buildings, even though 17.6% of the total number of *new* buildings is still missed by the algorithm. This is achieved at the expense of a relatively low correctness rate (59.4%), especially comparatively to those obtained in the Marseille and Lyngby test area. As detailed in the following sections, the corresponding *FP* new cases are caused by the size of the change and the quality of the input DSM (Figure 15d).

(a) **Champion**: *FP* case (**small** existing building)

(b) **Champion**: *FN new* case (**small** building).

(c) **Rottensteiner**: *FN new* case (**small** building).

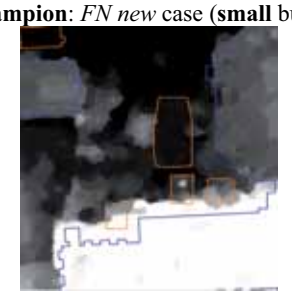

(d) **Rottensteiner**: *FP* case (DSM inaccuracies)

Figure 15. Evaluation details in Toulouse (the same colour code as Figure 14).

4.3.3 Summary

The main limitation in the satellite context appears to be the detection of *new* buildings. Thus, the completeness achieved both with (Champion, 2007) and (Rottensteiner, 2008) is clearly not sufficient to provide a full update of the database, which would require (in an operational context) a manual intervention in order to find the remaining *new* buildings. Detecting the changes of 2D buildings, starting with satellite images also appears too hard a challenge for the approaches of the current State-of-the-Art. This is corroborated by the fact that the ground classification performed in (Matikainen et al., 2007) did not give acceptable results for Toulouse when carried out in a fully automatic way.

The results may appear to be disappointing. However, one should note that, even though the completeness rates for *unchanged* buildings achieved by both methods are relatively low compared to those obtained in the Marseille and Lyngby test areas, they also indicate that more than 80% of *unchanged* buildings need not be investigated by an operator, even under challenging circumstances.

5. OUTCOMES ANALYSIS AND OVERALL FINDINGS

In order to obtain deeper insights into the reasons for failure, in the subsequent sections we will focus our analysis on some factors that affect the change detection performance, firstly the size of the change to detect, secondly the quality of the input data (including the DSM and DTM), thirdly the influence of other topographic objects present in the scene, lastly the primitives used in the system. This analysis is also used to propose some improvements to consider in the future change detection systems.

5.1 *Impact of the Size of a Change*

To analyse the performance of change detection as a function of the change size, we compute the completeness and correctness rates depending on this factor. For that purpose, *new* and *demolished* buildings are placed into bins representing classes of 20m² in width. Note that the buildings from all the test areas for which results were submitted are combined in order to have a significant number of changes for each bin. The graphs for (Champion, 2007) and (Rottensteiner, 2008) also contain the results from the Toulouse area. The completeness and correctness rates, computed independently for each bin, are presented in Figure 16 (left column) and demonstrate the close relation between the quality of change detection and the change size. This is true for the completeness with (Champion, 2007) and (Rottensteiner, 2008), but it is even more obvious for the correctness in all three graphs.

Looking at the curves that gives the cumulative correctness, computed by considering all buildings larger than a given size (Figures 16, right column), one can see that only buildings larger than 85m² for (Champion, 2007) – (Figure 16a), 65m² for (Matikainen et al., 2007) – (Figure 16b) and 45m² for (Rottensteiner, 2008) – (Figure 16c) can be detected with a satisfying correctness rate (70%)

From these new perspectives, it becomes obvious that the two major problems observed in Section 4, namely the potentially critical rate of missed *new* buildings (observed in the Toulouse test area, to a lesser extent in the Lyngby test area), which limits the qualitative effectiveness of change detection, and the poor correctness for *demolished* buildings (observed in the three test areas) are caused by the same underlying phenomenon i.e. the fact that small objects cannot be detected reliably by an automated procedure.

5.2 Impact of the *Quality of the Input Data*

Our experiments also identified the quality of the DSM and of the DTM as one of the main limiting factors of change detection.

5.2.1 Impact of the DSM

Regarding the first point, it mostly concerns the *correlation* DSM (used in Marseille and Toulouse). Three types of errors can be observed here.

- **Erroneous height** values, especially in **shadow areas** (where stereo-matching algorithms are known to worse perform) that are almost systematically alerted as new buildings, as depicted in Figures 17a, 17b, 17c and 17d, and contribute to lower the correctness of the systems for new buildings To limit this issue, the estimated position of buildings, given by the outdated database should be introduced in the system as an additional information. This solution is already implemented e.g. in (Rottensteiner, 2008) in order to improve the quality of the building

label image and clearly limits the number of the *FP* new cases, both observed with (Champion, 2007) and (Matikainen et al., 2007) in the Marseille test area (Figures 11a and 11e, page 24).

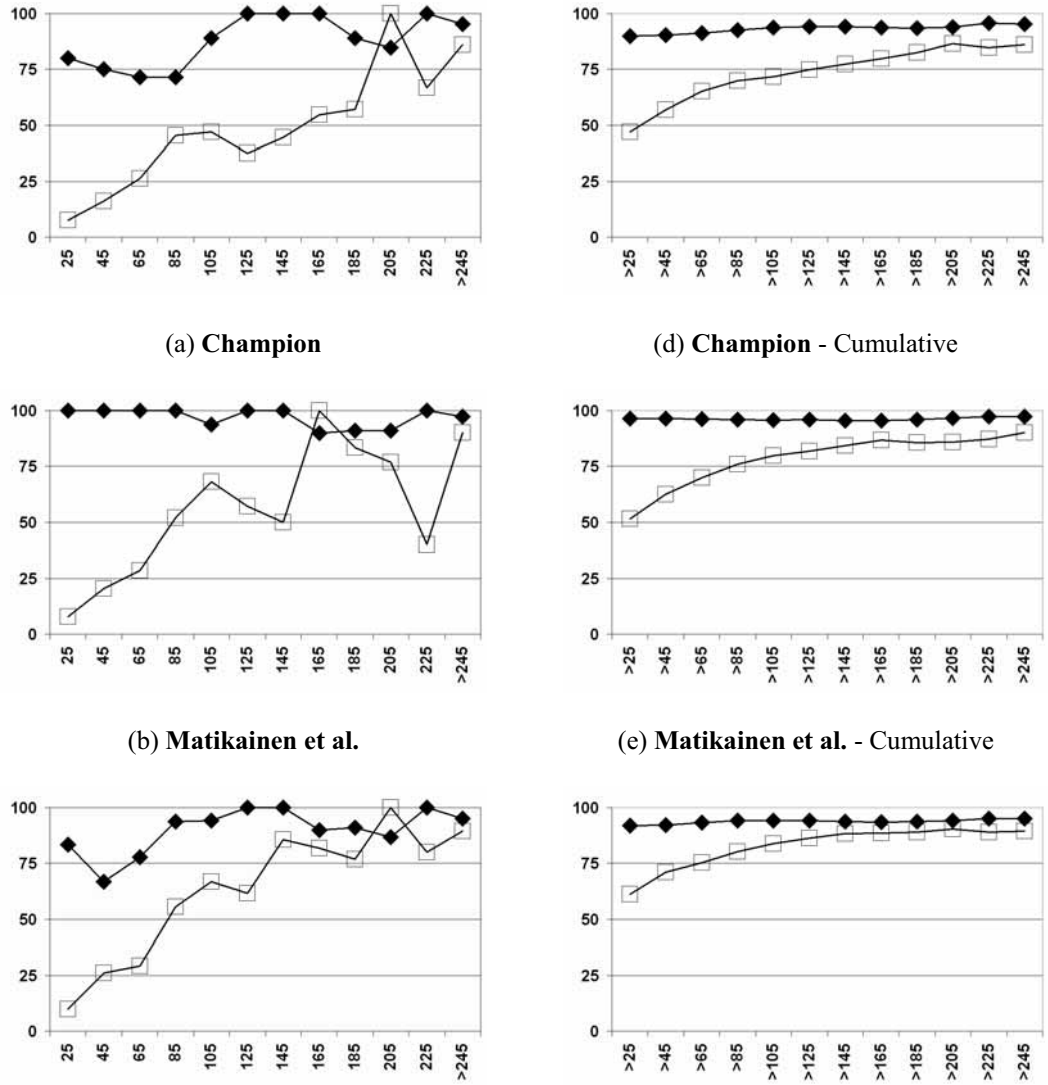

(a) **Champion**

(d) **Champion** - Cumulative

(b) **Matikainen et al.**

(e) **Matikainen et al.** - Cumulative

(c) **Rottensteiner**

(f) **Rottensteiner** - Cumulative

Figure 16. Completeness (black diamond) and correctness (white square) of the detection results as a function of the building size [m2] for (Matikainen, 2004), (Rottensteiner, 2008) and (Champion, 2007). First column: completeness and correctness for buildings of the size given in the abscissa. Second column: cumulative completeness and correctness computed for all buildings larger than the size given in the abscissa.

- The **quantization effects ("voxelling effect")** in the DSM i.e. the fact that the numerical resolution of height values is restricted to 20cm and 50cm (the size of one voxel), respectively in Marseille and Toulouse, which prevented the use of surface roughness as an input parameter for the Dempster-Shafer fusion process in (Rottensteiner, 2008) and altered the extraction of buildings. This effect mainly contributed to lower the correctness for demolished buildings.

- The errors, related to **classical problems of stereo-matching algorithms**, namely **repeating patterns** (demarcation lines in the sports field, rows of cars on the parking lot) and **poor contrast**, which entails height variations larger than 4m in the surface model in areas that are essentially horizontal and led in our experiments to errors in the final change map, especially in the Toulouse test areas with (Champion, 2007) and (Rottensteiner, 2008), as illustrated in Figures 17e, 17f, 17g and 17h. Here again, this effect clearly contributed to lower the correctness for new buildings.

As previously mentioned , some errors also occur in the LIDAR data set and are mostly related to the fact that the original LIDAR point cloud was re-sampled on a regular grid and to the absence of Last Pulse data.

Beyond the statistical aspects, our experiments show that the errors generated by the change detection approaches are often identical. Thus, the *FP* cases that occur in the Toulouse test area because of the DSM inaccuracies (Section 4.3) are both present in the outcomes of (Rottensteiner, 2008) and (Champion, 2007), as illustrated e.g. in Figures 17b and 17d respectively. That also highlights the impact of the context (here, the quality of input correlation DSM) on the change detection performance, regardless the methodology.

5.2.2 Impact of the DTM

As previously shown, the extraction of buildings and consequently the performance of the change detection process are the better the more accurate the DTM (or the classification into *ground* and *above-ground*) is.

In this study, the morphology-based method used in (Rottensteiner, 2008) and the surface-based method (Champion and Boldo, 2006) both fail in the presence of topographic discontinuities (cliffs). Refined approaches should be considered in the future to better model such terrain features. It must be noted here that manual corrections were not employed in this study, in order to keep the process fully automatic. The manual correction of difficult points is a normal practice in an operational context and could for instance have been used here to correct the initial classification into *terrain* vs. *off-terrain* points in (Matikainen et al., 2007). This would have given a better basis for the later classification stages and would also have improved the final change map.

(a) **Champion**: *FP* case (DSM inaccuracies – shadow areas), superimposed on the orthophoto.

(b) **Champion**: *FP* case (DSM inaccuracies – shadow areas), superimposed on the DSM.

(c) **Rottensteiner**: *FP* case (DSM inaccuracies – shadow areas), superimposed on the orthophoto.

(d) **Rottensteiner**: *FP* case (DSM inaccuracies – shadow areas), superimposed on the DSM.

(e) **Rottensteiner**: *FP* case (DSM inaccuracies – sport field), superimposed on the orthophoto.

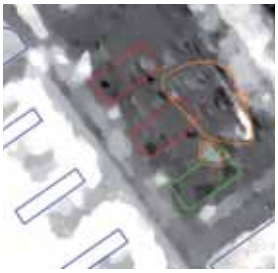

(f) **Rottensteiner**: *FP* case (DSM inaccuracies – sport field), superimposed on the DSM

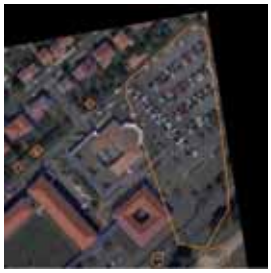

(g) **Rottensteiner**: *FP* case (DSM inaccuracies – repeating patterns), superimposed on the orthophoto

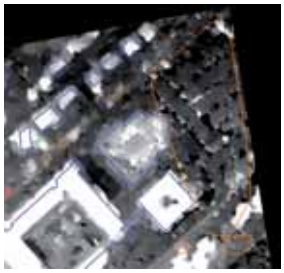

(h) **Rottensteiner**: *FP* case (DSM inaccuracies – repeating patterns), superimposed on the DSM.

Figure 17. Impact of the DSM quality of the input correlation DSM.

5.3 Impact of *Other Topographic Objects in the Scene*

Our experiments show some confusion between buildings and other *above-ground* objects, present in the scene and wrongly alerted as *new* buildings. Again, this contributes to lower the correctness achieved for *new* buildings. The methods presented here deal with this problem, but currently they only focus on one class of above-ground objects that is to be separated from buildings, namely trees. In general, these trees are identified with indicators based on the NDVI and then eliminated, as shown in Section 3.

Even though this strategy appears to be efficient, our experiments show that some confusion still occurs between buildings and trees, especially with (Champion, 2007) in the Marseille test area (Figure 18c). Here, thresholding the NDVI images to compute a vegetation mask, subsequently used to eliminate trees is clearly not robust enough. In this respect, using more robust criteria to extract vegetation and testing more sophisticated methods such as the classification-based method described in (Trias-Sanz et al., 2007) should be considered in the future to deal with the vegetation problem.

Our experiments also show that the remaining confusions are not limited to vegetation but concern other objects, not considered in the approaches presented in this study. For instance, some bridges or

elevated roads, present in the Lyngby test area are highlighted as *FP new* buildings both by (Rottensteiner, 2008) and (Olsen and Knudsen, 2005), as shown in Figures 18a, 18b, 18d and 18e. To limit the impact of these problems, two strategies could be considered in the future. The first one consists in developing more sophisticated methods that are capable of simultaneously extracting multiple object classes such as buildings, roads, and vegetation. Such methods would need to incorporate complex scene models that also consider the mutual interactions of the object classes in a scene. They could make use of recent developments in the field of Computer Vision that are related to the modelling context in image classification (Kumar and Hebert, 2006). The second strategy may use additional information on other objects, by incorporating e.g. an existing road database in the building change detection procedure.

(a) **Rottensteiner**: *FP* case (confusion with a bridge), superimposed on the orthophoto.

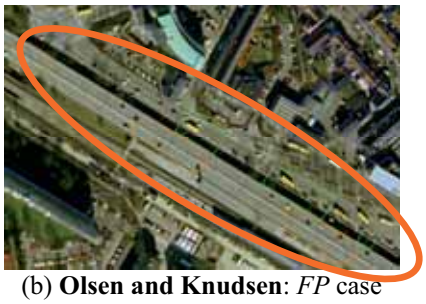

(b) **Olsen and Knudsen**: *FP* case (confusion with an elevated road / bridge), superimposed on the orthophoto.

(c) **Champion**: *FP* case, caused by omitted trees in the vegetation mask (in white)

(c) **Rottensteiner**: *FP* case (confusion with a bridge), superimposed on the DSM.

(e) **Olsen and Knudsen**: *FP* case (confusion with an elevated road / bridge), superimposed on the DSM

Figure 18. Impact of the other topographic objects in the scene.

5.4 Impact of the *Primitives used in the System*

In the approaches tested in this study, geometric primitives are preferred to radiometric features. If such an approach is valid in the LIDAR context (for which the geometry is known to be well described), it becomes uncertain in the imagery context (Marseille and most of all Toulouse) or when the quality of LIDAR data is lower (Lyngby). Thus, the 2D contours, extracted in the DSM with (Champion, 2007) are less accurate and the surface roughness computed in (Rottensteiner, 2008) is meaning-

less, which at the end contributes to alter the building extraction, ultimately the quality of the change map.

Two solutions could be considered in the future to overcome the problem. The first one consists in introducing *new* primitives, in particular 3D primitives in the change detection systems. These primitives may correspond to 3D building outlines (similar to those, produced with the algorithm by Taillandier and Deriche, 2002) or to the 3D roof planes, and should be constructed, by taking advantage of the high quality of *new* sensors and according to the *new* 3D acquisition capabilities, offered for instance by the latest generation spaceborne sensors (such as the Pléiades-HR system). The second one consists in using the colour information in order to limit e.g. the number of *FNs* (such as those produced by (Champion, 2007) in Marseille, as illustrated in Figure 11c) and avoid the large *FP* areas, generated in Toulouse with (Rottensteiner, 2008). The key point here obviously concerns the way to introduce this *new* information, either jointly with geometric primitives or in a sequential manner, e.g. in a post-processing step that would aim at reducing the number of false alarms and misdetections.

6 Conclusion

Four building change detection approaches have been tested in three different contexts. If the satellite context appears to be the most challenging for the current state-of-the-art, the aerial context and the LIDAR context appear to be a viable basis for building an operative system in the future. Thus, the high completeness rates for *demolished* buildings and the high correctness for *unchanged* buildings that could be achieved in these contexts highlight the effectiveness of the presented approaches in verifying the existing objects in the databases.

In summary, the main obstacle for making automatic change detection operational appears to be the inability of current algorithms to detect small changes. This affects the quality of the updated data base via missed *new* buildings, and reduces the economical efficiency via *FP demolished* buildings. Our experiments also show that a lot of false alarms are caused by the relatively poor quality of the input data (especially *correlation* DSM) and the presence of other topographic objects in the scene (in particular, vegetation and roads). In spite such drawbacks, the economical efficiency of the presented approaches seems to be promising, with 80-90% of the existing buildings that need no further attention by the operator, because these buildings are reported to be *unchanged*, which then provides a considerable amount of manual work saved.

Areas of improvement should concern input data and methodologies. Thus, the resolution of LIDAR data used in this test appeared to be critical and clearly limited the change detection performance. Using LIDAR points with a higher density (e.g. 5-10 points / m²) could improve the situation. Regarding the aerial context, the limiting factor here was the quality of the DSM that should be improved in the future, by using either multiple images with a better resolution (e.g. 10cm) or another method (Hirschmüller, 2006). As far as methodology is concerned, *new* primitives could be used in the algorithms, in particular 3D primitives (representing e.g. the 3D roof planes or building outlines) that can be reconstructed with the capabilities of latest generation sensors, in terms of ground resolution and 3D acquisition. Another concern should be the improvement of the scene models used in object detection such that they can deal with different object classes and their mutual interactions. By incorporating different object classes and considering context in the extraction process, several object classes could be detected simultaneously, and the extraction accuracy of all interacting objects could be improved. As long as such models are not readily available, existing databases containing other object classes can be used to improve the change detection performance.

In this project we learned how difficult it is to compare approaches of very different designs. To carry out a fair test, we chose to use the building label images and to limit the type of changes to *demolished* and *new* buildings. We are aware that this scheme is not sufficient to highlight the specificities of some methods, e.g. the thematic accuracy of the change map delivered by (Rottensteiner, 2008). However, we think that this scheme was sufficient to bring out the interesting findings presented here. We also hope that our results, in conjunction with those of other projects in the domain (e.g. WIPKA[5] and ARMURS[6]) will be helpful to create a nucleus of interested people, both in academia and the private sector, and to speed up the progress in the field of automated building change detection.

[5] http://www.tnt.uni-hannover.de/project/wipka/. Last visited: 04-08-09
[6] http://www.armurs.ulb.ac.be. Last visited: 04-08-09

Acknowledgments

We are grateful to EuroSDR for giving us the opportunity to conduct this test and CNES for providing Pléiades imagery. We thank the anonymous reviewers for their helpful comments about the two papers we submitted during the project (Champion et al., 2008) and (Champion et al., 2009)

References

Breiman, L., Friedman, J. H., Olshen, R. A., Stone, C. J., 1984. Classification and Regression Trees. The Wadsworth Statistics / Probability Series, Wadsworth, Inc., Belmont, California.

Champion, N., 2007. 2D building change detection from high resolution aerial images and correlation Digital Surface Models. In: Int'l Archives of the Photogrammetry, Remote Sensing and Spatial Information Sciences, Vol. XXXVI-3/W49A (on CD-ROM), pp. 197–202.

Champion, N., Matikainen, L., Rottensteiner, F., Liang, X., Hyyppä, J. A test of 2D Building Change Detection Methods: Comparison, Evaluation and Perspectives. International Archives of Photogrammetry, Remote Sensing and Spatial Information Sciences. Vol. XXXVII , Part 4, Beijing, China, July 2008.

Champion, N., Rottensteiner, F., Matikainen, L., Liang, X., Hyyppä, J., Olsen, B. P. A Test of Automatic Building Change Detection Approaches. In: International Archives of Photogrammetry, Remote Sensing and Spatial Information Sciences. Vol. XXXVIII, Part 3/W4. Paris, France, pp. 145–150.

Champion, N., Boldo, D., 2006. A robust algorithm for estimating Digital Terrain Models from Digital Surface Models in dense urban areas. In: Int'l Archives of the Photogrammetry, Remote Sensing and Spatial Information Sciences, XXXVI-3, pp. 111–116.

Definiens, 2008. ttp://www.definiens.com/.

Deriche, R. (1987), Using Canny's criteria to derive a recursively implemented optimal edge detector, International Journal of Computer Vision, Vol.1, pp.167-187

Heipke, C., Mayer, H., Wiedemann, C., Jamet, O., 1997. Automated reconstruction of topographic objects from aerial images using vectorized map information. In: Int'l Archives of Photogrammetry and Remote Sensing, XXXII, pp. 47–56.

Heipke, C., Cygan, M., Sester, M., Renlinag, Z. and Jie J. (2008), GIS Updating from imagery and collateral data sources, Tutorial jointly organized by ISPRS TC II & IV.

Hirschmüller, H., 2008. Accurate and efficient stereo processing by semi-global matching and mutual information. IEEE TPAMI 30(2), pp. 328-341.

Kumar, S. and Hebert, M.,, 2006. Discriminative random fields. International Journal of Computer Vision 68(2), pp. 179–201.

F. Lafarge, X. Descombes, J. Zerubia: "Building Reconstruction from a Single DEM", Proc. IEEE Computer Vision and Pattern Recognition (CVPR), 2008.

Matikainen, L., Hyyppä, J., Kaartinen, H., 2004. Automatic detection of changes from laser scanner and aerial image data for updating building maps. In: Int'l Archives of the Photogrammetry, Remote Sensing and Spatial Information Sciences, XXXV-B2, pp. 434–439.

Matikainen, L., Kaartinen, K., Hyyppä, J., 2007. Classification tree based building detection from laser scanner and aerial image data. In: Int'l Archives of the Photogrammetry, Remote Sensing and Spatial Information Sciences, XXXVI, pp. 280–287.

Mayer, H., Hinz, S., Bacher, U., Baltsavias, E., 2006. A test of automatic road extraction approaches. In: Int'l Archives of the Photogrammetry, Remote Sensing and Spatial Information Sciences, XXXVI-3, pp. 209–214.

Mayer, H., 2008. Object extraction in photogrammetric computer vision. ISPRS Journal of Photogrammetry and Remote Sensing 63(2008), pp. 213-222.

Olsen, B., Knudsen, T., 2005. Automated change detection for validation and update of geodata. In: Proceedings of 6th Geomatic Week, Barcelona, Spain.

Ortner, M., Descombes, X., Zerubia, J., 2008. A marked point process of rectangles and segments for automatic analysis of digital elevation models. IEEE Transactions on Pattern Analysis and Machine Intelligence 30 – Issue 1, 105 – 119.

Pierrot-Deseilligny, M., Paparoditis, N., 2006. An optimization-based surface reconstruction from Spot5- HRS stereo imagery. In: Int'l Archives of the Photogrammetry, Remote Sensing and Spatial Information Sciences,XXXVI-1/W41, pp. 73–77.

Rottensteiner, F., 2007. Building change detection from Digital Surface Models and multi-spectral images. In: Int'l Archives of the Photogrammetry, Remote Sensing and Spatial Information Sciences, XXXVI-3/W49B (on CD-ROM).

Rottensteiner, F., 2008 Automated updating of building data bases from digital surface models and multi-spectral images. In: IAPRSIS XXXVII – B3A, pp. 265-270.

Steinnocher, K., Kressler, F., 2006. Change detection. Technical report, EuroSDR Report.

Taillandier, F., Deriche, R., 2002. A reconstruction of 3D linear primitives from multiple views for urban areas modelisation. In: Int'l Archives of Photogrammetry and Remote Sensing, XXXIV-3B, pp. 267–272.

Terrasolid, 2008. http://www.terrasolid.fi/.

Trias-Sanz, R., Stamon, G., Louchet, J., To Appear. Using colour, texture, and hierarchial segmentation for high-resolution remote sensing. ISPRS Journal of Photogrammetry and Remote Sensing.

Annex

Paper presented at ISPRS Symposium 2008 in Beijing

Paper presented at ISPRS CMRT 2009 in Paris

A TEST OF 2D BUILDING CHANGE DETECTION METHODS: COMPARISON, EVALUATION AND PERSPECTIVES

Nicolas Champion[a], Leena Matikainen[b], Franz Rottensteiner[c], Xinlian Liang[b], Juha Hyyppä[b]

[a] IGN/MATIS, Saint-Mandé, France - nicolas.champion@ign.fr
[b] FGI, Dept. of Remote Sensing and Photogrammetry, Masala, Finland – (leena.matikainen, xinlian.liang, juha.hyyppa)@fgi.fi
[c] Cooperative Research Centre for Spatial Information, Dept. of Geomatics, University of Melbourne, Australia, franzr@unimelb.edu.au

Commission VI, WG VI/4

KEY WORDS: Change Detection, 2D vector databases, Algorithms Comparison, Quality Assessment

ABSTRACT:

In the past few years, 2D topographic databases have been completed in most industrialised countries. Most efforts in National Mapping and Cadastral Agencies (NMCAs) are now devoted to the update of such databases. Because t is generally carried out manually, by visual inspection of orthophotos, the updating process is time-consuming and expensive. The development of semi-automatic systems is thus of high interest for NMCAs. The obvious lack of expertise in the domain has driven EuroSDR to set up a test comparing different change detection approaches. In this paper, we limit the scope of the project to the imagery context. After describing input data, we shortly introduce the approaches of the working groups that have already submitted results. Preliminary results are assessed and a discussion enables to bring out first conclusions and directions.

1. INTRODUCTION

2D topographic databases have been completed in most National Mapping and Cadastral Agencies (NMCAs) during the last decade. The main issue now concerns the map revision. This procedure is known to be very tedious, time-consuming and expensive. There is also a growing need to automate it. The development of semi-automatic tools that are able to detect the changes in a database from recent data (typically imagery or LIDAR) and to present them to a human operator for verification is therefore highly desirable. Only a few solutions have been proposed by academic research, even fewer by private companies. Many questions that have arisen remain unanswered, e.g. those regarding the most efficient methodology, the type of primary data to use (LIDAR / imagery) or the most appropriate spatial resolution to choose. These considerations have driven EuroSDR (European Spatial Data Research - http://www.eurosdr.net) to set up a change detection project. This project is in line with previous EuroSDR projects, e.g. the project on road updating (Mayer et al., 2006) and the one on change detection (Steinnocher and Kressler, 2006). The aim of this new project is to evaluate the feasibility of semi-automatically detecting changes in a 2D building vector database from imagery or LIDAR. Three specific topics are investigated in detail: firstly, the impact of the type of data and methodology on the performance of the change detection; secondly, the impact of the spatial resolution of input data; finally, the impact of the complexity of the scene, especially with respect to topography and land use. The methodology of the project consists in a test comparing five different algorithms that are representative of the current state-of-the- art in the field of change detection. It is the main goal of this EuroSDR project to gather enough experience to identify key problems in change detection and to give promising directions for building an optimal operational system in the future.

In this paper, preliminary results achieved for three different algorithms, (Matikainen et al., 2007), (Rottensteiner, 2007) and (Champion, 2007), are presented. In Section 2, the datasets and the comparison method are described. In Section 3, the three approaches of the working groups that have already submitted results are shortly introduced. Results are given and evaluated in Section 4. We finally present a summary and conclusions.

2. INPUT DATA AND TEST SET-UP

2.1 Datasets Description

Two test areas are used in this study. The first test area is situated in Marseille (France). It has an area of about 0.4 km^2 and contains about 1300 buildings. The area corresponds to a very dense urban settlement and features a complicated urban configuration (lower buildings connected to higher buildings). The test area is hilly (with height differences of 150 m) and vegetated, especially along streets. The second test area is situated in Toulouse (France). It has an area of about 1 km^2 and contains about 200 buildings. It features a suburban area and is composed of detached buildings that are very different to each other with respect to the size, height, shape and roofing material. The terrain is also undulating (with height differences of 100 m) and vegetated. In this study, colour infrared (CIR) aerial images with a Ground Sample Distance (GSD) of 20 cm and multiple overlap (a forward and a side lap of minimum 60%) are used for Marseille. Pléiades tri-stereoscopic Satellite CIR images are used for Toulouse, with a GSD equal to 50 cm. In both cases, a Digital Surface Model (DSM) was computed using a stereo-matching algorithm based on the 2D minimization of a cost that takes into account discontinuities and radiometric similarities (Pierrot-Deseilligny and Paparoditis, 2006). The GSD of the DSM is equal to the GSD of the aerial images. CIR orthophotos were also computed from

input DSM and images. Reference (up-to-date) building databases were edited manually, by field surveying. Out-of-date databases were derived by simulating changes to the reference databases by inserting new and deleting some of the existing buildings. In Marseille, 107 changes were simulated (89 new and 18 demolished buildings) and 40 changes (23 new and 17 demolished buildings) were simulated in Toulouse. The out-of-date databases were converted to binary image files (building vs. no building) having the same GSD as the input data. These binary building masks were distributed to the participants along with the CIR orthophotos and the DSMs.

2.2 Evaluation Procedure

Each group participating in the test was asked to deliver a change map in which each building is labelled either as *unchanged*, *demolished* or *new*. However, both the representation of the results of change detection and the output formats varied considerably between the individual algorithms. In addition, the definitions of the classes that are discerned in the change detection algorithms are not identical. Whereas the algorithm by Champion (2007) exactly matches the test requirements, this is not the case for the other two algorithms used in this study. In these two cases it was thus decided to use a building label image representing the updated building map for the evaluation. The evaluation consists of a comparison of the outcomes of each algorithm to ground truth (i.e. the initial reference database). Two quality measures are computed for the evaluation: the *completeness*, i.e. the percentage of the actual changes that are detected by an algorithm, and the *correctness*, i.e. the percentage of the changes detected by an algorithm that correspond to real changes (Heipke et al., 1997):

$$Completeness = \frac{TP}{TP + FN} \in [0,1]$$
$$Correctness = \frac{TP}{TP + FP} \in [0,1] \quad (1)$$

In Equation 1, *TP*, *FP*, and *FN* are the numbers of true positives, false positives, and false negatives, respectively. They refer to changes in the change map compared to actual changes in the reference. Thus, a *TP* is an entity reported as *changed* (*demolished* or *new*) that is actually changed in the reference. A *FP* is an entity reported as *changed* by an algorithm that has not *changed* in the reference. A *FN* is an entity that was reported as *unchanged* by an algorithm, but is *changed* in the reference. Finally, an entity reported as *unchanged* by an algorithm and also being *unchanged* in the reference is a true negative (*TN*). In this context, the entities to compare can be buildings, which results in per-building quality measures, or pixels in a rasterised version of the change map, which results in per-pixel quality measures. In the cases where it was decided to use a building label image representing the updated map for the evaluation, the rules for classifying an entity as a *TP*, a *FP*, a *FN*, or a *TN* had to be defined in a slightly different way. Any existing (i.e. *unchanged*) building in the reference database is considered a *TN* if a predefined percentage (T_h) of its area is covered with buildings in the new label image. Otherwise, it is considered a *FP*, because it does not have a substantial correspondence in the new label image, which thus indicates a change. A *demolished* building in the reference database is considered a *TP* if the percentage of its area covered by any building in the new label image is smaller than T_h. Otherwise, it is considered to be a *FN*, because the fact that it corresponds to buildings in the new label image indicates that the change detection algorithm has not found this building to have been demolished. A *new* building in the reference database is considered a *TP* if the cover percentage is greater than T_h. Otherwise, it is considered a *FN*. The remaining large areas in the new label image that do not match any of the previous cases correspond to objects wrongly alerted as *new* by the algorithm and thus constitute *FP*s.

3. CHANGE DETECTION APPROACHES

3.1 Method 1 - (Matikainen et al., 2007)

The building detection method of the Finnish Geodetic Institute (FGI) was originally developed to use laser scanning data as primary data. In this study, it is directly applied to input correlation DSM and orthophotos. The method includes the following stages:

1. Pre-classification of DSM height points to separate ground points from above-ground points, using (Terrasolid, 2008).
2. The region-based segmentation of the DSM into homogeneous regions and calculation of various attributes for each segment, using (Definiens, 2008)
3. The classification of the segments into ground and above-ground classes by using the pre-classification.
4. The definition of training segments for buildings and trees on the basis of training data sets.
5. The construction of a classification tree by using the attributes of the training segments (Breiman et al., 1984).
6. The classification of above-ground segments into buildings and trees on the basis of their attributes and the classification tree.
7. A post-processing to correct small, misclassified areas by investigating the size and neighbourhood of the areas.

The output of the method also consists of a building label image representing the new state of the database, which is used for evaluation in this study.

3.2 Method 2 - (Rottensteiner, 2007)

The input data of this method consist of a DSM obtained by LIDAR or stereo-matching techniques. A geocoded NDVI image, the initial building data base, and a Digital Terrain Model (DTM) can optionally be used. If no DTM is available, it is derived from the DSM by hierarchic morphologic filtering. If the initial database is available, it can be used to introduce a bias that favours a classification consistent with the initial data base, because in most scenes only a small percentage of buildings will actually have changed. The workflow of the method consists of three stages. First, a Dempster-Shafer fusion process is carried out on a per-pixel basis and results in a classification of the input data into one of four predefined classes: *buildings*, *trees*, *grass* land, and *bare soil*. Connected components of building pixels are grouped to constitute initial building regions. A second Dempster-Shafer fusion process is then carried out on a per-region basis to eliminate regions corresponding to trees. The third stage of the work flow is the actual change detection process, in which the detected buildings are compared to the existing map. A very detailed change map is generated in this process. The output of the method consists of a building label image representing the new state of the data base and in change maps describing the change status both on a per-pixel and a per-building level (Refer to (Rottensteiner, 2007) for more details). Since the definitions of the classes in the change map do not match those required in Section 2.2, the building label image is used for evaluation in this study.

3.3 Method 3 - (Champion, 2007)

The input data of the method are a DSM, a vegetation mask, computed from CIR orthophotos and NDVI index, and a DTM, automatically derived from the DSM using the algorithm described in (Champion and Boldo, 2006). The workflow consists of 2 stages: in a first step, geometric primitives, extracted from the DSM (2D contours i.e. height discontinuities) or from multiple images (3D segments, computed with (Taillandier and Deriche, 2002)), are collected for each building and matched with primitives derived from the existing vector map. A final decision about acceptance or rejection is then achieved per building. In the second step, the DTM is combined with the DSM to process an above-ground mask. This mask is morphologically compared to the initial building mask (derived from the vector database) and the vegetation mask and new buildings are extracted. The output of the method consists of a change map, in which each building is labelled as *unchanged*, *demolished* or *new*.

4. RESULTS AND DISCUSSION

The evaluation outputs are summarized in Table 1. The completeness and correctness are given for each test area and for each approach, both on a per-building basis and on a per-pixel basis. Values in bold indicates for which methods the best results are achieved. In an optimal system, completeness and correctness are equal to 1: in that case, there is no *FN* (no under-detection) and no *FP* (no overdetection). To be of practical interest, i.e. to consider the system effective and operational, previous works on change detection (Steinnocher and Kressler, 2006), (Mayer et al., 2006) expect a completeness rate close to 1 (typically 0.85) and a high correctness rate (typically 0.7). These recommendations are true for completeness (the new map must be really *new*) but must be modulated for correctness, with respect to the type of change. In our opinion, the effectiveness of a system is mostly related to the amount of work saved for a human operator. That also corresponds to the number of *unchanged* buildings that are correctly detected, because these buildings need no longer be inspected. As a consequence, the correctness rate has to be high during the verification of the database (i.e. for *demolished* buildings). By contrast, a low correctness rate for new buildings is less problematic: without the support of automatic techniques, the entire scene has to be examined by a human operator and therefore, a system that delivers a set of potential new buildings is effective if the true changes are contained in the set and if the number of *FP* s is not overwhelmingly large.

4.1 Marseille Test Area

4.1.1 (Matikainen et al., 2007): The evaluation of this method is illustrated in Fig. 1-a. The method best operates in term of completeness (0.98). Only two changes are missed by the algorithm and are related to errors in the initial "ground"/"above-ground" classification. Most false alarms are caused by one of two problems, namely the uncertainty of the classification in shadow areas (e.g. Fig. 2-a) and errors in the DSM between buildings that cause a misclassification of street areas as *new* buildings (e.g. Fig. 2-b).

4.1.2 (Rottensteiner, 2007): The evaluation of this method is illustrated in Fig. 1-b. Overall, the changes are detected correctly. Compared to (Matikainen et al., 2007), there are only three additional *FN*s. Five new buildings are missed by the algorithm (Fig. 2-c), which is caused by errors that occur in the DTM, by complicated topographic features (cliffs). In presence of such features, the DTM, derived from the DSM by hierarchic morphological opening, is less accurate, which predictably limits the extraction of new buildings that is partly based on the difference between the DSM and DTM. Quantisation effects in the DSM (the numerical resolution of height values is restricted to 20 cm) prevented the use of surface roughness as an input parameter for the Dempster-Shafer fusion process, which might have helped to overcome such problems. However, the correctness of the system is acceptable, which implies a limited number of *FP*s. Compared to (Matikainen et al., 2007) and (Champion, 2007), no *FP*s are generated during the detection of new buildings (e.g. Fig. 2-d). *FP*s are mostly caused by small buildings, located in inner yards and in shadow areas: the complexity of the urban scene and the relatively poor quality of the DSM in shadow areas clearly and significantly deteriorate the change detection correctness here.

Method	Completeness		Correctness	
	per building	per pixel	per building	per pixel
Marseille Test Area				
Matikainen	**0.98**	**0.99**	0.54	0.79
Rottensteiner	0.95	0.98	**0.58**	**0.83**
Champion	0.94	0.94	0.45	0.75
Toulouse Test Area				
Rottensteiner	**0.85**	0.90	0.49	0.53
Champion	0.80	**0.95**	**0.55**	**0.85**

Table 1. Completeness and Correctness achieved by the three algorithms for both data sets.

4.1.3 (Champion, 2007): The evaluation of this method is illustrated in Fig. 1-c. Five *FN*s appear with the method. Two of them (in the north-western corner of the scene - Fig. 2-e) occur during the first stage of the algorithm. They are caused by extracted primitives that are wrongly used to validate demolished buildings. Remaining *FN*s are related to inaccuracies in the processed DTM and occur where topography is particularly difficult. Here again, the overestimation of the terrain height in the DTM prevents the complete extraction of new buildings. Regarding *FP*s, those that occur in the first stage of the algorithm are related to the complexity of the scene: the extraction of pertinent primitives for inner and lower buildings is more difficult and makes the verification more uncertain. Most *FP*s that occur in the second stage are related to building-like structures (walls that are wrongly considered to be new buildings), errors in the vegetation mask (omitted trees) and the same inaccuracies in the correlation DSM (large overestimated areas in narrow streets) that caused errors in the classification of (Matikainen et al., 2007) (Fig. 2-f).

4.1.4 Remark concerning the aerial context: In the context of aerial imagery, there is not a visible predominance of an approach over another one. The three of them perform well in terms of completeness. The differences almost entirely appear in terms of correctness: classification-based methods, i.e. (Matikainen et al., 2007) and (Rottensteiner, 2007), seem to be more efficient than (Champion, 2007) and deliver fewer *FP*s. The per-building correctness rates obtained with the three approaches (0.54, 0.58 and 0.45, respectively) are relatively low, and none of the approaches appears to be a viable basis for a practical solution. However, this consideration must be modulated by the good correctness values (of 0.79, 0.83 and

0.75), that are computed on a per-pixel basis. Since the per-pixel values are directly linked to the area that has been classified correctly or not, these values clearly highlight that the change detection is mostly uncertain for small buildings.

(a) Matikainen

(b) Rottensteiner

(c) Champion

Figure 1. Change Detection Evaluation in Marseille Test Area. In green, *TP* cases; in red, *FN* cases; in orange, *FP* cases; in blue, *TN* cases.

4.2 Toulouse Test Area

4.2.1 (Rottensteiner, 2007): The evaluation of this method is illustrated in Fig. 3-a. Again, major changes are well detected. However, changes affecting small buildings are missed, which results in a high number of *FN*s for small buildings (Fig. 4-a). There are also many *FP*s that are mostly caused by inaccuracies in the DSM. Shadow areas are also systematically overestimated in the DSM, which generates *FP*s during the detection of new buildings. Two very large areas of false alarms appear in the eastern part of the scene (a sports field - Fig. 4-b) and in the north-eastern corner (a parking lot) and are related to classical problems of stereo-matching algorithms, namely repeating patterns (demarcation lines in the sports field, rows of cars on the parking lot) and poor contrast. This entails height variations larger than 4 m in the surface model in areas that are essentially horizontal.

4.2.2 (Champion, 2007): The evaluation of this method is illustrated in Fig. 3-b. Overall, the results are similar to those computed by (Rottensteiner, 2007) and particularly poor for small buildings (Fig. 4-c). The difficulty to extract pertinent primitives for small buildings entails 8 *FN* cases during the detection of new buildings and many *FP*s during the verification of the database (cf. Fig. 4-d for an example).

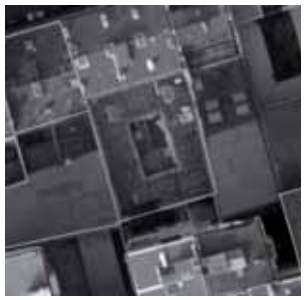

(a) Matikainen: *FP* case

(b) Matikainen: *FP* case

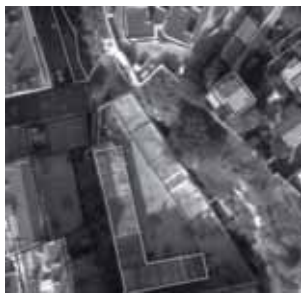

(c) Rottensteiner: *FN* case

(d) Rottensteiner: no *FP* case

(e) Champion: FN cases

(f) Champion: *FP* cases

Figure 2. Evaluation details in Marseille. The same colour code as Fig. 1 is used.

4.2.3 Remark concerning the satellite context: The change detection is clearly limited by the resolution of input satellite data in relation to the size of changes to be detected. The completeness and correctness values are (0.85, 0.50) and (0.80, 0.55) for the two methods, respectively. Such values clearly reflect that detecting 2D building changes in a satellite context is too hard a challenge for the current state-of-the-art. This observation is corroborated by the fact that the ground classification performed in (Matikainen et al., 2007) does not give acceptable results for Toulouse when carried out in a fully automatic way. The results may appear to be disappointing. However, the completeness of the two systems both turn out to be very close to the values found in (Mayer et al., 2006) and expected for a system to be operational. Regarding the correctness, the low rate is mostly related to a high number of *FP*s during the detection of new buildings, especially for (Rottensteiner, 2007). As mentioned at the beginning of section 4, it is less problematic as the corresponding *FP* objects would inescapably be checked by a human without the support of automatic techniques. The results that are achieved here clearly demonstrate that it is worth while to carry out research in the satellite context, especially towards the reduction of *FP*s.

(a) Rottensteiner

(b) Champion

Figure 3. Change Detection Evaluation in Toulouse Test Area (with the same colour code as in Fig. 1).

4.3 Factors affecting the accuracy

In this section, we will try to sum up some preliminary results based on the experiences of this EuroSDR project. We will focus the analysis on the impact of input data on the change detection performance on the one hand, on the features of the method on the other hand, more specifically on the type (geometric/radiometric) of primitives to use.

4.3.1 Impact of the DSM: The limiting factor of change detection appears to be the quality of the DSM. The erroneous height values present in the initial DSM between some buildings (i.e. nearby step edges) and the quantization effect observed in both areas and that prevents to exploit surface roughness in the change detection process clearly affect the quality of output change maps. It should be possible to overcome such drawbacks by using LIDAR data, as indicated by the completeness and correctness computed in (Matikainen et al., 2004) and (Rottensteiner, 2007). The results achieved for the EuroSDR test dataset based on LIDAR data have not been evaluated yet but should confirm those results. Improving the performance of an image-based change detection system implies a higher robustness of stereo-matching techniques with respect to shadow areas and a higher preservation of object details, especially step edges.

(a) Rottensteiner: *FN* case

(b) Rottensteiner: *FP* case

(c) Champion: *FN* cases

(d) Champion: *FP* cases

Figure 4. Evaluation details in Toulouse.

4.3.2 Impact of the DTM: As previously highlighted, the extraction of buildings and consequently the performance of the change detection process are the better the more accurate the DTM is. In this study, the morphology-based method used in (Rottensteiner, 2007) and the surface-based method (Champion and Boldo, 2006) both fail in the presence of topographic discontinuities (cliffs). Refined approaches should be considered in the future to better model such terrain features. It must also be noted that in order to keep the process fully automatic, manual corrections were not employed for this study. Manual corrections of difficult points are a normal practice in operational processing and could for instance be used to correct the initial classification into terrain vs. off-terrain points required for DTM generation. This would give a better basis for the later classification stages and improve the final change map.

4.3.3 Impact of the vegetation mask: As previously mentioned, some confusion occurs in this test between trees and buildings. One solution may consist in using more robust criteria to extract vegetation. Classification-based methods, similar to (Trias-Sanz et al., to appear) could also be preferred to NDVI-based methods. Another hint consists in introducing an ontology for objects of interest in the scene (at least for buildings and trees): simple rules such as, “a tree cannot be entirely contained in a building”, could easily limit the number

of errors, such as the *FN* case produced by (Champion, 2007) in the north-western part of Marseille test (Fig. 2-e).

4.3.4 Impact of the primitives used in the system: In the three approaches, geometric primitives are preferred to radiometric features. In a LIDAR context, such an approach is valid, as the geometry is known to be well described. The image context is more difficult: the 2D contours, extracted in the DSM with (Champion, 2007) are less accurate and the surface roughness computed in (Rottensteiner, 2007) is meaningless. Finding alternative and robust geometric primitives, such as 3D segments (Taillandier and Deriche, 2002), is therefore of high interest. Another solution consists in using radiometric primitives. The use of colour information could also limit the number of *FN*s, such as those produced by (Champion, 2007) in Marseille (Figure 2-f) and could limit the large *FP* areas that occur in Toulouse with (Rottensteiner, 2007). The performance of a change detection system also seems to be closely related to the right combination of radiometric and geometric features.

5. CONCLUSION

Three change detection methods have been tested and compared in this study. The scope has been limited to the imagery context, although two of the three methods, i.e. (Matikainen et al., 2007) and (Rottensteiner, 2007) were not originally designed to deal with imagery. The results presented in this paper demonstrate their high transferability on the one hand and the potential of imagery as an alternative to LIDAR data to detect changes in a 2D building database on the other hand. The results are particularly good, especially in terms of completeness and show the significance to use such interactive techniques in an updating process. The remaining work to be done concerns the reduction of false alarms. The study clearly shows that geometric primitives (height, roughness. . .) that are known to be pertinent in a LIDAR context are less accurate when imagery is used. The improvement of DSM quality is a key point, but other solutions (extraction of new geometric primitives, better modelling of the terrain, and integration of radiometric primitives) are interesting research directions, too. The main focus of the project now is on evaluating more thoroughly the performance of the system with respect to the update status of the building (*unchanged*, *demolished* or *new*) and its size on the one hand, on evaluating the results processed for an area that contains LIDAR data (Lyngby, Denmark) on the other hand. The preliminary visualization of the results on this test area shows a good behaviour of (Matikainen et al., 2007) and (Rottensteiner, 2007). Quantitative evaluation is still necessary to evaluate their performance and the transferability of (Champion, 2007) that is originally built to deal with aerial images. Finally, we plan to expand this test to other methods, namely those described in (Olsen and Knudsen, 2006) and (Katartzis and Sahli, 2008). Beyond scientific results, we hope that this project will be a good opportunity to create a network of interested people both in academia and in the private sector that can speed up the progress in the field of automated building change detection.

ACKNOWLEDGEMENTS

We are grateful to EuroSDR for giving us the opportunity to conduct this test and CNES for providing Pléiades imagery.

REFERENCES

Breiman, L., Friedman, J. H., Olshen, R. A., Stone, C. J., 1984. Classification and Regression Trees. The Wadsworth Statistics / Probability Series, Wadsworth, Inc., Belmont, California.

Champion, N., 2007. 2D building change detection from high resolution aerial images and correlation Digital Surface Models. In: Int'l Archives of the Photogrammetry, Remote Sensing and Spatial Information Sciences, Vol. XXXVI-3/W49A (on CD-ROM), pp. 197–202.

Champion, N., Boldo, D., 2006. A robust algorithm for estimating Digital Terrain Models from Digital Surface Models in dense urban areas. In: *Int'l Archives of the Photogrammetry, Remote Sensing and Spatial Information Sciences*, XXXVI-3, pp. 111–116.

Definiens, 2008. ttp://www.definiens.com/.

Heipke, C., Mayer, H., Wiedemann, C., Jamet, O., 1997. Automated reconstruction of topographic objects from aerial images using vectorized map information. In: *Int'l Archives of Photogrammetry and Remote Sensing*, XXXII, pp. 47–56.

Katartzis, A., Sahli, H., 2008. A stochastic framework for the identification of building rooftops using a single remote sensing image. *IEEE Transactions on Geoscience and Remote Sensing* 46, pp. 259–271.

Matikainen, L., Hyyppä, J., Kaartinen, H., 2004. Automatic detection of changes from laser scanner and aerial image data for updating building maps. In: *Int'l Archives of the Photogrammetry, Remote Sensing and Spatial Information Sciences*, XXXV-B2, pp. 434–439.

Matikainen, L., Kaartinen, K., Hyyppä, J., 2007. Classification tree based building detection from laser scanner and aerial image data. In: *Int'l Archives of the Photogrammetry, Remote Sensing and Spatial Information Sciences*, XXXVI, pp. 280–287.

Mayer, H., Hinz, S., Bacher, U., Baltsavias, E., 2006. A test of automatic road extraction approaches. In: *Int'l Archives of the Photogrammetry, Remote Sensing and Spatial Information Sciences*, XXXVI-3, pp. 209–214.

Olsen, B., Knudsen, T., 2006. Building change detection: a case study comparing results from analog and digital imagery. Technical report, KMS (National Survey and Cadastre) and Danish National Space Centre.

Pierrot-Deseilligny, M., Paparoditis, N., 2006. An optimization-based surface reconstruction from Spot5- HRS stereo imagery. In: *Int'l Archives of the Photogrammetry, Remote Sensing and Spatial Information Sciences*,XXXVI-1/W41, pp. 73–77.

Rottensteiner, F., 2007. Building change detection from Digital Surface Models and multi-spectral images. In: *Int'l Archives of the Photogrammetry, Remote Sensing and Spatial Information Sciences*, XXXVI-3/W49B (on CD-ROM).

Steinnocher, K., Kressler, F., 2006. Change detection. Technical report, EuroSDR Report.

Taillandier, F., Deriche, R., 2002. A reconstruction of 3D linear primitives from multiple views for urban areas modelisation. In: *Int'l Archives of Photogrammetry and Remote Sensing*, XXXIV-3B, pp. 267–272.

Terrasolid, 2008. http://www.terrasolid.fi/.

Trias-Sanz, R., Stamon, G., Louchet, J., To Appear. Using colour, texture, and hierarchial segmentation for high-resolution remote sensing. *ISPRS Journal of Photogrammetry and Remote Sensing*.

A TEST OF AUTOMATIC BUILDING CHANGE DETECTION APPROACHES

Nicolas Champion[a], Franz Rottensteiner[b], Leena Matikainen[c], Xinlian Liang[c], Juha Hyyppä[c] and Brian P. Olsen[d]

[a] IGN, MATIS – Saint-Mandé, France – Nicolas.Champion@ign.fr
[b] FGI, Dept. of Remote Sensing and Photogrammetry – Masala, Finland –
(leena.matikainen, xinlian.liang, juha.hyyppa)@fgi.fi
[c] Institute of Photogrammetry and GeoInformation,
Leibniz Universität Hannover – Germany – rottensteiner@ipi.uni-hannover.de
[d] National Survey and Cadastre (KMS) – Copenhagen, Denmark – bpo@kms.dk

Commission III, WG III/4

KEY WORDS: Change Detection, Building, 2D Vector Databases, Algorithms Comparison, Quality Assessment

ABSTRACT:

The update of databases – in particular 2D building databases – has become a topical issue, especially in the developed countries where such databases have been completed during the last decade. The main issue here concerns the long and costly change detection step, which might be automated by using recently acquired sensor data. The current deficits in automation and the lack of expertise in the domain have driven the EuroSDR to launch a test comparing different change detection approaches, representative of the current state-of-the-art. The main goal of this paper is to present the testbed of this comparison test and the results that have been obtained for two different contexts (imagery and LIDAR). In addition, we give the overall findings that emerged from our experiences and some promising directions to follow for building an optimal operative system in the future.

1. INTRODUCTION

The production of 2D topographic databases has been completed in many industrialised countries. Presently, most efforts in the National Mapping and Cadastral Agencies (NMCAs) are devoted to the update of such databases. As the update process is generally carried out manually by visual inspection of orthophotos, it is time-consuming and expensive. As a consequence, its automation is of high practical interest for the NMCAs. The update procedure can be split into two steps: *change detection*, in which the outdated database is compared to recently collected sensor data in order to detect changes, and *vectorization*, i.e. the digitization of the correct geometry of the changed objects. Given the state-of-the-art in automatic object detection (Mayer, 2008), only the automation of the change detection step seems to be possible at this time. The key idea is to focus the operator's attention on the areas that may have changed. Work is saved because the operator needs not inspect areas classified as *unchanged* by the automatic procedure.

The current deficits in automation and the lack of expertise within the NMCAs have driven the EuroSDR (European Spatial Data Research - http://www.eurosdr.net) to lauch a project in the topic. It also aims at evaluating the feasibility of semi-automatically detecting changes in a 2D building vector database from optical imagery or LIDAR. Three subtopics are investigated in detail, firstly the impact of methodology; secondly, the impact of the type and spatial resolution of input data; lastly, the impact of the complexity of the scene in terms of interfering objects such as roads. The methodology consists in comparing four different algorithms representative for the current state-of-the-art in the field of change detection. First results, achieved for the cases where only aerial and satellite images are used, were presented in (Champion et al., 2008). The results obtained there showed the limitations of change detection methods, especially in relation to the quality of input data. The main goal of this paper is to present the final results of the project, including a LIDAR dataset, and to give a detailed evaluation of the outcomes delivered by the approaches compared here.

After describing the datasets and the evaluation procedure (Section 2), the methods compared in the test are concisely introduced (Section 3). In Section 4, a thorough evaluation is carried out, including an analysis of the performance of change detection with respect to the update status of the building and its size. The weak and strong points, regarding the datasets and methodologies, are then identified and used to give overall findings and recommendations for building an optimal operative system for change detection in the future.

2. INPUT DATA AND TEST SET-UP

Three test areas are used for the comparison: Marseille (France), Toulouse (France), and Lyngby (Denmark). The area covered by the test sites is 0.9 x 0.4 km^2 in Marseille, 1.1 x 1.1 km^2 in Toulouse, and 2.0 x 2.0 km^2 in Lingby. The test areas differ considerably regarding topography, land use, urban configuration and roofing material. The terrain is hilly in Marseille and Toulouse and relatively flat in Lyngby. Marseille features a densely built-up area consisting of small buildings of variable height, all connected to each other and mostly covered with red tile. Toulouse and Lyngby feature a suburban area, mostly composed of detached buildings and characterised by a large variety of roofing materials such as slate, gravel, or concrete. Colour Infrared (CIR) orthophotos and Digital Surface Model (DSMs) are available for all test areas. In Marseille and Toulouse (imagery context), an image matching algorithm (Pierrot-Deseilligny and Paparoditis, 2006) was used to derive the DSM from input images. In Marseille, these images are multiple aerial images having a forward and side overlap of 60%. The Ground Sample Distance (GSD) of all

input data is 0.2 m. In Toulouse, these images are Pléiades tri-stereoscopic satellite images. The GSD of all input data is 0.5 m. Lastly, the DSM used in Lyngby was derived from first pulse LIDAR data, and the digital orthophoto was generated from a scanned aerial image, both with a GSD of 1 m. For the three test areas, up-to-date vector databases representing the 2D outlines of buildings were available. They served as a reference in the test. In order to achieve an objective evaluation, the outdated databases were simulated by manually adding or removing buildings Thus, 107 changes (out of 1300 buildings in the scene) were simulated in Marseille (89 *new* and 18 *demolished* buildings); 40 (out of 200) in Toulouse (23 *new*, 17 *demolished*) and 50 (out of 500) in Lyngby (29 *new*, 21 *demolished*). The outdated databases were converted to binary building masks having the same GSD as the input data and then distributed to the participants along with input data.

Each group participating in the test was asked to deliver a change map in which each building of the vector database is labelled either as *unchanged*, *demolished* or *new*. Because the methods have been developed in different contexts, their designs noticeably differ, for instance regarding the definitions of the classes considered in the final change map – e.g. four classes for (Champion, 2007) and six classes for (Rottensteiner, 2008) – and the format of the input data – e.g. vector for (Champion, 2007) and raster for (Matikainen et al., 2007). As a work-around, it was decided to use the building label image representing the updated version of the building map (cf. Section 3) for the evaluation of those methods that do not deliver the required change map in the way described above. Only the method by (Champion, 2007) delivered such a change map, which was also directly used in the evaluation.

In order to evaluate the results achieved by the four algorithms, they are compared to the reference database, and the *completeness* and the *correctness* of the results (Heipke et al., 1997) are derived as quality measures:

$$Completeness = \frac{TP}{TP + FN}$$
$$Correctness = \frac{TP}{TP + FP} \quad (1)$$

In Equation 1, *TP*, *FP*, and *FN* are the numbers of True Positives, False Positives, and False Negatives, respectively. They refer to the update status of the vector objects in the automatically-generated change map, compared to their real update status given by the reference. In the case where the final change map is directly used for the evaluation, i.e. with (Champion, 2007), a *TP* is an object of the database reported as *changed* (*demolished* or *new*) that is actually changed in the reference. A *FP* is an object reported as *changed* by the algorithm that has not *changed* in the reference. A *FN* is an object that was reported as *unchanged* by the algorithm, but is *changed* in the reference. In the three other cases, where a building label image representing the updated map is used for the evaluation, the rules for defining an entity as a *TP*, a *FP*, a *FN* had to be adapted. In these cases, any *unchanged* building in the reference database is considered a *TN* if a predefined percentage (T_h) of its area is covered with buildings in the *new* label image. Otherwise, it is considered a *FP*, because the absence of any correspondence in the *new* label image indicates a change. A *demolished* building in the reference database is considered a *TP* if the percentage of its area covered by any building in the *new* label image is smaller than T_h. Otherwise, it is considered to be a *FN*, because the fact that it corresponds to buildings in the *new* label image indicates that the change has remained undetected. A *new* building in the reference is considered a *TP* if the cover percentage is greater than T_h. Otherwise, it is considered a *FN*. The remaining areas in the *new* label image that do not match any of the previous cases correspond to objects wrongly alerted as *new* by the algorithm and thus constitute *FP*s.

The quality measures are presented in the evaluation on a per-building basis (rather than on a per-pixel basis), as the effectiveness of a change detection approach is limited by the number of changed buildings that is missed or over-detected and not by the area covered by these buildings. As explained in the Section 4, these quality measures are also computed separately for each change class.

3. CHANGE DETECTION APPROACHES

The four methods tested in this study are concisely presented, ordered alphabetically according to the corresponding author.

Champion, 2007: The input of the method is given by a DSM, CIR orthophotos and the outdated vector database. Optionally, the original multiple images can also be used. The outcome of the method is a modified version of the input vector database, in which *demolished* and *unchanged* buildings are labelled and vector objects assumed to be *new* are created. The method starts with the *verification of the database*, where geometric primitives extracted from the DSM (2D contours, i.e. height discontinuities) and, optionally, from multiple images (3D segments), are collected for each object of the existing database and matched with primitives derived from it. A similarity score is then computed for each object and used to achieve a final decision about acceptance (*unchanged*) and rejection (*changed* or *demolished*). The second processing stage, i.e. the *detection of new buildings,* is based on a Digital Terrain Model (DTM) automatically derived from the DSM (Champion and Boldo, 2006), a normalised DSM (nDSM), defined as the difference between the DSM and the DTM, and an above-ground mask, processed from the nDSM by thresholding. Appropriate morphological tools are then used to compare this latter mask to the initial building mask derived from the vector database and a vegetation mask computed from CIR orthophotos and an image corresponding to the Normalised Difference Vegetation Index (NDVI), which results in the extraction of *new* buildings.

Matikainen et al., 2007: The building detection method of the Finnish Geodetic Institute (FGI) was originally developed to use laser scanning data as primary data. In this study, it is directly applied to the input DSM and CIR orthophotos. A raster version of the database (for part of the study area) is used for training. The method includes three main steps. It starts with segmentation and a two-steps classification of input data into *ground* and *above-ground*, based on a point then object analysis, using the Terrasolid[1] and Definiens[2] software systems. This is followed by the definition of training segments for buildings and trees and the classification of the *above-ground* segments into *buildings* and *trees*. This classification is based on predefined attributes and a classification tree (Breiman et al., 1984). A large number of attributes can be used, e.g. mean values, standard deviations, texture and shape of the segments. The method automatically selects the most useful ones for

[1] http://www.terrasolid.fi/. Last visited: 03-31-09.
[2] http://www.definiens.com/. Last visited: 03-31-09.

classification. In the Marseille area, the criteria selected in the tree included only NDVI. In the Lyngby area, NDVI and a shape attribute were selected. The third stage consists of a post-processing step that analyses the size and neighborhood of building segments and corrects their class accordingly. The result of building detection is a building label image which is used here for the comparison test.

Olsen and Knudsen, 2005: The input of the method is a DSM, CIR orthophotos and a raster version of the outdated database. The method starts with the generation of a DTM, estimated from the DSM through appropriate morphological procedures, a nDSM and an Object Above Terrain (OAT) mask. This is followed by a two-step classification that aims at distinguishing *building* from *no building* objects. This classification is based on criteria that best characterise buildings (especially in terms of size and form) and results in the building label image that is used for the evaluation in this study. The last stage is the actual change detection step, in which the classification outcomes is compared to the initial database in order to extract a preliminary set of potential changes (on a per-pixel basis) that is then post-processed in order to keep only the objects that are assumed to have changed.

Rottensteiner, 2008: This method requires a DSM as the minimum input. Additionally it can use an NDVI image, height differences between the first and the last laser pulse, and the existing database, available either in raster or vector format. The workflow of the method starts with the generation of a coarse DTM by hierarchical morphological filtering, which is used to obtain a nDSM. Along with the other input data, the nDSM is used in a Dempster-Shafer fusion process carried out on a per-pixel basis to distinguish four object classes: *buildings*, *trees*, *grass* land, and *bare soil*. Connected components of *building* pixels are then grouped to constitute initial building regions and a second Dempster-Shafer fusion process is performed on a per-region basis to eliminate remaining trees. Finally, there is the actual change detection step, in which the detected buildings are compared to the existing map, which produces a change map that describes the change status of buildings, both on a per-pixel and a per-building level. Additionally, a label image corresponding to the *new* state of the data base is generated. In spite of the thematic accuracy of the change map produced by this method, it was decided to use this building label image for the evaluation in this test.

4. EVALUATION AND DISCUSSION

In our opinion, the effectiveness of a change detection system is related to its capacity to guide the operator's attention only to objects that have changed so that *unchanged* buildings do not need to be investigated unnecessarily. These considerations result in the evaluation criteria used in this paper to analyze the change detection performance. On the one hand, to support the generation of a map that is really up-to-date, i.e. to be effective qualitatively, the *completeness* of the system for buildings classified as *demolished* and the *correctness* for *unchanged* buildings are required to be high. The *completeness* of *new* buildings also has to be high if the operator is assumed not to look for any *new* building except for those which are suggested by the system. (Note that this also holds true for *modified* buildings, a case not considered in this study because the simulated changes only consisted in *new* and *demolished* buildings). On the other hand, to reduce the amount of manual work required by the operator i.e. to be effective economically, the *correctness* of the changes highlighted by the system and the *completeness* of *unchanged* buildings must be high. However, if a low *completeness* of *unchanged* buildings implies that many buildings are checked uselessly, this is not necessarily critical for the application itself, because the updated database is still correct. Moreover, the economical efficiency that could then appear to be low has to be put into perspective according to the size of the building database to update. For instance, if a change detection system reports 60% of a *national* database as changed, we cannot necessarily conclude about the inefficiency of this system because it still means that 40% of the buildings need not be checked, which amounts to millions of buildings.

4.1 Overall Analysis

Figure 1 presents the evaluation of the results achieved by the methods that processed the Lingby test area (LIDAR context). Table 1 gives the per-building completeness and correctness, obtained for each test area and each approach. Note that the T_h parameter (Cf. Section 2.) is set in this study to 0.2 for the Marseille and Lyngby test areas and 0.26 for the Toulouse test area. The values in bold indicate for which methods the best results are achieved. The completeness of detected changes is high for all the methods, especially in the aerial (Marseille) and LIDAR (Lyngby) contexts. By contrast, the correctness observed in our experiments is relatively poor, which indicates that there are many *FP* changes reported by the systems. In this respect, only the results obtained in the Lyngby test area with (Rottensteiner, 2008) seem to achieve a relatively acceptable standard.

Approach	Completeness	Correctness
Marseille (Imagery – Aerial context)		
(Champion, 2007)	94.1%	45.1%
(Matikainen et al., 2007)	**98.8%**	54.3%
(Rottensteiner, 2008)	95.1%	**59.1%**
Toulouse (Imagery – Satellite context)		
(Champion, 2007)	78.9%	**54.5**%
(Rottensteiner, 2008)	**84.2%**	47.1%
Lyngby (LIDAR context)		
(Matikainen et al., 2007)	94.3%	48.8%
(Olsen and Knudsen, 2005)	**95.7%**	53.6%
(Rottensteiner, 2008)	91.4%	**76.1%**

Table 1. Completeness and Correctness achieved by the four algorithms for the three datasets.

To take the analysis further, we also determined the quality measures separately for *unchanged*, *demolished* and *new* buildings. They are presented in Tables 2 (Marseille), 3 (Lyngby) and 4 (Toulouse), respectively. Focusing on the Marseille test area first, it can be seen in Table 2 that all algorithms are effective in detecting the actual changes. Thus, (Matikainen et al., 2007) and (Rottensteiner, 2008) achieve a completeness of 100% for *demolished* buildings. The correctness for *unchanged* buildings is also 100%. The few (11.1%) *demolished* buildings missed by (Champion, 2007) are caused by extracted primitives that are erroneously used in the *verification* procedure. All three methods also feature a high completeness for *new* buildings. Here, (Matikainen et al., 2007) performs best, with only 2.4% of the *new* buildings missed. The main limitation of this context appears to be the poor correctness rate achieved for *demolished* buildings, which ranges from 18.4% with (Champion, 2007) to 23.7% with


(a) Matikainen et al. (2007)


(b) Rottensteiner (2008)


(c) Olsen and Knudsen (2005)

Figure 1. Evaluation of change detection in Lyngby, for (a), (b) and (c) Green: TP; red: FN; orange: FP; blue: TN.

	Unchanged	*Demolished*	*New*
(Champion, 2007)			
Completeness [%]	93.5	88.9	95.2
Correctness [%]	99.8	18.4	63.5
(Matikainen et al., 2007)			
Completeness [%]	94.7	100	97.6
Correctness [%]	100	23.7	75.6
(Rottensteiner, 2008)			
Completeness [%]	94.1	100	94.0
Correctness [%]	100	22.0	96.3

Table 2. Completeness and correctness for the Marseille test area, depending on the update status.

	Unchanged	*Demolished*	*New*
(Matikainen et al., 2007)			
Completeness [%]	81.7	100	91.8
Correctness [%]	100	22.6	100
(Olsen and Knudsen, 2005)			
Completeness [%]	87.8	100	93.9
Correctness [%]	100	30.4	82.1
(Rottensteiner, 2008)			
Completeness [%]	95.9	100	87.8
Correctness [%]	100	56.8	91.8

Table 3. Completeness and correctness for the Lyngby test area, depending on the update status.

	Unchanged	*Demolished*	*New*
(Champion, 2007)			
Completeness [%]	82.8	100	75.0
Correctness [%]	100	42.9	65.2
(Rottensteiner, 2008)			
Completeness [%]	80.2	86.7	82.6
Correctness [%]	97.9	36.1	59.4

Table 4. Completeness and correctness for the Toulouse test area, depending on the update status.

(Matikainen et al., 2007). The situation is a bit better for *new* buildings, with a correctness rate larger than 63% for all the methods and even rising to 96.8% with (Rottensteiner, 2008). In spite of such limitations, all the methods presented here are very efficient in classifying *unchanged* buildings, for which the completeness rates are higher than 93%, which indicates that a considerable amount of manual work is saved and also demonstrates the economical efficiency of these approaches, in the aerial context.

Analyzing Table 3 leads to similar conclusions for the LIDAR context. The correctness rate for the reported *demolished* buildings are again poor and only (Rottensteiner, 2008) achieves less than 50% false positives. However, the methods are very effective in detecting *demolished* buildings and achieve a completeness rate of 100% for this class. Compared to the outcomes obtained in Marseille, the main difference concerns the *new* buildings, which appear to be more difficult to extract. Thus, between 6.1% (Olsen and Knudsen, 2006) and 12.2% (Rottensteiner, 2008) of the *new* buildings are missed. If these percentages of missed *new* buildings can be tolerated, our tests indicate that LIDAR offers a high economical effectiveness and thus may be a viable basis for a future application. If these error rates for *new* buildings are unacceptable, manual post-process is required to find the missed buildings, at the expense of a lower economical efficiency.

The situation is not quite as good with the satellite context (Table 4). The method by (Champion, 2007) is very effective in detecting *demolished* buildings (100%), but this is achieved at the expense of a low correctness rate (42.9%). The same analysis can be carried out with (Rottensteiner, 2008), but this method even misses quite a few *demolished* buildings. It has to be noted that, even though the completeness rates for *unchanged* buildings achieved by both methods are relatively low compared to those obtained in the Marseille and Lyngby test areas, they also indicate that even under challenging circumstances, 80% of *unchanged* buildings need not be investigated by an operator. The main limitation appears to be the detection of *new* buildings. Thus, as illustrated in Figures 3e and 3f, 17.4% and 25% of *new* buildings are missed with (Rottensteiner, 2008) and (Champion, 2007) respectively, which is clearly not sufficient to provide a full update of the database and requires a manual intervention in order to find the remaining *new* buildings.

In order to obtain deeper insights into the reasons for failure, in the subsequent sections we will focus our analysis on some factors that affect the change detection performance.

4.2 Impact of the Size of a Change

To analyse the performance of change detection as a function of the change size, we compute the completeness and correctness rates depending on this factor. For that purpose, *new* and *demolished* buildings are placed into bins representing classes of 20 m² in width. Note that the buildings from *all* the test areas for which results were submitted are combined in order to have

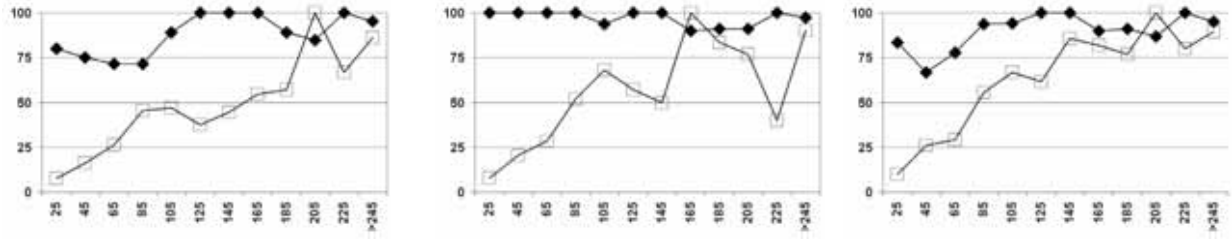

(a) Champion, 2007 (b) Matikainen et al., 2007 (c) Rottensteiner, 2008

Figure 2. Completeness (diamonds) and correctness (squares) of the detection results as a function of the building size [m²].

a significant number of changes for each bin. The graphs for (Champion, 2007) and (Rottensteiner, 2008) also contain the results from the Toulouse area. The completeness and correctness rates, computed independently for each bin, are presented in Figure 2 and demonstrate the close relation between the quality of change detection and the change size. This is true for the completeness with (Champion, 2007) and (Rottensteiner, 2008), but it is even more obvious for the correctness in all three graphs. Correctness is particularly poor for buildings smaller than 100 m². Attentive readers may also notice that a low correctness occurs with (Matikainen et al., 2007) and (champion, 2007) with the {225m²-245m²} building class: it is due to large ground areas in the Marseille test area, mistakenly classified as above-ground and wrongly alerted as *new* buildings. Looking at these graphs it becomes obvious that the two major problems observed in Section 4.1, namely the potentially critical rate of missed *new* buildings, which limits the qualitative effectiveness of change detection, and the poor correctness for *demolished* buildings are caused by the same underlying phenomenon i.e. the fact that small objects cannot be detected reliably by an automated procedure.

4.3 Impact of the Quality of the Input Data

Our experiments show that many *FP* cases are related to the quality of the input DSM. Thus, the *correlation* DSMs used in the imagery context contain a lot of erroneous height values, especially in shadow areas (where stereo-matching algorithms are known to worse perform) that are almost systematically alerted as *new* buildings, as depicted in Figures 3a, 3b, 3c, and 3d. These errors contribute to lower the correctness rate, especially for new buildings, which drops to 63.5% with (Champion, 2007) in Marseille. The high rate of 96.3% obtained here with (Rottensteiner, 2008) may be related to the use of the initial description of the database as a priori information for producing and improving the building label image. In Toulouse, *FP new* buildings were also related to DSM errors, caused by repeating patterns. Another problem concerns the quantisation effects i.e. the fact that the numerical resolution of height values in the *correlation* DSM is restricted to the GSD, which for instance prevents the use of surface roughness as an input parameter for the Dempster-Shafer fusion process in (Rottensteiner, 2008) and ultimately contributes to lower the correctness rate for *demolished* buildings.

Regarding the Lyngby test area, it was a problem that the original data were not available. Single points inside water areas were not eliminated from the data, but used in an interpolation process based on a triangulation of the LIDAR points, producing essentially meaningless data in these water areas that for example caused *FP new* cases with (Olsen and Knudsen, 2005). The other problem was that first pulse (rather than last pulse) data were provided, which caused *FP*s in areas with dense vegetation, e.g. along rivers with (Rottensteiner, 2008). Combined with a relatively low resolution (1 m), these problems contribute to lower the correctness of the systems.

4.4 Impact of Other Topographic Objects in the Scene

In our experiments, some confusion occurs between buildings and other above-ground objects, present in the scene and wrongly alerted as *new* buildings. Again, this contributes to lower the correctness achieved for *new* buildings. The methods deal with this problem, but currently they only focus on one class of above-ground objects that is to be separated from buildings, namely trees. In general, these trees are identified with indicators based on the NDVI and then eliminated, as shown in Section 3. Even though this strategy appears to be efficient, our experiments show that such confusions are not limited to vegetation but concern other objects, not considered in the approaches presented in this study. For instance, bridges or elevated roads are highlighted as *FP new* buildings in the Lyngby test area by (Rottensteiner, 2008) and (Olsen and Knudsen, 2005), as shown in Figures 3g and 3h. To limit the impact of these problems, two strategies could be considered in the future. The first one consists in developing more sophisticated methods that are capable of simultaneously extracting multiple object classes such as buildings, roads, and vegetation. Such methods would need to incorporate complex scene models that also consider the mutual interactions of the object classes in a scene. They could make use of recent developments in the field of Computer Vision that are related to the modelling context in image classification (Kumar and Hebert, 2006). The second strategy may use additional information on other objects, by incorporating e.g. an existing road database in the building change detection procedure.

Additional Remark: Beyond the statistical aspects, our experiments show that the errors generated by the change detection approaches are often identical. Thus, the *FP* cases that occur in the Marseille test area because of the DSM inaccuracies (Section 4.3) are both present in the outcomes of (Matikainen et al., 2007) and (Champion, 2007), as illustrated in Figures 3a and 3b respectively. Some of other errors shared at least by two approaches are also illustrated in Figure 3.

5. CONCLUSION

Four building change detection approaches have been tested in three different contexts. If the satellite context appears to be the most challenging for the current state-of-the-art, the aerial context and the LIDAR context appear to be a viable basis for building an operative system in the future. Thus, the high completeness rates for *demolished* buildings and the high correctness for *unchanged* buildings that could be achieved in

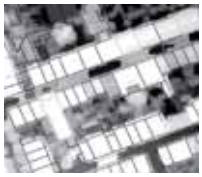
(a) Matikainen et al., 2007


(c) Rottensteiner, 2008


(e) Rottensteiner, 2008


(g) Rottensteiner, 2008


(b) Champion, 2007

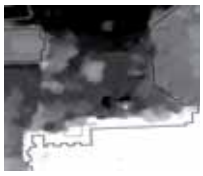
(d) Champion, 2007


(f) Champion, 2007


(h) Olsen and Knudsen, 2005

Figure 3. Evaluation Details (same colour code as Figure 1). *FP new* cases related to DSM errors (shadow areas), in Marseille streets (a)-(b) and Toulouse (c)-(d); (e)-(f) *FN new* cases (small changes); (g)-(h) *FP* new buildings related to bridges.

these contexts highlight the effectiveness of the presented approaches in verifying the existing objects in the databases. The main limitation in terms of qualitative efficiency concerns the relatively high number of *FN new* buildings – raising 12.1% in the Marseille test area with (Rottensteiner, 2008) – that are mostly related to the object change size. The economical efficiency of the presented approaches seems to be promising, with 80-90% of the existing buildings that need no further attention by the operator, because these buildings are reported to be *unchanged*, which then provides a considerable amount of manual work saved. In terms of the economical efficiency, the main limitation is a high number of *FP demolished* buildings that have to be inspected unnecessarily. Again, the main reason is problems of the algorithms to detect small changes.

Areas of improvement should concern input data and methodologies. Thus, the resolution of LIDAR data (1 point / m²) used in this test appeared to be critical for the change detection performance: using higher density LIDAR data (e.g. 5-10 points / m²) should improve the situation. As far as methodology is concerned, new primitives should be used in the algorithms, in particular 3D primitives (representing e.g. the 3D roof planes or building outlines) that can now be reliably reconstructed with the 3D acquisition capabilities, offered by recent airborne/spaceborne sensors. Another concern should be the improvement of the scene models used in object detection such that they can deal with different object classes and their mutual interactions. By incorporating different object classes and considering context in the extraction process, several object classes could be detected simultaneously, and the extraction accuracy of all interacting objects could be improved.

In this project, we learned how difficult it is to compare approaches of very different designs. To carry out a fair test, we chose to use the building label images and to limit the type of changes to *demolished* and *new* buildings. In addition, we chose to compare the building label images to the initial vector database, basing on a coverage rate featured by a T_h parameter. In our experiments, this parameter appeared to be critical. Further investigations are also necessary to study the actual impact of this parameter on the quality of the computed change maps i.e. completeness and correctness rates. However, if we are aware of these drawbacks, we think that this scheme was sufficient to bring out the interesting findings presented here. We also hope that our results – in conjunction with those of e.g. the ARMURS[3] project – will be helpful to create a nucleus of interested people, both in academia and private sector, and to speed up the progress in the field of automated building change detection.

REFERENCES

Breiman, L., Friedman, J. H., Olshen, R. A., Stone, C. J., 1984. Classification and Regression Trees. The Wadsworth Statistics / Probability Series, Wadsworth, Inc., Belmont, California.

Champion, N., 2007. 2D building change detection from high resolution aerial images and correlation Digital Surface Models. In: *IAPRSIS* XXXVI-3/W49A, pp. 197–202.

Champion, N., Boldo, D., 2006. A robust algorithm for estimating Digital Terrain Models from Digital Surface Models in dense urban areas. In: *IAPRSIS* XXXVI-3, pp. 111–116.

N. Champion, L. Matikainen, F. Rottensteiner, X. Liang, J. Hyyppä, 2008. A test of 2D Building Change Detection Methods: Comparison, Evaluation and Perspectives. In: *IAPRSIS* XXXVII – B4.

Heipke, C., Mayer, H., Wiedemann, C., Jamet, O., 1997. Automated reconstruction of topographic objects from aerial images using vectorized map information. In: *IAPRS*, XXXII, pp. 47–56.

Kumar, S. and Hebert, M.,, 2006. Discriminative random fields. *International Journal of Computer Vision* 68(2), pp. 179–201.

Matikainen, L., Kaartinen, K., Hyyppä, J., 2007. Classification tree based building detection from laser scanner and aerial image data. In: *IAPRSIS* XXXVI, pp. 280–287.

Mayer, H., 2008. Object extraction in photogrammetric computer vision. *ISPRS Journal of Photogrammetry and Remote Sensing* 63(2008), pp. 213-222.

Olsen, B., Knudsen, T., 2005. Automated change detection for validation and update of geodata. In: *Proceedings of 6th Geomatic Week*, Barcelona, Spain.

Pierrot-Deseilligny, M., Paparoditis, N., 2006. An optimization-based surface reconstruction from Spot5- HRS stereo imagery. In: *IAPRSIS* XXXVI-1/W41, pp. 73–77.

Rottensteiner, F., 2008 Automated updating of building data bases from digital surface models and multi-spectral images. In: *IAPRSIS* XXXVII – B3A, pp. 265-270.

[3] http://www.armurs.ulb.ac.be. Last visited: 09-06-30

EuroSDR-Project

Commission 1 “Sensors, Primary Data Acquisition and Georeferencing”

NEWPLATFORMS

Unconventional Platforms (Unmanned Aircraft Systems) for Remote Sensing

Final Report

Report by Jurgen Everaerts

Remote Sensing Research Unit – VITO, Belgium

Abstract

This final report of the EuroSDR project "NEWPLATFORMS" gives an overview of a very promising new class of platforms for remote sensing, unmanned aircraft systems or UAS. Although unmanned aircraft have been around for many years, they are now becoming available for scientific and civil use, as low-altitude systems that provide an "eye in the sky" for small photogrammetry projects (the size of a construction site), and for the development of new remote sensing applications.

First, the concept of an UAS is described. It is not just about the aircraft, but also about its ground control system (which gives the remote pilot the ability to control the aircraft). Two ways of classification are given, one more descriptive (based on physical properties such as total mass, range, endurance, etc.), and one based on the flight clearance potential. The latter is important, since there is a total lack of coherent regulations across Europe. A summary of the regulatory authorities is presented in chapter 2.

The report concludes with a review of the (potential) applications in remote sensing that can be conducted with UAS.

Introduction

The NEWPLATFORMS project was formally proposed to the EuroSDR Science Meeting in Madrid, in the Autumn of 2004.

Initially, the project's aim was to inventorise the unconventional platforms, to assess their ability and to compare that to the more traditional platforms for remote sensing, satellites and manned aircraft. However, although there were many systems then (and even more today), there was no consolidation yet; it did not seem very useful to make a list of systems that would potentially not exist any more when the list was published. Furthermore, the UAV community already has an extensive list of platforms published yearly an maintained at www.uvs-info.com.

From then on, the NEWPLATFORMS project aimed at keeping the EuroSDR community up to date on this evolving technology, on a yearly basis.

At the ISPRS Congress in Beijing, 2008, a working group "UVS for Mapping and Monitoring Applications" was set up, with an explicit desire to liaise with EuroSDR. This working group has now taken up its activities, and those will be reported to EuroSDR on the same basis as NEWPLATFORMS did.

As this subject may be slightly unfamiliar to the remote sensing community, a list of abbreviations is added. However, this introduction is a good place to clarify the meaning of some of the most common ones:

- UAV stands for Unmanned Aerial Vehicle
- UAS is an Unmanned Aircraft System, which is composed of a UAV and its on-ground command-and-control system
- UVS is an Unmanned Vehicle System, which could operate in the air (UAS), on the ground, on or under water.

In this report, the focus is on UAS.

1 Unmanned aircraft systems

1.1 System, not aircraft

Although the flying component of an unmanned system is by far the most exciting, it is useless and inoperable without the on-ground supporting systems. This is illustrated in figure 1.

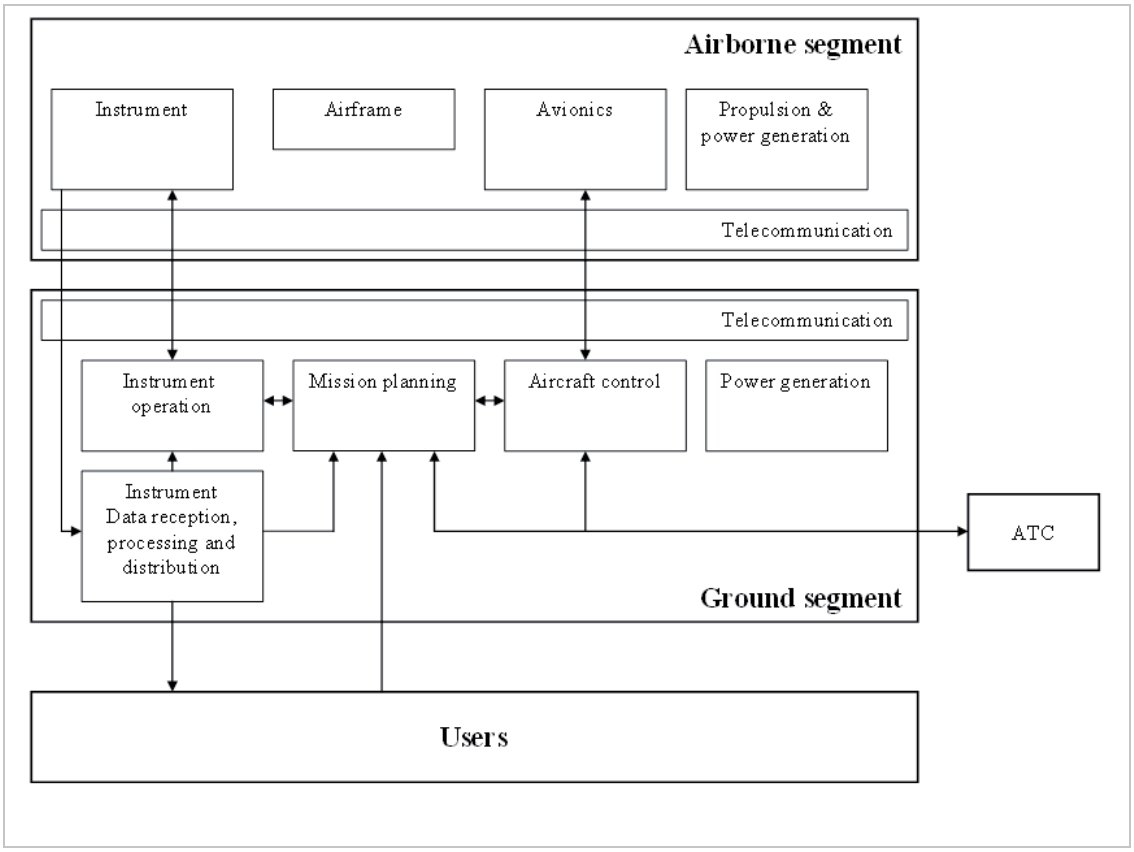

Figure 1: Schematic overview of the components of a UAS and its relation to the outside world (Everaerts, 2008)

The airborne segment (the aircraft) consists of

- The airframe: the mechanical structure that allows flight (wings, fuselage, tail, flaps, …) and provides space for the other airborne parts. UAV airframes take many forms, which are sometimes unlike what we consider to be a "regular" aircraft. This is possible, because they need not take the presence of a human pilot into consideration.
- The avionics: the electro-mechanical system that controls the aircraft. This includes servos to deflect moving parts (rudder, flaps), sensors that provide information on the environment (pressure, temperature) and the behaviour of the aircraft within that environment (angle of attack, …). An autopilot, GPS positioning, inertial measurement system, and altimeter (pressure based) are also required. In many cases, forward and nadir looking (low resolution) cameras are used to assist the on-ground pilot.

- Preferably, the avionics also contain a central processing unit that executes the commands given by the pilot and instrument operators, and that monitors all onboard systems. In case of a communication malfunction, this unit then takes control of the aircraft to execute a predefined sequence of operations (e.g. fly to a pre-set way point and circle there while trying to re-establish communication; eventually force the aircraft to descend).
- When operating the UAS in controlled airspace, a location transponder may be required. This device responds to interrogation by RADAR signals by transmitting the aircraft identity, its position and altitude.
- Power and propulsion system is required to maintain flight. Conventional fuel engines require fuel tanks, electric engines require batteries or fuel cells to be taken. Solar cells are also used for power generation.
- Instrument: this is the reason for the aircraft to fly. For short duration flights, onboard storage is used; long duration flights need a data downlink capability. Many types of instruments, stand-alone or combined, have been integrated on UAS platforms.
- Telecommunication: this is used to command and control the UAV (via the avionics), to downlink telemetry data (on the status of the airborne systems) and potentially instrument data as well.

The ground segment is composed of:

- Mission planning: based on the mission goals, and taking telemetry, instrument and weather data into account, the mission planner determines the best way to achieve the goals (in terms of instrument settings and flight plan). This is then given to the pilot. Mission planning interfaces with Air Traffic Control (ATC) for flight permission.
- Aircraft control: the pilot controls the aircraft on the basis or the UAV telemetry and the mission requirements. Even when the UAV is in autonomous mode, a pilot is required to be present. The pilot communicates with ATC during the mission. In most cases, ATC prefers to receive that communication via the aircraft, so that it behaves in the same way as conventional aircraft do.
- Telecommunication: this is used to command and control the UAV (via the avionics), to receive telemetry data (on the status of the airborne systems) and potentially also to control the instrument.
- Instrument operation: based on the mission planning, the instrument is operated to collect the data that are required. This may involve setting frame rates, aperture and integration time setting, zooming and pointing (e.g. in a gimballed system), for imaging systems.
- Instrument data reception, processing and distribution: the raw data that are received are used for mission planning and instrument operation (processed in a basic way so that the integrity and quality of the data can be assessed); they are then transferred to the processing system. After archiving and applying all necessary processing steps, the results can then be distributed. For high altitude, long endurance (HALE) systems, this processing facility is very much comparable to satellite processing centres.

1.2 Classification

As with every attempt to bring order in chaos, the UAS community has made great efforts in classifying the systems into clear categories. However, there is not one universally accepted. In paragraph 1.2.1, Table 1 describes of the more commonly used classification, and so it is placed first in the discussion, followed by some examples. It is not completely unambiguous, however, and it doesn't address one of the major issues with UAS: their ability to fly legally. Therefore, another classification is proposed in paragraph 1.2.2., which groups UAS that are thought to have the same likelihood of getting cleared for flight.

1.2.1 Based on size, mass and performance

A common classification of UAS is given in table 1.

Category	**Acronym**	**Range (km)**	**Flight Altitude (m)**	**Endurance (h)**	**MTOW (kg)**
Nano	η	< 1	100	<1	< 0,025
Micro	μ	<10	250	1	<5
Mini	Mini	<10	150-300	<2	<30
Close Range	CR	10-30	3000	2-4	150
Short Range	SR	30-70	3000	3-6	200
Medium Range	MR	70-200	5000	6-10	1250
Medium Range Endurance	MRE	>500	8000	10-18	1250
Low Altitude Deep Penetration	LADP	>250	50-9000	0.5-1	350
Low Altitude Long Endurance	LALE	>500	3000	>24	<30
Medium Altitude Long Endurance	MALE	>500	14000	24-48	1500
High Altitude Long Endurance	HALE	>2000	20000	24-48	4500-12000
Unmanned Combat Aerial Vehicle	UCAV	~1500	10000	~2	10000.
Lethal	LETH	300	4000	3-4	250
Decoy	DEC	0-500	5000	<4	250
Stratospheric	STRATO	>2000	20000-30000	>48	30-?

Table 1: UAS classification based on physical properties (van Blyenburg, 2009)

For the categories that are of interest to EuroSDR, one or a few examples are given. For a more comprehensive list, please refer to van Blyenburg, 2009 or UVS Info, 2009

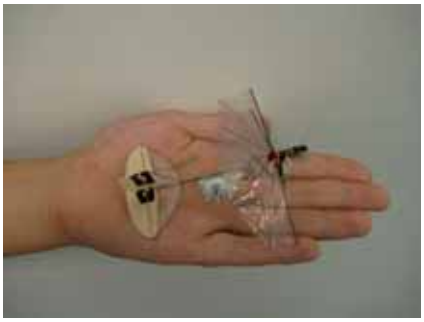

Figure 2: Delfly micro (http://www.delfly.nl), a nano UAS

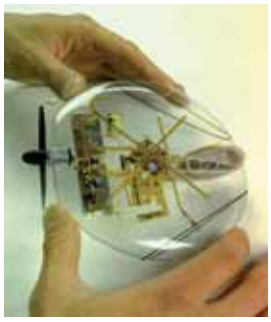

Figure 3: AerovVironment Micro UAV (http://www.avinc.com), a nano UAS

Figure 4: Draganflyer X6 (http://www.draganfly.com), a micro UAS

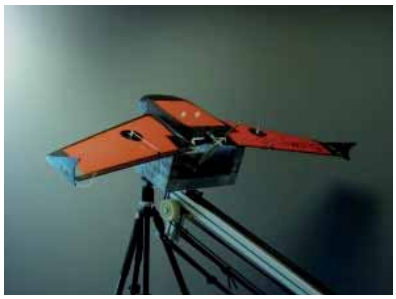

Figure 5: Gatewing K-120 (http://www.gatewing.com), a micro UAS

Figure 6: Cropcam (http://cropcam.com), a micro UAS

Figure 7: Geocopter (http://geocopter.nl), a mini UAS

Figure 8: Altair Insect (http://www.atair.com), a close range UAS

Figure 9: QinetiQ Zephyr (http://www.qinetiq.com), a HALE UAS

1.2.2 Based on certification potential

A more practical classification method, adapted to the EuroSDR participants' needs is given by UVS International. This approach is driven by the aircraft certification/flight permission process. Before discussing this, let us review the structure of the airspace in Europe.

ICAO has defined airspace classes as shown in Table 2. Classes A-E are called controlled airspace, F and G are uncontrolled. The classes are based on

- Flight rules: these are Instrument Flight Rules (IFR) where a pilot can fly his aircraft by using the aircraft instruments only (e.g. at night, in clouds); Visual Flight Rules (VFR) require weather conditions that are clear enough for the pilot to control the aircraft's attitude, navigation and to avoid obstacles and other aircraft. In exceptional cases, Special Visual Flights Rules (SVFR) are applied when VFR flights are conducted when IFR rules should be applied. UAS flights are not conducted under IFR nor VFR, because these flight rules require a pilot to be in the aircraft, but it is very likely that Air Traffic Control (ATC) will require the UAS pilot to behave in the same way as all other pilots that share the airspace with the UAS.
- Flight clearance: whether permission to fly is to be requested from ATC or not
- Flight separation: this can be managed by ATC or by the pilots themselves. In many cases, this implies that the aircraft should carry a transponder.

Class	Flight rules	Flight clearance	Separation
A	IFR/SVFR	ATC	ATC
B	IFR/SVFR/VFR	ATC	ATC
C	IFR/SVFR/VFR	ATC	IFR/SVFR are separated from IFR/SVFR/VFR flights; VFR flights are given traffic information about VFR flights
D	IFR/SVFR/VFR	ATC	IFR/SVFR are separated from IFR/SVFR/VFR flights; VFR flights are given traffic information about IFR/SVFR/VFR flights
E	IFR/SVFR/VFR	ATC for IFR/SVFR	IFR/SVFR are separated from IFR/SVFR flights; all flights are given traffic information about VFR flights
F	IFR/VFR		IFR flights are separated from IFR flights if practical; traffic information may be given about other flights
G	IFR/VFR		Traffic information may be given about other flights

Table 2: ICAO airspace classes

The layout (geolocation and altitude) of the different airspace classes is a national responsibility. For instance, Figure 10 shows the situation in Germany. Across Europe, there are no common altitudes to separate airspace classes. To complicate things even further, Air Traffic Control responsibility is shared between national ATC for the lower air space and EUROCONTROL for the upper air space.

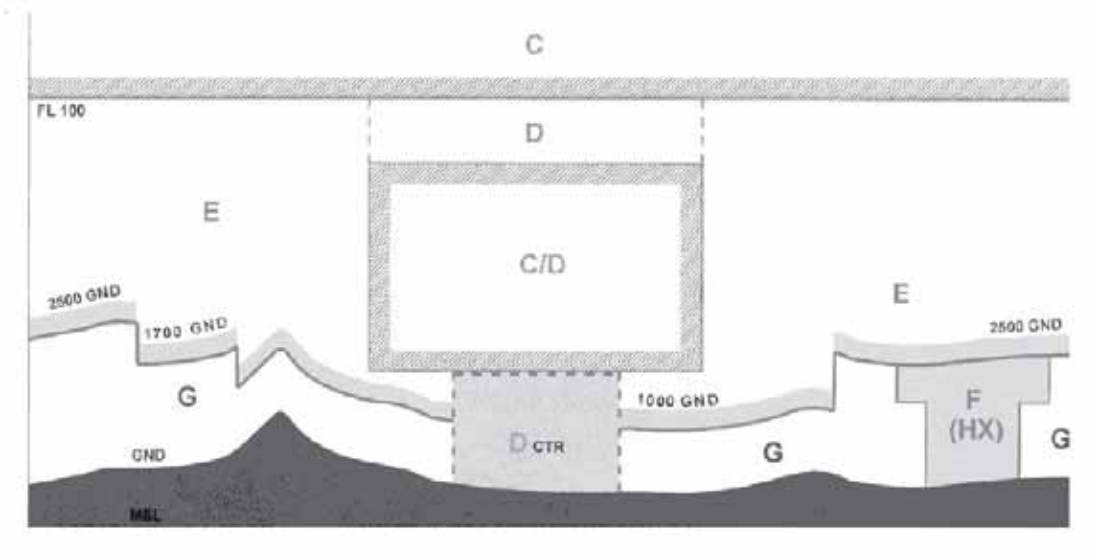

Figure 10: the airspace layout in Germany

Low altitude UAS will usually operate in class G airspace, which is uncontrolled. Therefore, other users of the airspace need to be informed through NOTAM (Note to Airmen) of the UAS flights. At higher altitude, in controlled airspace, separation can be handled by ATC; note however that not all countries allow manned and unmanned aircraft to mix. Then, the UAS will need to fly in segregated airspace (a three-dimensional box of airspace closed for all other air traffic), again published in a NOTAM.

1.2.2.1 Light UAS – Class I

	MTOM	Flight altitude	Distance to pilot	Flight mode
Micro	<1.5 kg	< ~150 m AGL	< ~500 m	Visual LoS
GRP A	1.5 – 7 kg			
GRP B	7 – 20/25 kg			
GRP C	20/25 – 150 kg			

Table 3: properties of Light UAS-Class I

Light UAS, class I systems usually operate in uncontrolled airspace, under very close supervision of the pilot (within Line of Sight (LoS)). To conduct these flights is expected to be relatively easy, requiring operational approval including:

- Proof of safe flight: this can be based on existing flight practise, and be determined by examining the aircraft and its control systems.
- Approved documentation: the civil aviation authority will review the document packs, and verify that the safety of people and property is adequately assured
- Licensing & Training: the pilot will have to demonstrate that he is fully capable of operating the aircraft
- Limitations, etc: the operating area shall be defined, acceptable environmental circumstances described (visibility, wind, …)

- Occurrence reporting mandatory: a system shall be put in place to report on unexpected events, so that the authorities have sufficient visibility in the operation of the aircraft.
- NOTAM informing other airspace users of the flights.

This class of UAS is already flying in many countries, under varying regulations. The EuroSDR community should focus on these, as the next two classes are unlikely to be available in the near future. They have been divided into 4 groups (Micro, GRP A, B and C) to indicate some of the regulation "boundaries" in terms of mass. Clearly, a lighter system will usually be more likely to be accepted by authorities.

Note that these regulations are set on a national level, although there are initiatives to harmonize these across Europe.

- Examples of Light UAS-Class I are :
- Model aircraft, transformed into a remote sensing platform;
- Fixed wing UAS;
- Rotary wing UAS, both model helicopters and radically different designs;
- Powered paraglider UAS;
- Blimp UAS.

During conversations with Belgian CAA, it became clear that a popular UAS, a quadrocopter, is considered to be too unsafe to be allowed to fly. Although several companies in Belgium actively promote this system (and show images acquired by them), clearly, these have not been through the certification process. In Germany, the state of Saxony has give a flying permit to micro drones; a new generation of micro drones will be required to carry an emergency parachute.

1.2.2.2 Light UAS - Class II

	MTOM	Flight altitude	Distance to pilot	Flight mode
Micro	<1.5 kg	> ~150 m AGG	> ~500 m	Beyond visual LOS
GRP A	1.5 – 7 kg			
GRP B	7 – 20/25 kg			
GRP C	20/25 – 150 kg			

Table 4: properties of Light UAS-Class II

Light UAS, class II systems are of a much more important complexity. They are to fly beyond the pilot's direct observation, so they should have adequate means to detect and avoid other air traffic. To fly, they need to coordinate with ATC, and follow the Rules of the Air. These systems will have to

- Comply to a full set of regulations, possibly based on EASA CS23 or CS-VLA (Very Light Aircraft)
- Obtain an Air Operator Certificate
- Obtain a formal registration of the aircraft
- Obtain aircraft Certification of Airworthiness
- Use a licensed pilot
- Obtain a Type certification
- Comply to EASA Maintenance Part 66 & 145

- Be produced by an Approval of Design & Production Organisation, or demonstrate similar capability
- NOTAM informing other airspace users of the flights.

This is no small task at all; some of these requirements are as yet not totally clear, as regulation is evolving. At present, there does not seem to be a sufficiently promising application of UAS to justify the associated cost.

1.2.2.3 UAS under EASA regulation

	Flight altitude	Distance to pilot	Flight mode
MTOM > 150 kg Including optionally piloted aircraft	> 150 m AGL	> 500 m	Beyond visual LOS

Table 5: properties of UAS heavier than 150 kg

UAS heavier than 150 kg MTOM are being regulated by EASA. The requirements for these aircraft will be more stringent than for Light UAS, class II. This raises the same concerns as above.

1.2.2.4 Balloons

Balloons are another possibility to lift remote sensing instrumentation. A distinction is made between manned (need certification and a licensed pilot) and unmanned balloons (e.g. weather balloons); if tethered or moored, the unmanned balloons need not go through as many qualification steps; if they are used in uncontrolled airspace, it should be easy to deploy them.

1.3 UAS evolution in the past 6 years

Although a clear legal framework has not been established for unmanned aircraft, the number of systems has been steadily increasing over the past years. Table 6 to Table 7 illustrate this evolution. On a whole, the number of UAS in the inventory of UVS International has more than doubled in the 2004-2008 time window. This growth was even stronger in the Light UAS-Class I category, where a 260 % increase is observed.

When we look at the purpose of the UAS, it is clear that it is still dominated by the military and dual purpose applications, but the strongest growth is seen in the civil/commercial category , which has grown by almost 350 % between 2004 and 2008.

Finally, an overview is given of the UAS producing countries; the number of Light UAS and the total number of UAS. An extensive list of civil, commercial, research and dual purpose UAS can be found in annex.

	2004	2005	2006	2007	2008	2009
Total number of UAS	477	544	603	789	974	1190
Number of producers/developers	203	207	252	312	369	422
International teamed efforts	12	20	32	34	35	38
Number of Producing countries	40	43	42	48	48	50

Table 6: evolution of UAS over the past 5 years (van Blyenburg, 2009)

	2004	2005	2006	2007	2008	2009
Light UAS-Class I	194	-	267	383	505	658

Table 7: evolution of Light UAS-Class I. No information for 2005 could be found (van Blyenburg, 2009)

	2004	2005	2006	2007	2008	2009
Civil/Commercial	33	55	47	61	115	150
Military	362	397	413	491	578	683
Dual Purpose	39	44	77	117	242	260
Research	43	35	31	46	54	66
Developmental		219	217	269	293	329

Table 8: evolution of UAS involved in different applications (van Blyenburg, 2009)

	2006		2007		2008		2009	
	Light UAS	total	Light UAS	total	Light UAS	total	Light UAS	total
Argentina				1	9	13	11	15
Australia	7	14	9	18	14	23	15	24
Austria		2		2		2	5	7
Belgium	1	1	1	1	1	1	2	2
Brazil		1	1	4	1	4	3	6
Bulgaria	1	1	1	1	1	1	2	2
Canada	1	2	3	4	4	5	13	14
Chili		1		1		2		2
China (PR)	8	19	8	20	9	28	9	29
Colombia			2	2	3	4	3	4
Croatia		3		3		3		3
Czech Republic		1		1		1		1
Finland			1	1	1	1	1	1
France	30	52	34	56	34	65	55	77
Germany	14	22	22	31	26	36	29	39
Greece		1		1		1	1	3
Hungary			1	1	1	1	1	1
India	1	2	2	3	4	5	5	6
International	3	32	4	34	4	35	4	38
Iran	3	3	5	6	5	6	28	38
Israel	25	52		62	35	72	42	83
Italy	4	11	10	19	19	30	23	37
Japan	14	15	14	15	14	16	14	16
Jordan	2	3	2	3	2	3	2	3
Malaysia		1		1	2	3	2	3
Mexico				3		4		4

	2006		2007		2008		2009	
	Light UAS	total	Light UAS	total	Light UAS	total	Light UAS	total
Netherlands	5	6	6	7	10	11	11	12
New Zealand		2		2		2	3	5
Norway	4	6	5	7	7	10	8	12
Pakistan	12	23	12	23	17	29	20	33
Phillipines							1	1
Poland	2	2	4	4	5	5	5	5
Portugal		1	2	3	2	3	2	3
Romania		1	1	2	1	2	2	4
Russian Federation	9	25	11	35	24	53	29	59
Serbia			3	4	3	4	3	4
Singapore	5	8	6	9	6	9	6	9
Slovakia							1	1
Slovenia		1		1	3	4	5	6
South Africa		7	2	9	2	9	4	16
South Korea	4	8	4	8	5	11	17	25
Spain	6	8	6	9	10	15	14	19
Sweden		2	1	4	1	8	1	8
Switzerland		1	7	9	9	9	17	19
Taiwan ROC	3	6	4	7	4	7	5	8
Tunisia		2		2		2		2
Turkey	4	5	6	8	9	12	10	13
U.A.E.		1	1	6	1	6	2	8
UK	18	29	30	45	35	51	42	65
Ukraine	2	3	2	3	2	3	4	7
USA	79	217	119	288	151	341	176	386

Table 9: number of Light UAS and total number of UAS developed in '06-'09 around the world (Van Blyenburg, 2009)

2 The legislative perspective

The legal framework within which a UAV is operating is highly complicated. The main issue for UAS flights in non-segregated airspace at present is "equivalence":

"Regulatory airworthiness standards should be set to be no less demanding than those currently applied to comparable manned aircraft nor should they penalize UAS systems by requiring compliance with higher standards simply because technology permits" (EASA, 2005).

This implies:

- Equivalent behaviour: for air traffic control (ATC), a UAS should behave as all other controlled air traffic. This means: provide a means to determine its position (a transponder) and communicate via the normal channels (so radio communication from the on-ground pilot should pass through the UAS)
- See-and-avoid capability: the UAS should be able to detect other aircraft in its vicinity and execute standard avoidance actions. It should also be visible from other aircraft (so it needs to carry navigation lights)

The second condition is a very difficult one to address, and this currently inhibits most flights beyond line-of-sight. Many experimental approaches using optical, acoustic and other means have been proposed for the "sense" part.

National and International authorities and organisations all have their own partial responsibility. In what follows, the actors in this field that play a role in Europe are described. Figure 3 below shows the result of a study made for the European Commission, DG Enterprise and Industry on the European UAS market (EC, 2008a and 2008b). Figure 11 summarizes the factors that govern the development of the European civil UAS market, and the players involved., while Figure 12 shows how an incremental approach could be set up.

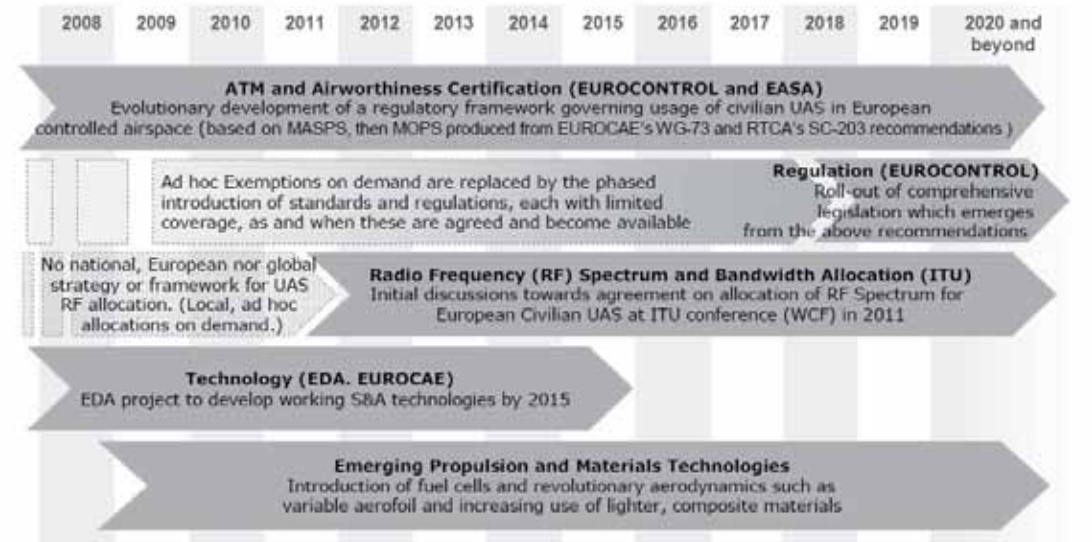

Figure 11: Factors that govern the development of the civil UAS market in Europe (EC, 2008a)

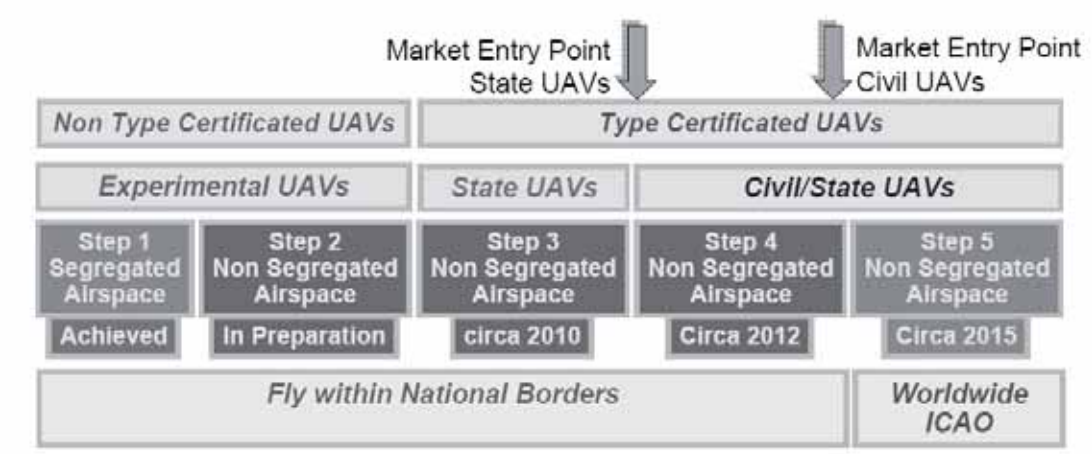

Figure 12: Steps for the integration of UAS into the airspace (Kershaw, 2008)

2.1 ICAO

The **International Civil Aviation Organisation** (ICAO; www.icao.int) Convention (ICAO, 2006), has following articles that are relevant for UAV flight:

Article 1 : Sovereignty

The contracting States recognize that every State has complete and exclusive sovereignty over the airspace above its territory.

Article 8 : Pilotless aircraft

No aircraft capable of being flown without a pilot shall be flown without a pilot over the territory of a contracting State without special authorization by that State and in accordance with the terms of such authorization. Each contracting State undertakes to insure that the flight of such aircraft without a pilot in regions open to civil aircraft shall be so controlled as to obviate danger to civil aircraft.

Article 12 : Rules of the air

Each contracting State undertakes to adopt measures to insure that every aircraft flying over or manoeuvring within its territory and that every aircraft carrying its nationality mark, wherever such aircraft may be, shall comply with the rules and regulations relating to the flight and manoeuvre of aircraft there in force. Each contracting State undertakes to keep its own regulations in these respects uniform, to the greatest possible extent, with those established from time to time under this Convention. Over the high seas, the rules in force shall be those established under this Convention. Each contracting State undertakes to insure the prosecution of all persons violating the regulations applicable.

In 2007, ICAO has established the Unmanned Aircraft Systems Study Group (UASSG), which will *"… assist the Secretariat in coordinating the development of ICAO Standards and Recommended Practices (SARPS), Procedures and Guidance material for civil unmanned aircraft systems (UAS), to support a safe, secure and efficient integration of UAS into non-segregated airspace and aerodromes*" (ICAO, 2008). UASSG' work program is to"

1. Serve as the focal point and coordinator of all ICAO UAS related work, with the aim of ensuring global interoperability and harmonization;
2. Develop a UAS regulatory concept and associated guidance material to support and guide the regulatory process;

3. Review ICAO SARPS, propose amendments and coordinate the development of UAS SARPS with other ICAO bodies;

4. Contribute to the development of technical specifications by other bodies (e.g., terms, concepts), as requested; and

5. Coordinate with the ICAO Aeronautical Communications Panel (ACP), as needed, to support development of a common position on bandwidth and frequency spectrum requirements for command and control of UAS for the International Telecommunications Union (ITU) World Radio Conference (WRC) negotiations."

This last point shows another important party in the UAV operation: no UAV is allowed to fly without direct communication with the on-ground controller. For this, a command-and-control radio link has to be guaranteed.

2.2 EASA

The European Aviation Safety Agency (EASA; www.easa.europa.eu) is a European Union agency, which groups the member states Civil Aviation Authorities (CAA). It is developing a UAV systems certification process, for UAV systems with a maximum take-off mass of more than 150 kg (UAS lighter than 150 kg are explicitly not subject to EASA regulation). It will deal with airworthiness (protection of people and property on the ground). EASA intends to do this on a type certification basis (comparable to what commercial aircraft manufacturers go through when they design a new type of aircraft), which is a very costly affair. The UAV certification specification will be a tailored version of CS-23 "Certification Specifications for Normal, Utility, Aerobatic, and Commuter Category Aeroplanes".

EASA has published an Advanced Notice for Proposed Amendment, "Policy for Unmanned Aerial Vehicle (UAV) certification" in 2005 (EASA, 2005), inviting comments from its stakeholders. This has resulted in a Comment Response Document, published in 2007 (EASA, 2007), which was itself open for feedback for one year (until February 2008). Now, EASA should publish a new policy.

2.3 EUROCONTROL

The mission of the European Organisation for the Safety of Air Navigation, EUROCONTROL (www.eurocontrol.int), *is to harmonise and integrate air navigation services in Europe, aiming at the creation of a uniform air traffic management (ATM) system for civil and military users, in order to achieve the safe, secure, orderly, expeditious and economic flow of traffic throughout Europe, while minimising adverse environmental impact.*(EUROCONTROL, 2009)

EUROCONTROL has issued "Specifications for the Use of Military UAVs as Operational Air Traffic Outside Segregated Airspace" in 2007 (EUROCONTROL, 2007). This should be followed by a similar document for civil UAS, with a requirement that UAS performance is equivalent to that of manned aircraft.

EUROCONTROL is not in favour of segregated operations of UAS, mainly due to the already crowded skies over Europe. Integrating UAS in the airspace should also not disrupt other civil air traffic. It also wants UAS to behave in an equivalent way as IFR aircraft.

In the near future, it is expected that UAS will be integrated in the Single European Sky ATM Research Program (SESAR), which will be deployed in 2014-2020. (SESAR, 2008)

2.4 EDA

The European Defence Agency (EDA; www.eda.europa.eu) is a European Union agency which aims *"to support the Member States and the Council in their effort to improve European defence capabili-*

ties in the field of crisis management and to sustain the European Security and Defence Policy as it stands now and develops in the future" (EDA, 2004)

One of the topics in its work programme 2009 (EDA, 2009) are Unmanned Air Vehicles (UAVs), with emphasis on following aspects:

- Air Traffic Insertion and airworthiness: pursue challenge of standardisation and certification to operate in regulated airspace.
- Future UAVs: pursue work on long Endurance and Tactical Unmanned Aerial System.
- Frequency management: harmonise needs on the military use of the spectrum and frequencies required for UAVs.

In the past, EDA has sponsored several UAS related studies, usually on long endurance UAVs:

- Technology Demonstration Study On Sense & Avoid Technologies For Long Endurance Unmanned Aerial Vehicles [LE-UAVs] (2006-2007) (EDA, 2007a)
- Technology Demonstration Study on Data Links for LE-UAV (2005-2007) (EDA, 2007b)

Finally, EDA is funding the AIR4ALL project, that is developing a route map for UAS traffic insertion (www.air4all.net). The extended consortium is also planning to address the radio frequency allocation issue (see ITU; Henley, 2008)

2.5 NATO

The **North Atlantic Treaty Organisation** (NATO; www.nato.int) is responsible for the military regulations in most of the European countries. It is involved in the regulatory process via its Flight in non-segregated airspace (FINAS) group, which intends to recommend and document NATO-wide guidelines to allow the cross-border operation of unmanned aerial vehicles (UAVs) in non-segregated airspace. Although NATO clearly states that it is not a regulatory body, it advocates standardisation to promote interoperability, economy of effort and mutual trust.

Figure 13: an overview of the UAV related activities and documents. (Snow, 2008) shows the UAV related activities at NATO. Its Standardisation Agreements (STANAGs) have already developed a considerable amount of good practise:

- STANAG 4670 "Recommended Guidance for the Training of Designated Unmanned Aerial Vehicle Operator (DUO)" deals with the UAV operator (i.e. pilot) training, and lists the required skills. This STANAG is currently undergoing ratification by the NATO member states.(STANAG 4670, 2006)
- STANAG 4671 "UAV Systems Airworthiness Requirements (USAR)" is a certification standard, for fixed wing UAVs, of 150 to 20 000 kg mass. It is closely related to EASA CS-23. This STANAG has been ratified by US, UK, FR, NL, with reservations. (STANAG 4671, 2007)
- Study 4685 "Human Factors and UAV Systems Safety" is a FINAS activity that will analyse UAV accidents, and the human factors that have contributed to them; it will then make recommendations (Snow, 2008)

Special attention is also given to the "Sense-and-Avoid" issue. A UAV has to be able to detect surrounding air traffic and perform the same type of collision avoidance as a manned aircraft. A target level of safety (TLOS) of 5.10^{-9} collisions/flight hour is proposed.

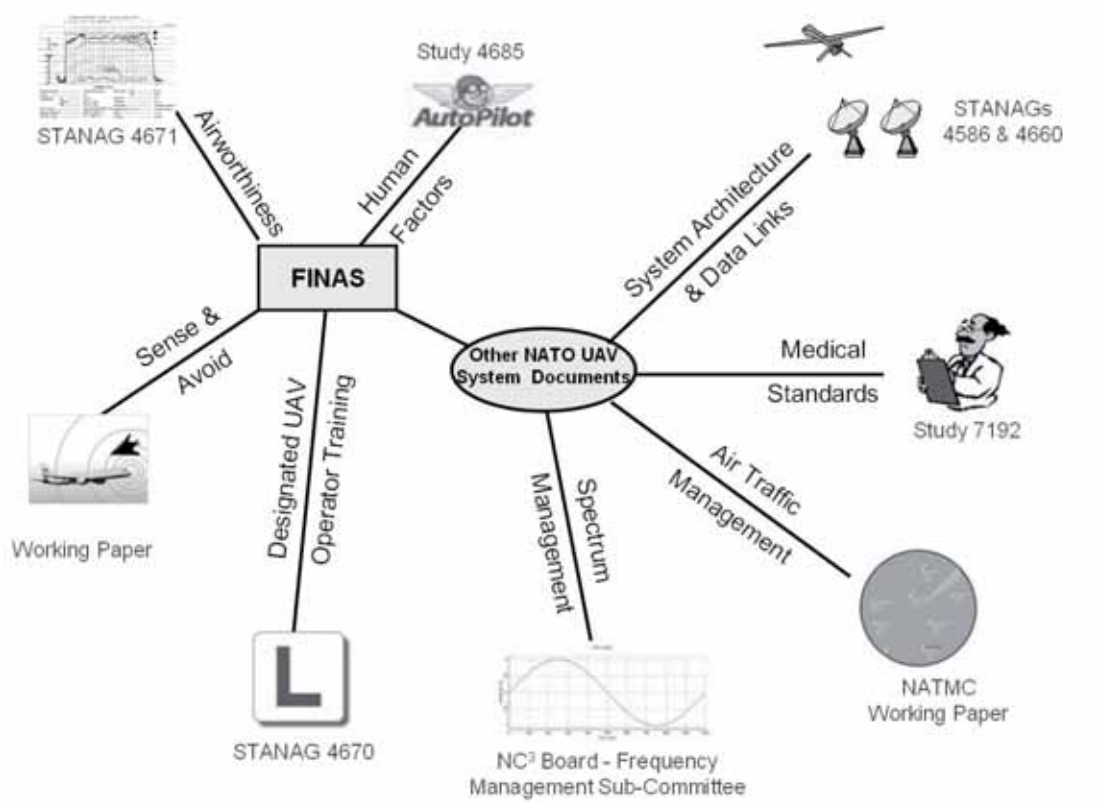

Figure 13: an overview of the UAV related activities and documents. (Snow, 2008)

2.6 AUVSI

The Association for Unmanned Vehicle Systems International (AUVSI; www.auvsi.org) is "the world's largest non-profit organization devoted exclusively to advancing the unmanned systems community. AUVSI, with members from government organizations, industry and academia, is committed to fostering, developing, and promoting unmanned systems and related technologies."

2.7 EuroCAE

The European Organisation of Civil Aviation Equipment (EuroCAE; www.eurocae.eu) is a not-for-profit association of aviation manufacturers, regulators, European and national Aviation Authorities, Air Navigation Service providers, Airlines, Airports and other users. It Working Group 73 "Un-manned Aircraft Systems", has been established to deliver standards and guidance that will ensure the safety and regularity of unmanned aircraft (UA) missions.

2.8 JARUS – Light UAS

JARUS stands for Joint Authorities for Rulemaking on UAS (Hermans and Leijgraaf, 2008), and it groups civil aviation authorities of Austria, Belgium, Czech Republic, France, Germany, Italy, The Netherlands, Spain and the UK; EASA and Eurocontrol are active members as well. This group wants to draft a single set of airworthiness, operational and airspace requirements, for civilian UAS lighter than 150 kg or for research purposes. These drafts are expected to be ready in 2009.

Note that regulation for aircraft lighter than 150 kg is a strictly national matter in Europe. JARUS requirements will have to be introduced in every single national legislation, so it is likely that they will vary to some extent across Europe.

The UK CAA Directorate or Airspace Policy has published CAP722 "Unmanned Aircraft System Operations in UK Airspace – Guidance" (UKCAA, 2008) "*…to assist those who are involved in the development of UAS to identify the route to certification, in order to ensure that the required standards and practices are met by all UAS operators."*

The Swedish Aviation Safety Authority has issued an air safety and approvals procedure in 2003 (Wiklund, 2003).

The Danish CAA has issued regulations on UAS lighter than 25 kg (DKCAA, 2004), which essentially limits UAS operation to low altitude (<100m) and away from people and property.

The French CAA allows flight of UAS beyond line-of-sight, and even independent flight ("évoluer de manière autonome"), but only in segregated airspace (FRCAA, 2007)

The UK CAA Directorate or Airspace Policy has published CAP722 "Unmanned Aircraft System Operations in UK Airspace – Guidance" (UKCAA, 2008) "*…to assist those who are involved in the development of UAS to identify the route to certification, in order to ensure that the required standards and practices are met by all UAS operators."* Its CAP 722 regulation discusses non-segregated flight from its third edition in 2008.

The Belgian CAA has decided to base its certification process on a well-established standard: EASA CS-23. (BE-CAA, 2007), regardless of the aircraft mass. Before that, it had already granted an airworthiness certificate for the military B-Hunter, based on a tailoring of EASA CS-VLA (Very light aircraft). From my own experience, Belgian CAA may well be the most willing to consider granting permission to fly UAVs in non-segregated airspace.

2.9 UVS International

UVS International (www.uvs-international.com) is a not-for-profit organisation for the promotion of unmanned vehicle systems. It has instigated an "Interim WG on Light UAS", with participants for industry, authorities and organisations from Europe, and observers from US FAA and RTCA.

It works within the EuroCAE, NATO FINAS, ICAO, EUROCONTROL UAS initiatives and is as such a co-ordinating organisation. It has corporate as well as institutional members.

2.10 Other UAS associations

UAV Dach is the German language UAS working group, with members from Germany, Austria, Switzerland and the Netherlands.

2.11 Research Projects

On top of the official activities, the EC, EDA and others are sponsoring research projects to develop regulation for the insertion of UAS into the civil non-segregated airspace. To mention just two:

- Air4All, an EDA study for "Formulation of a route map for the technology and system demonstrations required to achieve the evolving regulatory requirements for State and Civil UASs"
- INOUI (Innovative Operational UAS Integration, EC FP6).
- ASTRAEA (Autonomous Systems Technology Related Airborne Evaluation & Assessment, a UK private/public initiative)

2.12 ITU

The International Telecommunication Union (ITU; www.itu.int) is the leading United Nations agency for information and communication technology issues, and the global focal point for governments and the private sector in developing networks and services. Amongst other duties, ITU is coordinating the shared global use of the radio spectrum. As of today, there are no globally accepted frequencies allocated for UAV operation. This may be resolved at the next World Radio Conference, in 2011.

Until then, the use of radio links for command & control, telemetry and communication with Air Traffic Control (see Figure 14: an overview of the communication links that are required for UAS operation.) needs to be settled locally. This obviously inhibits the development of UAV related technology, as it reduces the number of identical items that can be sold.

ITU doesn't seem to be very proactive in this area, as it is estimating that the use of civil UAS will only be an issue by 2020.

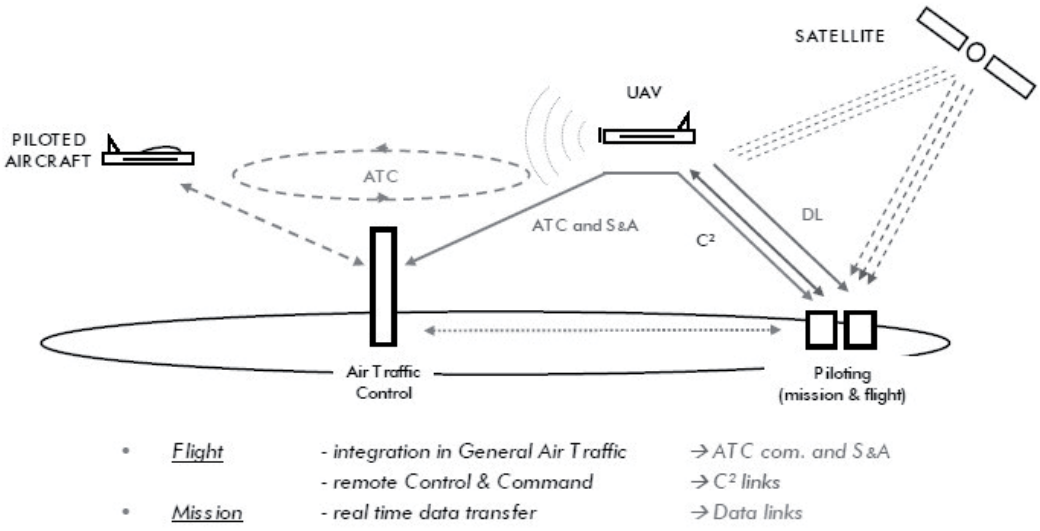

Figure 14: an overview of the communication links that are required for UAS operation.

3 UAS for photogrammetry and remote sensing

The Air4All consortium (www.air4all.net; Kershaw, 2008) summarizes the expected steps for integration of UAS as a confidence building sequence (Figure 12: Steps for the integration of UAS into the airspace (Kershaw, 2008)):

- First prove the airworthiness of the UAS in segregated airspace
- Then prove that is can be integrated in the non-segregated airspace.
- Then start type certification for UAS (first for State UAS, i.e. military ones), so that they can be produced in larger numbers
- Type certification of civil UAS then benefits from the lessons learnt in the previous step
- Finally, the legal (ICAO) framework for crossing borders can be tested.

3.1 Strengths

Figure 15 highlights the strengths of UAS:

Figure 15: UAS applications and UAS advantages (adapted from UASUK, 2009)

- Scalability: there are UAS of virtually ever size, so there is always one that meets the needs of the particular user or application. A small UAS (including control system and a consumer digital camera) is available at a cost lower than 20 000 Systems with higher performance cost up to 1 million €.
- Persistence: depending on the application, short to very long duration flights may be necessary. Again, this is addressed in the inventory of existing UASs. The unique feature of a pilotless aircraft is that it does not need to land for crew rotation. This saves time and thus increases the ability to continue the observation.
- Flexibility: mostly, the UAS is deployed within the area of interest, and it can be brought there by car or a small truck; usually there is no need for an airfield and its installations. After an initial flight clearance procedure, a flight can be organised in a matter of hours or days.
- Technology: micro-electronics and other technological developments are easily integrated; for short-range missions, existing ICT solutions can be used for command and control (e.g. IEEE 802.11 wireless ethernet).
- New opportunities: this is illustrated by the applications that have been reported, e.g. archaeology. The cost of using a small light UAS is considerably lower than that of conventional aerial survey. Also, UAS are operable in dangerous environments: since there are no lives at risk, a UAS can be flown in places where manned aircraft cannot be sent (e.g. flying through clouds of harmful chemicals after an industrial accident, or monitoring volcanic activity)

Table 10 shows how UAS compare to conventional remote sensing platforms.

	Airborne platforms	Satellite platforms	Low altitude UAV	High altitude UAV
Coverage	**Local to Regional** 10 – 10 000 km^2	**Global reach** Only low resolution satellites provide a true global coverage; HR satellites take snap-shots.	**Local** Up to ~1 km^2 Within sight of the controller.	**Regional** Up to 200 000 km^2
Update rate	**Low or non-existing** Multi-year update programs at NMCAs	**High** Within days or weeks	**Ad-hoc** No programs in place	**Weeks-months**
Flexibility	**Flight plans** Needs to be integrated in other air traffic; is dependent on weather	**Orbit constraints** The orbit determines the time of overpass	**Total** Below air traffic, flies whenever required (and if weather allows)	**Flight plans + ad-hoc** Above air traffic, can avoid underlying weather or be sent to crisis events
Quality	**?** Many private companies have high standards, but these may not be interchangeable	**Constant** Satellite observations are usually processed by a very limited number (usually : one only) of processing centres.	**?** These systems are mostly under development, their quality will improve.	**Constant** Follows the satellite data processing philosophy
Spatial Resolution	High to Very High cm to dm	Low to Medium m to km	**Very high** Cm	**High** dm
Positional Accuracy	**High** Well established methods for sub-pixel accuracy	**Low to medium** Stand-alone precision of several pixels	**High** Well established methods for sub-pixel accuracy	**High** Well established methods for sub-pixel accuracy
Spectral Resolution and accuracy	**Not always well controlled** Film is qualitative only; commercial digital systems have wide bands, in photogrammetry this is not an issue.	**Calibrated** Only digital sensors are used on satellites nowadays, all well calibrated.	**?** Depends on the instrument that is carried	**Calibrated** Purpose designed instruments.
Target application(s)	**Mapping, image acquisition**	**Environmental, image acquisition**	**Experimental, crisis management, traffic monitoring, …**	**Mapping, environmental, crisis management**
System cost (order of magnitude, €)	**1-10 M€**	**10-1000 M€**	**10 -1000 k€**	**10 – 100 M€**

Table 10: Properties of traditional and UAV platforms (Everaerts, 2008)

3.2 Applications

In short, UAS have been used in a wide variety of remote sensing applications. They have also inspired photogrammetrists to adapt their methods for the imagery produced by UAS, and computer vision methods have been used to control UAS. So, UAS are not just another platform for remote sensing, they define new challenges and stimulate new applications.

The EC civil UAS market study (EC, 2008a) has a list of applications:

- Government
    - Law enforcement (Police, Civil Security)
    - Border security
    - Coastguard
- Fire and Rescue
    - Forest fires
    - Other major incidents
    - Emergency rescue (e.g. Mountain rescue)
- Energy Sector
    - Oil and gas industry distribution infrastructure monitoring
    - Electricity grids / distribution network monitoring
- Agriculture, Forestry and Fisheries
    - Environmental monitoring
    - Crop dusting
    - Optimising use of resources
    - Fisheries Protection
- Earth Observation and Remote Sensing
    - Climate monitoring
    - Aerial photography, mapping and surveying
    - Seismic events
    - Major incident and pollution monitoring
- Communications and Broadcasting
    - VHALE platforms as proxy-satellites
    - MALE / S/MUAS as short-term, local communications coverage
    - Camera platforms (e.g. broadcasting, and film industry)

Roughley and Meredith (2008) raise the question of integration of UAS in the airspace. This is regarded as the make-or-break issue in many UAS studies, but is it really? The integration question can be reversed: is integration with other traffic in the airspace necessary? Which applications can be developed while the UAS stays segregated from other traffic? Also, there are CAAs that will allow UASs to operate in non-controlled airspace under a NOTAM. This question may help us more when we evaluate the potential of UAS operation for a certain application.

Application	Segregated flying possible or under NOTAM
Aerial photogrammetry survey	Yes, away from cities
Archaeology site survey	Yes
Agricultural monitoring	Yes
Border security (maritime)	Dependent on circumstances
Border security (over land)	No
Communications relay	Dependent on circumstances
Crop spraying	Yes
Rapid response & crisis management	Yes
Environmental Monitoring	Yes
Fisheries monitoring, oceanography	Yes
Forest fire monitoring	Yes
Forestry survey and mapping	Yes
Law enforcement	Under strict rules
Maritime surveillance and patrol	No
Monitoring of energy transmission infrastructure	Yes
Natural resource survey	Yes
Search and rescue	Yes
Traffic management	Under strict rules
Weather and environmental monitoring	Yes
Wildlife monitoring	Yes

Table 11: potential for remote sensing applications using UAS under NOTAM or in segregated airspace

3.2.1 Aerial photogrammetry survey

Many small UAS are being used for traditional photogrammetry applications, such as aerial image acquisition, and with that, vector mapping, DSM extraction, orthophoto generation, etc., … The constraints imposed on the flight within line-of-sight limit the extents of the areas that can be covered in a single flight. Nevertheless, many projects have been reported with very good accuracies, mainly due to the very high resolution (mm to cm) of the imagery and the limited flying height (50-200 m).

Haarbrink *et al.* (2008) show that a 200 x 300 m^2 area can be surveyed in 5 minutes, and that the resulting DSM, compared to very precise tachymetric survey, has an average difference of 3.5 mm, with a 25.6 mm standard deviation.

Private companies such as Germatics in Germany (www.germatics.com) or SmartPlanes (www.smartplanes.se) produce high resolution orthophotos for golf courses, agriculture, forestry and construction. Gatewing in Belgium (gatewing.com) targets open pit mining and quarries for regular monitoring, as well as infrastructure building site planning and monitoring.

3.2.2 Archaeology

Martinez-Rubio *et al.* (2005) have used a tethered small Zeppelin type aerostat to carry a Nikon D70 digital camera to image the Clvnia Sulpicia site in Spain. From 80 m altitude, 0.05 m image resolution was obtained. Using a 70% forward and lateral overlap, planimetric and altimetric precision of 0.05 and 0.03 m were obtained.

Eisenbeiss and Zhang (2006) used an unmanned helicopter to survey the Pinchango Alto site in Peru. They used a Canon D60 and D10 (Eisenbeiss,2005) to produce 0.03 cm resolution imagery to derive a

DSM of the site; this was compared to a ground based laser scanning DSM (Lambers *et al.*, 2007), with good agreement.

More archaeological sites have been imaged using unmanned platforms (Çabuk *et al.*, 2007, Verhoeven, 2006), with less geometric precision, but integrating other instruments (such as infrared imagery). Mostly, these images are used to provide the "bigger picture", not for measurement.

3.2.3 Agriculture

In Japan, 2000 UAS were used in 2003 for farming. This includes mapping (water stress, disease, crop loss mapping), but other farming activities as well: ploughing, seeding and application of fertiliser and pesticide (Newcombe, 2007). Interestingly, these UAS are under regulatory authority of the Ministry of Agriculture, Forestry and Fisheries. They are called "flying ploughs" in this regulation.

The CropCam company (cropcam.com) offers a highly integrated system that is designed to hand launched. It features automatic navigation, and takes images at predefined GPS positions. Finally, the results are georeferenced, so they can be used instantaneously after landing.

A HALE (High Altitude, Long Endurance) UAV, Pathfinder Plus was used on a coffee plantation in Hawaii (Herwitz, 2004), to provide planters information on the best time for harvesting.

3.2.4 Border security

The U.S. Customs and Border protection agency is using a (military) Predator-B system, equipped with both electro-optical and RADAR instruments to routinely monitor its borders (CBP, 2009).

3.2.5 Forest fire monitoring

The yearly impact of forest fires in the Mediterranean countries, Australia and California has made forest fire monitoring an urgent need. UAS have been used in this respect (Réstas, 2006; Martínez-de Dios, 2006; Casbeer, 2006).

3.2.6 Rapid response and crisis management

Rapid response imaging using UAVs has received a lot of attention as well. This has been demonstrated for road accident simulations (Haarbrink, 2006). In the framework of the EC FP6 OSIRIS project, a micro UAV was used to make *in situ* measurements for the determination of atmospheric stability. Using this, the dispersion of a toxic plume can be accurately monitored. (Smeets, 2009).

UAVs have also been proposed and operated as platforms to monitor volcanoes (Buongiorno, 2005).

3.2.7 Traffic monitoring

A final example of the flexibility of UAVs is their use in traffic monitoring (Puri, 2007; Doherty, 2004; Haarbrink)

3.3 Test platform

UAS are ideal for testing new remote sensing equipment and for validation of new methods. Some examples are

- Goniometer alternative: BRDF measurements require the observation of targets under multiple orientations. This can be done using bulky equipment, but just as well using a small UAS helicopter.
- Upscaling: it is well known that in situ field spectrometer data are difficult to correlate to airborne hyperspectral images, probably due to spectral mixing and atmospheric effects. A

UAS can take in situ measurements at different altitudes (different scales), and these may very well correlate better to the airborne data.

- Imaging spectrometer testing: VITO has received several requests to fly experimental imaging spectrometers in its light UASs.
- Use cases have been developed to use UAS in close range applications: one example is to image wind turbine propellers at very high resolution (and potentially in more than just the visual spectrum) to look for corrosion and other defects (e.g. from lightning impacts). This currently involves a long wind turbine downtime and a high altitude crane to lift an inspector (and this is very hard to do at sea). Data acquisition is one of the new aspects, but crack and corrosion detection is another challenge, which may require multispectral images and computer vision techniques.

4 Conclusion

Unmanned aircraft systems have been growing in numbers in the past four years; they have been used in many remote sensing activities, albeit in small projects almost exclusively. This is due to the lack of regulation to allow them to fly in controlled air space. In uncontrolled airspace (usually at very low altitude), there seem to be sufficient possibilities for UASs to become an important tool for remote sensing (in education, instrument development as well as in operational use).

5 References

BE-CAA, 2007. Belgian Certification Specification for UAV systems.

Billen, E., 2009. Development of legal framework for civil UAS activities in controlled airspace. Proceedings of International Symposium "Light Weight Unmanned Aerial Vehicle Systems and Subsystems", Oostende, Belgium.

CBP, 2009. http://www.cbp.gov/xp/cgov/border_security/air_marine/uas_program/uasoverview.xml

Çabuk, A., Deveci A. & Ergincan F. 2007. Improving Heritage Documentation. GIM International 21, 9, September 2007

Dalamagkidis, K., Valavanis, K.P., Piegl, L.A., 2009. On Integrating Unmanned Aircraft Systems into the National Airspace System. Springer Science+Business Media B.V., Berlin, Germany.

DKCAA, 2004. BL 9-4 Regulations on unmanned aircraft not weighting more than 25 kg.

EASA, 2005. European Aviation Safety Agency (EASA) A-NPA, No. 16/2005 "Policy for unmanned aerial vehicle (UAV) certification.

EASA, 2007. . European Aviation Safety Agency (EASA), CRD to A-NPA 16/2005.

EC, 2008 ENTR/2007/065 Study Analysing the current activities in the field of UAV; first element: status.

EC, 2008 ENTR/2007/065 Study Analysing the current activities in the field of UAV; second element: way forward.

EDA, 2004. Council joint action 2004/551/CFSP of 12 July 2004 on the establishment of the European Defense Agency.

EDA, 2007a. Technology Demonstration Study On Sense & Avoid Technologies For Long Endurance Unmanned Aerial Vehicles [LE-UAVs]. http://www.eda.europa.eu/genericitem.aspx?area=31&id=305

EDA, 2007b. Technology Demonstration Study – LE_UAV Datalink Study. http://www.eda.europa.eu/genericitem.aspx?area=31&id=171

EDA, 2009. EDA Work programme 2009. http://www.eda.europa.eu/WebUtils/downloadfile.aspx?fileid=467

Eisenbeiss, H. and Zhang, L., 2006. Comparison of DSMs generated from mini UAV imagery and terrestrial laserscanner in a cultural heritage application. In: The International Archives of Photogrammetry, Remote Sensing and Spatial Information Sciences, Dresden, Germany, Vol. XXXVI part 5.

EUROCONTROl, 2007. Specifications for the Use of Military UAVs as Operational Air Traffic Outside Segregated Airspace. EUROCONTROL-SPEC-0102

EUROCONTROL, 2008. Unmanned Aircraft Systems (UAS) Market Outlook.

EUROCONTROL, 2009. http://www.eurocontrol.int/corporate/public/standard_page/org_mission.html

Everaerts, 2008. Unmanned aerial vehicles for photogrammetry and remote sensing. In: Advances in Photogrammetry, Remote Sensing and Spatial Information Sciences: 2008 ISPRS Congress Book. Taylor&Francis Group, London, UK.

FRCAA, 2007. Arrêté du 1er août 2007 relatif aux condition d'insertion et d'évolution dans l'espace aérien des aéronefs civils ou de la défense non habités.

Haarbrink, R.B., Eisenbeiss, H., 2008. Accurate DSM production from unmanned helicopter systems. In: The International Archives of Photogrammetry, Remote Sensing and Spatial Information Sciences, Beijing, PRC, Vol. XXXVII part B1.

Henley, 2008. A Proposed European Route Map for UAS Traffic Insertion. UAS Information Workshop – 10 November 2008

Hermans, R. and van de Leijgraaf, R., 2009. The co-ordinated European certification approach for Light UAS. In UVS International Yearbook 2008/2009 UAS: The Global Perspective. UVS International, Paris, France.

ICAO, 2006. Convention of International Civil Aviation, ninth edition. http://www.icao.int/icaonet/arch/doc/7300/7300_9ed.pdf

ICAO, 2008. SAR operational principles, procedures and techniques – Development of procedural strategies for the practical provision of SAR services, Unmanned Aircraft Systems/ UAS. ICAO/IMO joint working group on harmonization of aeronautical and maritime search and rescue (ICAO/IMO JWG-SAR), Fifteenth meeting, Canberra, Australia.

Kershaw, D., 2008. Presentation at the Air4All 2nd Stakeholder meeting, Brussels, Belgium, 6 May 2008.

Martinez Rubio, J. et al., 2005. IMAP3D: Low cost photogrammetry for cultural heritage. Proceedings of CIPA2005 XX International Symposium, Torino, Italy.

Newcombe, L., 2007. Green fingered UAVs. Unmanned Vehicle, November 2007.

Smeets, N. et al., 2009. User of a Micro UAV for the determination of Atmospheric Stability in Accidental Air Dispersion Modelling. Proceedings of International Symposium "Light Weight Unmanned Aerial Vehicle Systems and Subsystems", Oostende, Belgium.

Roughley, D.J. and Meredith, K., 2008. Canadian Market Opportunities for UAS: Non-Military Applications. National Research Council Canada, Institute for Aerospace Research, May 2008.

SESAR, 2008. SESAR Consortium Work Programme for 2008-2013. http://www.eurocontrol.int/sesar/gallery/content/public/docs/DLM-0710-002-02-00-D6.pdf

Snow, M, 2008. "NATO FINAS", EASA UAV Workshop, Paris, France.

STANAG 4670, 2006. http://www.barnardmicrosystems.com/download/STANAG_4670_Ed_1_2006.pdf

STANAG 4671, 2007. http://www.mae.ncsu.edu/courses/mae589c/cook/USAR_Edition_1.pdf

Van Blyenburg, 2009. Unmanned Aircraft Systems, The Global Perspective 2009/2010. 7th Edition

Verhoeven,G., Loenders, J.O., 2006. Looking through Black-Tinted Glasses – A Remotely Controlled Infrared Eye in the Sky. BAR International Series, 200§, Volume 1568, pp.73 -80.

UASUK, 2009. http://www.uavsuk.com

UKCAA, 2008. CAP 722 Unmanned Aircraft System Operations in UK Airspace – Guidance.

Wiklund, E., 2003. Flying with unmanned aircraft (UAVs) in airspace involving civil aviation activity: Air safety and the approvals procedure. http://www.luftfartsstyrelsen.se/upload/In_english/Aviation%20Safety%20Authority/UAV.pdf

Index of Figures

Index of Tables

Annex

List of civil, commercial, research and dual purpose UAS (van Blyenburg, 2009)

Nr.	Country	Producers/Developers	System Designation	Category
1	Argentina	AeroDreams UAV	ADS-101 Strix	02-Mini
2	Argentina	AeroDreams UAV	ADS-301 Nancu	02-Mini
3	Argentina	AeroDreams UAV	ADS-401	02-Mini
4	Australia	AAI Corp - Aerosonde	Aerosonde Mk III & IV	08-LALE
5	Australia	ADRO	Pelican Observer	03-CR
6	Australia	AeroCam Australia	Trainer	02-Mini
7	Australia	AeroCam Australia	Shadow UAV	02-CR
8	Australia	BAE Systems & University of Sydney	Brumby Mk3	05-MR
9	Australia	BAE Systems & University of Sydney	Kingfisher Mk1	04-SR
10	Australia	BAE Systems & University of Sydney	Kingfisher Mk2	04-SR
11	Australia	Codarra Advanced Systems	Avatar	02-Mini
12	Australia	CSIRO	Mantis	02-Mini
13	Australia	Sonacom & University of Sydney	Mirli	05-MR
14	Australia	University of South Australia & Aerospace Sciences Corp.	Tandem Wing	03-CR
15	Australia	UAV Vision	G18 Aeolus	03-CR
16	Australia	UAV Vision	T21	02-Mini
17	Australia	UAV Vision	T26	02-Mini
18	Australia	V-TOL Aerospace	i-copter Phantom	03-CR
19	Australia	V-TOL Aerospace	i-copter Seeker	03-CR
20	Australia	V-TOL Aerospace	Warrigal	02-Mini
21	Austria	AeroSpy	Quadrocopter	01-Micro
22	Austria	AeroSpy	unnamed	01-Micro
23	Austria	FH Joanneum (Univ. Graz)	JXP-S	01-Micro
24	Austria	KameraDrohne	KamerDrohne HD35	02-Mini
25	Austria	Schiebel Elektronische Geräte	Camcopter	04-SR
26	Austria	University of Salzburg	Javiator	01-Micro
27	Belgium	Flying-Cam	FlyingCam	02-Mini
28	Belgium	Gatewing	K120	01-Micro
29	Brazil	Incubaero	Embravant	03-CR
30	Brazil	Gyrofly Innovations	Gyro 500	01-Micro
31	Canada	Advanced Subsonics	Grasshopper	02-Mini
32	Canada	Aerial Insight	Ai-extended	01-Micro
33	Canada	Aerial Insight	Ai-multi	01-Micro
34	Canada	Aerial Insight	Ai-solo	01-Micro
35	Canada	Aerion Labs	Scout	01-Micro
36	Canada	CropCam	CropCam	02-Mini
37	Canada	Draganfly Innovations	DF-SAVS	02-Mini
38	Canada	Draganfly Innovations	DF-TSU	02-Mini
39	Canada	Draganfly Innovations	DX-PRO	02-Mini
40	Canada	Draganfly Innovations	Tango	02-Mini

Nr.	Country	Producers/Developers	System Designation	Category
41	Canada	Draganfly Innovations	X6	02-Mini
42	Canada	MicroPilot	MP-Trainer	02-Mini
43	Canada	MicroPilot	MP-Vision	02-Mini
44	Chili	Chilean Air Force Polytechnical Academy	Vantapa X-02	05-MR
45	Colombia	FromSky	Terraco	02-Mini
46	Croatia	Soko	B3	04-SR
47	Croatia	Soko	B4	04-SR
48	France	ABS Aerolight	Maxi	03-CR
49	France	ABS Aerolight	Pixy	03-CR
50	France	Aeroart	A100	02-Mini
51	France	Aeroart	Aves	02-Mini
52	France	Aeroart	H250	03-CR
53	France	Aeroart	Seagos	02-Mini
54	France	Aeroart & Mercury Computer	Aelius 0	02-Mini
55	France	Aeroart & Mercury Computer	Aelius 1	02-Mini
56	France	EADS Military Aircraft & Dyn'Aéro (airframe	Surveyor 2500	05-MR
57	France	EADS Military Aircraft &SurveyCopter	Scorpio 30	04-SR
58	France	EADS Military Aircraft &SurveyCopter	Scorpio 6	04-SR
59	France	EuroMC	Aero-Drone 50	02-Mini
60	France	EuroMC	Aero-Drone 70	02-Mini
61	France	EuroMC	Aero-Drone 120	02-Mini
62	France	Flying Robots	FR 101	05-MR
63	France	Flying Robots	FR A2	02-Mini
64	France	Flying Robots	FR E1	02-Mini
65	France	Gates Technology	GT Aircraft	03-CR
66	France	Infotron	IT 180-5 EL	02-Mini
67	France	Infotron	IT 180-5 TH	02-Mini
68	France	Lehmann Aviation	LP960	01-Micro
69	France	Lehmann Aviation	LV580	01-Micro
70	France	Novadem	NX110	02-Mini
71	France	Novadem	U130	02-Mini
72	France	Pix-Air & AirStar	Soulcam	02-Mini
73	France	PR Aviation (based on Viario, Germany)	PY Copter	02-Mini
74	France	Sagem Défense Sécurité (Safran)	Merlin	02-Mini
75	France	Sagem Défense Sécurité (Safran) & Onéra, France & Stemme, Germany (airframe)	Busard	06-MRE
76	France	Sirehna & KYU Micodrones & PY Automation, France	Cybird	02-Mini
77	France	Sirehna & KYU Micodrones & PY Automation, France	Elytre (Elsa)	02-Mini

Nr.	Country	Producers/Developers	System Designation	Category
78	France	Survey-Copter	unnamed	01-Micro
79	France	Survey-Copter	Copter 1	02-Mini
80	France	Survey-Copter	Copter 1b	02-Mini
81	France	Survey-Copter	Copter 4	03-CR
82	France	Survey-Copter	DVF-2000	02-Mini
83	France	Vision du ciel	Cyclope 4.0	02-Mini
84	France	Vision du ciel	I.Z.I 1.0	02-Mini
85	France	Vision du ciel	Pixy 26-40	02-Mini
86	France	Vision du ciel	Pixy 29-40	02-Mini
87	Germany	AirRobot	AR70	01-Micro
88	Germany	AirRobot	AR100	01-Micro
89	Germany	AirRobot	Mikado	01-Micro
90	Germany	Borjet	CoRex	01-Micro
91	Germany	Borjet	FlyEye	01-Micro
92	Germany	Diehl (see Microdrones, Germany)	SensoCopter	01-Micro
93	Germany	Mavionics	Carolo P70	02-Mini
94	Germany	Mavionics	Carolo T140	02-Mini
95	Germany	Mavionics	Carolo T200	02-Mini
96	Germany	Microdrones	Md4-1000	02-Mini
97	Germany	Microdrones (see Diehl)	Md4-200	02-Mini
98	Germany	Rheinmetall Defense Electronics	Opale	05-MR
99	Germany	Rotrob	Rotrob	02-Mini
100	Germany	Scalecopter	CamClone	02-Mini
101	Germany	TFH Wildau	Bully	01-Micro
102	Germany	UAV Services & Systems	X-Sight	02-Mini
103	Germany	UAV Services & Systems	MX-Sight	02-Mini
104	Greece	EADS - 3 Sigma	Nearchos	05-MR
105	Hungary	HI Aero	Gabbiano	02-Mini
106	International	Airscan Consortium (EC funded)	Airscan	04-SR
107	International	VITO, Belgium & Verhaert, Belgium & QinetiQ, UK	Pegasus	12-STRA
108	International	Composites Technology, Malaysia & BAE Systems, USA	Eagle 150	05-MR
109	International	Kawada, Japan & Schweizer, USA	RoboCopter 300	03-CR
110	International	Politecnico Torino & Euro Consortium	Heliplat	12-STRA
111	International	SmartFish, Switzerland & DLR, Germany	HyFish	02-Mini
112	Iran	Aero Pars	R3	01-Micro
113	Iran	Aero Pars	R4	01-Micro
114	Iran	Aero Pars	R5	01-Micro
115	Iran	Aero Pars	R6	01-Micro
116	Iran	Amirkabir University of Technology	Electric UAV	02-Mini
117	Iran	Iran Aircraft Manufacturing Industries (HESA)	Ababil A	02-Mini

Nr.	Country	Producers/Developers	System Designation	Category
118	Iran	Iran Aircraft Manufacturing Industries (HESA)	Ababil B	02-Mini
119	Iran	Iran Aircraft Manufacturing Industries (HESA)	Ababil C	02-Mini
120	Iran	Mechanics College fo Isfahan University	Aria	05-MR
121	Israel	Aeronautics Defense Systems	Aerosky	04-SR
122	Israel	Aeronautics Defense Systems	Aerosky 2	04-SR
123	Israel	Aeronautics Defense Systems	Aerostar	04-SR
124	Israel	BlueBird Aero Systems	MicroB	01-Micro
125	Israel	Elbit Systems & IAI & Urband Aerospace	Mule	04-SR
126	Israel	Elbit Systems & IAI & Urband Aerospace	Panda	02-Mini
127	Israel	IAI-Malat	EyeView B	04-SR
128	Israel	IAI-Malat	Firebird	04-SR
129	Israel	Steadicopter	STD-5	03-CR
130	Israel	Topi-Vision	Casper-420	03-CR
131	Italy	A2Tech	RV-02	02-Mini
132	Italy	A2Tech	RV-160TD	02-Mini
133	Italy	Aermatica	Anteos	01-Micro
134	Italy	Alenia Aeronautica & Selex Galileo & Thales Alenia Space	Molynx	10-HALE
135	Italy	CIRA	Castore	12-STRA
136	Italy	International Aviation Supply	Archimede	05-MR
137	Italy	International Aviation Supply	Raffaello	05-MR
138	Italy	MAVTech	MH600-AP	01-Micro
139	Italy	MAVTech	MH2000	02-Mini
140	Italy	Nautilus	NRC-Class D	02-Mini
141	Italy	Nautilus	NRC-Class E	02-Mini
142	Italy	Nimbus	NBS 20	02-Mini
143	Italy	Nimbus	NBS 35	02-Mini
144	Italy	Siralab	SR-H3	02-Mini
145	Japan	Fuji Heavy Industries	HSFD	03-CR
146	Japan	Fuji Heavy Industries	RPH-2A	02-Mini
147	Japan	Hirobo	Sky Surveyor	03-CR
148	Japan	Kawada Industries & Hitachi	Colugo	02-Mini
149	Japan	Nara Institute of Science and Technology	XB-2	05-MR
150	Japan	Nara Institute of Science and Technology & TAO	Skyblade	02-Mini
151	Japan	Yamaha Motors	Aerial RMAX	03-CR
152	Japan	Yamaha Motors	Agricultural RMAX	03-CR
153	Japan	Yamaha Motors	Autonomous RMAX II	03-CR

Nr.	Country	Producers/Developers	System Designation	Category
154	Japan	Yamaha Motors	Autonomous RMAX IIG	03-CR
155	Japan	Yanmar Agricultural Equipment Co.	YH-300SL	02-Mini
156	Japan	Yanmar Heli Services & Kobe Giken	KG-135	02-Mini
157	Malaysia	Composites Technology Research (CTRM)	Eagle ARV	05-MR
158	Malaysia	System Consultancy Services	UAV	02-Mini
159	Mexico	Hydra Technologies	S4	04-SR
160	Mexico	Hydra Technologies	S5	05-MR
161	Netherlands	ASTI & TNO	DelFly I	00-Nano
162	Netherlands	ASTI & TNO	DelFly II	00-Nano
163	Netherlands	Delft Dynamics	Robot helicopter	02-Mini
164	Netherlands	E-Producties	EKH-001	03-CR
165	Netherlands	Geocopter	Furore	03-CR
166	Netherlands	HighEye	HE 26	02-Mini
167	Netherlands	HighEye	HE 26C	02-Mini
168	Netherlands	HighEye	HE 3.6 t	02-Mini
169	Netherlands	HighEye	HE 60	02-Mini
170	Netherlands	HighEye	HE80	02-Mini
171	Netherlands	UAV-Europe	MH 23	04-SR
172	New Zealand	Skycam UAV	Kahu-2E-B	02-Mini
173	New Zealand	Skycam UAV	Kahu Hawk	02-Mini
174	New Zealand	Skycam UAV	Kahu silver eye	02-Mini
175	New Zealand	TGR Helicopr Ltd.	Wasp	09-MALE
176	Norway	Norut IT	CryoWing	08-LALE
177	Norway	Odin Aero	Recce D6	02-Mini
178	Norway	Prox Dynamix	Black Hornet PD-100	00-Nano
179	Norway	Prox Dynamix	Hornet-3	00-Nano
180	Norway	Proxflyer	BladeRunner	01-Micro
181	Norway	Proxflyer	MicroFlyer	01-Micro
182	Norway	Proxflyer	Mosquito	01-Micro
183	Norway	Proxflyer	Nanoflyer	01-Micro
184	Norway	Robot Aviation	unnamed	03-CR
185	Norway	Scandicraft & CybAero, Sweden	Apid 55	04-SR
186	Pakistan	Integrated Dynamics	Explorer	02-Mini
187	Pakistan	Integrated Dynamics	Rover	02-Mini
188	Poland	Air Force Institute of Technology	HOB-bit	02-Mini
189	Poland	Air Force Institute of Technology	unnamed	02-Mini
190	Portugal	Faculty of Engineering, University of Porto	ASASF	02-Mini
191	Russian Federation	A-Level Aerosystems	ZALA 421-01	01-Micro
192	Russian Federation	A-Level Aerosystems	ZALA 421-02	03-CR
193	Russian Federation	A-Level Aerosystems	ZALA 421-03	02-Mini
194	Russian Federation	A-Level Aerosystems	ZALA 421-04 electric	02-Mini
195	Russian Federation	A-Level Aerosystems	ZALA 421-04 thermic	02-Mini

Nr.	Country	Producers/Developers	System Designation	Category
196	Russian Federation	A-Level Aerosystems	ZALA 421-06	02-Mini
197	Russian Federation	A-Level Aerosystems	ZALA 421-07	
198	Russian Federation	A-Level Aerosystems	ZALA 421-08	01-Micro
199	Russian Federation	A-Level Aerosystems	ZALA 421-09	03-CR
200	Russian Federation	A-Level Aerosystems	ZALA 421-12	01-Micro
201	Russian Federation	Irkut	Irkut-10	03-CR
202	Russian Federation	Irkut	Irkut-20	03-CR
203	Russian Federation	Irkut	Irkut-2F	02-Mini
204	Russian Federation	Irkut	Irkut-2T	02-Mini
205	Russian Federation	Irkut	Irkut-2M	02-Mini
206	Russian Federation	Irkut & Aeronautics, Israel (airframe)	Irkut-60	03-CR
207	Russian Federation	Irkut & Aeronautics, Israel (airframe)	Irkut-200	05-MR
208	Russian Federation	Irkut & Stemme, Germany (airframe)	Irkut-850	05-MR
209	Russian Federation	Radio	MMS	02-Mini
210	Russian Federation	Sukhoi	Zond-1	10-HALE
211	Russian Federation	Sukhoi	Zond-2	10-HALE
212	Russian Federation	Sukhoi	Zond-3	09-MALE
213	Russian Federation	Teknol	Mini UAV System	01-Micro
214	Russian Federation	Teknol	Tactical UAV System	02-Mini
215	Russian Federation	Tranzas (Kronshtadt)	Dozor 2	03-CR
216	Russian Federation	Tranzas (Kronshtadt)	Dozor 3	04-SR
217	Russian Federation	Tranzas (Kronshtadt)	Dozor 4	03-CR
218	Russian Federation	Tranzas (Kronshtadt)	Dozor 5	03-CR
219	Russian Federation	Tupolev	Berkut	05-MR
220	Serbia	EMA	Nikola Tesla 150	02-Mini
221	Singapore	Cradance	Golden Eagle	02-Mini
222	Singapore	Singapore Technologies Aerospace	Skyblade II	02-Mini
223	Singapore	Singapore Technologies Aerospace	Skyblade IV	02-Mini
224	Slovakia	Advanced Unmanned Systems Interna-tional	AirSniper	02-Mini
225	South Africa	ABAT	Posduif	02-Mini
226	South Africa	Advanced Technologies & Engineering	Civil Vulture	05-MR
227	South Africa	Advanced Technologies & Engineering	Kiwit	02-Mini
228	South Africa	Advanced Technologies & Engineering	Roadrunner	02-Mini
229	South Africa	Advanced Technologies & Engineering	Sentinel 500 M	05-MR
230	South Africa	Advanced Technologies & Engineering	Sentinel 620	05-MR
231	South Africa	Advanced Technologies & Engineering	Sentinel 800	05-MR
232	South Africa	Advanced Technologies & Engineering	Vigil EE	04-SR
233	South Africa	Advanced Technologies & Engineering	Vigil SR	03-CR
234	South Korea	Korean Aeronautical Research Institue	Durumi	08-LALE
235	South Korea	Korean Aerospace Industries& Daewoo	Arch-50	05-MR
236	South Korea	Microaerobot	Flying Robot	01-Micro
237	South Korea	Microaerobot	FM-07	01-Micro
238	South Korea	Microaerobot	MA1	01-Micro

Nr.	Country	Producers/Developers	System Designation	Category
239	South Korea	Microaerobot	MA2	01-Micro
240	South Korea	Oneseen Skytech	Cine-Copter	02-Mini
241	South Korea	Oneseen Skytech	MAVtronix7000	02-Mini
242	South Korea	Oneseen Skytech	X-Copter	02-Mini
243	South Korea	Ucon Systems	RemoH-C100	02-Mini
244	Spain	Aerovision	Fulmar	03-CR
245	Spain	Airview	AV-01	02-Mini
246	Spain	Airview	AV-02	02-Mini
247	Spain	Airview	AV-03	02-Mini
248	Spain	Aitem	Dedalo	02-Mini
249	Spain	Aitem	Horus	02-Mini
250	Spain	Alpha Unmanned Systems	Atlantic	02-Mini
251	Spain	Alpha Unmanned Systems	Atlas	02-Mini
252	Spain	Alpha Unmanned Systems	Commando	02-Mini
253	Spain	Alpha Unmanned Systems	Sniper	02-Mini
254	Spain	Robotnik Automation	X4	02-Mini
255	Spain	UAV Navigation	KUAV	03-CR
256	Sweden	CybAero	APID 55	04-SR
257	Sweden	Saab	Skeldar V-150	04-SR
258	Sweden	SmartPlanes	Smart-1	02-Mini
259	Switzerland	Aeromedia	Aerocopter 1	02-Mini
260	Switzerland	Aeromedia	Aerocopter 2	02-Mini
261	Switzerland	Aeromedia	AeroStar 1	02-Mini
262	Switzerland	Aeromedia	AeroStar 2	02-Mini
263	Switzerland	Aeroscout	B2-120	02-Mini
264	Switzerland	Aeroscout	T5	02-Mini
265	Switzerland	Minizepp	Z10000Pro	02-Mini
266	Switzerland	Minizepp	Z13000	02-Mini
267	Switzerland	SenseFly	Swinglet	01-Micro
268	Switzerland	Skive Avoiation	Skive	02-Mini
269	Switzerland	Skybotix	Skybox	01-Micro
270	Switzerland	Skybotix	Coax	01-Micro
271	Switzerland	Skybotix	OS4	01-Micro
272	Switzerland	Skybotix	Planemini	01-Micro
273	Switzerland	Skybotix	Skybox	01-Micro
274	Switzerland	Swiss Federal Institute of Technology	Sky-Sailor	01-Micro
275	Switzerland	Swiss UAV	NEO S-300	03-CR
276	Switzerland	Swiss UAV	KOAX X-240	03-CR
277	Taiwan ROC	Aero Flight Technology Enterprises	Mx-1	04-SR
278	Taiwan ROC	National Cheng Kung University	Swan	02-Mini
279	Turkey	Kale & Baykar Technologies	Bayraktar	02-Mini
280	Turkey	Kuzgun High Technology Design	Kuzgun	02-Mini
281	Turkey	METU - Dept. Of Aerospace Engineering	Mini UAV	02-Mini

Nr.	Country	Producers/Developers	System Designation	Category
282	UK	Fanwing	Fanwing	03-CR
283	UK	GFS Projects	GFS-7	02-Mini
284	UK	MagSurvey	Prion	02-Mini
285	UK	Nitrohawk	Nitrohawk	02-Mini
286	UK	SkyShips	C1000	03-CR
287	UK	SkyShips	Cirrus 840	03-CR
288	UK	Swarn Systems	Owl	01-Micro
289	UK	Universal Target Systems	Spotter	02-Mini
290	UK	VTOL Technologies	Aerial Police Dog	03-CR
291	Ukraine	Scientific Industrial Service	A-10 Phoenix	04-SR
292	Ukraine	Scientific Industrial Service	A-12 Hurricane	02-Mini
293	Ukraine	Scientific Industrial Service	A-160	05-MR
294	Ukraine	Scientific Industrial Service	A-5 SeaEAgle	03-CR
295	USA	AAI Corp	Aerosonde Mk 4.4	08-LALE
296	USA	AAI Corp	Aerosonde MK 4.7	05-MR
297	USA	AC propulsion	So Long	03-CR
298	USA	Adaptive Fight	Hornet	01-Micro
299	USA	Advanced Ceramics Research (BAE Systems)	Manta B	04-SR
300	USA	Advanced Ceramics Research (BAE Systems)	SilverFox	04-SR
301	USA	Advanced Hybrid Aircraft	Hornet	06-MRE
302	USA	Advanced Hybrid Aircraft	Wasp	05-MR
303	USA	Advanced Soaring Systems & NASA	Apex	10-HALE
304	USA	AeroCam	23F	02-Mini
305	USA	AeroCam	60F	02-Mini
306	USA	Aerotonomy	Nanos	
307	USA	AeroVironment	Centelios	10-HALE
308	USA	AeroVironment	Global Observer	10-HALE
309	USA	AeroVironment	Global Observer G0-1	10-HALE
310	USA	AeroVironment	Global Observer G0-2	10-HALE
311	USA	AeroVironment	Helios	10-HALE
312	USA	AeroVironment	Hiline	10-HALE
313	USA	AeroVironment	Hornet	01-Micro
314	USA	AeroVironment	MicroBat	01-Micro
315	USA	AeroVironment	Pathfinder Plus	10-HALE
316	USA	AeroVironment	Wasp	01-Micro
317	USA	Aerotonomy	Nanos	00-Nano
318	USA	Agrarius (& Advanced Ceramics Research)	HawkEye	02-Mini
319	USA	Airscooter	Airscooter E70	01-Micro
320	USA	Airscooter	Airscooter G70	01-Micro
312	USA	Airship	Surveillance L15	05-MR?
322	USA	Arcturus	T-15	02-Mini

Nr.	Country	Producers/Developers	System Designation	Category
323	USA	Arcturus	T-16	02-Mini
324	USA	Aurora Flight Sciences	Chiron	06-MRE
325	USA	Aurora Flight Sciences	GoldenEye-100	04-SR
326	USA	Aurora Flight Sciences	Marsflyer	13-EXO
327	USA	Aurora Flight Sciences	Orion HALL	10-HALE
328	USA	Aurora Flight Sciences	Perseus	10-HALE
329	USA	Aurora Flight Sciences	SkyWatch	09-MALE
330	USA	Aurora Flight Sciences	Theseus	10-HALE
331	USA	Autonomous Airborne Systems	HOVTOL	05-MR
332	USA	Biorobotics (Case Western Univ. & Univ. Of Florida)	MMALV series	01-Micro
333	USA	Blackwater Aeroships	Polar 400	04-SR
334	USA	Boeing	X-48B	03-CR
335	USA	Carolina Airships	Guardian 31	04-SR
336	USA	Carolina Airships	Guardian 34	04-SR
337	USA	Charles Stark Draper Laboratory	NAV	01-Micro
338	USA	Charles Stark Draper Laboratory	SARD	02-Mini
339	USA	CIRPAS	Pelican (Cesna-based)	05-MR
340	USA	Continental Controls and Design	LOCUST MAV	01-Micro
341	USA	Coptervision	CVG 2002	02-Mini
342	USA	Cyber Defense Systems	Cyberscout	02-Mini
343	USA	Dara Aviation	D-1 Heavy Payload	05-MR
344	USA	Dara Aviation	D-1 Long Mission	06-MRE
345	USA	Dara Aviation	D-1 Short Mission	05-MR
346	USA	Dragonfly Pictures	DP-4X Mule	05-MR
347	USA	Dragonfly Pictures	DP-4XT	05-MR
348	USA	Dragonfly Pictures	DP-5	04-SR
349	USA	Dragonfly Pictures	DP-5T	03-CR
350	USA	Dragonfly Pictures	DP-5X Wasp	04-SR
351	USA	Dragonfly Pictures	DP-5XT Gator	05-MR
352	USA	Flight Systems	Tracker UAV	02-Mini
353	USA	General Atomics Aeronautical Systems	Altair	10-HALE
354	USA	General Atomics Aeronautical Systems	Altus	10-HALE
355	USA	General Atomics Aeronautical Systems	Ikhana	10-HALE
356	USA	Georgia Tech Research Institute	MarsFlyer	13-EXO
357	USA	Georgia Tech Research Institute	UAV	02-Mini
358	USA	HEI Group	Blicopter	02-Mini
359	USA	Honeywell	gMAV	01-Micro
360	USA	Honeywell	T-Hawk	01-Micro
361	USA	Insitu	GeoRanger	04-SR
362	USA	Insitu	SeaScan	04-SR
363	USA	Insitu & Boeing	ScanEagle	04-SR
364	USA	IntelliTech Microsystems	Vector P	05-MR

Nr.	Country	Producers/Developers	System Designation	Category
365	USA	Iron Bay	XTM	05-MR
366	USA	Iron Bay	Fatboy	03-CR
367	USA	Iron Bay	Knighthawk	05-MR
368	USA	Iron Bay	Sabre	02-Mini
369	USA	ISL Inc. Bosch Aerospace	Lears IV	08-LALE
370	USA	ISL Inc. Bosch Aerospace	SASS LITE	05-M
371	USA	ISL Inc. Bosch Aerospace	WASP	02-Mini
372	USA	Kaman Aerospace & Lockheed Martin	K-Max Burro	05-MR
373	USA	Kuchera Defence	Falcon	02-Mini
374	USA	L3 & BAI Aerosystems	Javelin	02-Mini
375	USA	L3 & Geneva Aerospace	Dakota	05-MR
376	USA	Lew Aerospace Inc	Inventus E	02-Mini
377	USA	Lew Aerospace Inc	Inventus S-1	03-CR
378	USA	Marcus UAV	Marcus 100	01-Micro
379	USA	Nascent Technology	AHMMH-1 XS	02-Mini
380	USA	Naval Research Lab.	AME	03-CR
381	USA	Naval Research Lab.	Ghost/Dakota	03-
382	USA	Naval Research Lab.	Ion Tiger	03-CR
383	USA	Naval Research Lab.	Mares	04-SR
384	USA	Naval Research Lab.	NDM-1/2/3	03-CR
385	USA	Neany (Titan Aircraft airframe)	Arrow	05-MR
386	USA	Neural Robotic Industries	AutoCopter	02-Mini
387	USA	Octatron	SkySeer	02-Mini
388	USA	Optimum Solutions	Condor 300	02-Mini
389	USA	Oregon Iron Works	Sea Scout	04-SR
390	USA	Orion Aviation	Model 706 Seabat	05-MR
391	USA	Procerus Technology	Unicorne 1	02-Mini
392	USA	Procerus Technology	Unicorne 2	02-Mini
393	USA	Procerus Technology	Unicorne 3	02-Mini
394	USA	Raytheon Missile Systems	Cobra	03-CR
395	USA	Rotomotion	SR 20	02-Mini
396	USA	Rotomotion	SR 30	02-Mini
397	USA	Rotomotion	SR 100	02-Mini
398	USA	Rotomotion	SR 200	02-Mini
399	USA	RP Flight Systems	Shaker AP	02-Mini
400	USA	RP Flight Systems	Slipstream II	02-Mini
401	USA	RP Flight Systems	Slipstream III	02-Mini
402	USA	SAIC	Vigilante 496	05-MR
403	USA	Sanswire-TAO	SAS-51	05-MR
404	USA	Sanswire-TAO	Skysat	05-MR
405	USA	Sanswire-TAO	Stratellite	05-MR
406	USA	Scaled Composites	Proteus	10-HALE
407	USA	Tactronix-Tactical Airspace Group (TAG)	TAG-M2600	03-CR

Nr.	Country	Producers/Developers	System Designation	Category
408	USA	Thorpe Seeop Corp.	P10	?
409	USA	Thorpe Seeop Corp.	P10A	04-SR
410	USA	Thorpe Seeop Corp.	P10B	04-SR
411	USA	Thorpe Seeop Corp.	P40	04-SR
412	USA	Thorpe Seeop Corp.	P7108	04-SR
413	USA	Thorpe Seeop Corp.	TS1000	04-SR
414	USA	Thorpe Seeop Corp.	TS2000	05-MR
415	USA	Trek Aerospace	DragonFly	05-MR
416	USA	University of Florida	SUAV	01-Micro
417	USA	University of Kansas	Meridian	05-MR
418	USA	Victory Systems	Mini-UAV	01-Micro

Catergory explanations

CR	Close Range
SR	Short Range
MR	Medium Range
MRE	Medium Range Endurance
LADP	Low Altitude Deep Penetration
LALE	Low Altitude Long Endurance
MALE	Medium Altitude Long Endurance
HALE	High Altitude Long Endurance
UCAV	Unmanned Combat Aerial Vehicle
STRA	Stratospheric
EXO	Exo stratrospheric

LIST OF OEEPE/EuroSDR OFFICIAL PUBLICATIONS

State – Dec. 2009

1 *Trombetti, C.:* „Activité de la Commission A de l'OEEPE de 1960 à 1964" – *Cunietti, M.:* „Activité de la Commission B de l'OEEPE pendant la période septembre 1960 – janvier 1964" – *Förstner, R.:* „Rapport sur les travaux et les résultats de la Commission C de l'OEEPE (1960–1964)" – *Neumaier, K.:* „Rapport de la Commission E pour Lisbonne" – *Weele, A. J. v. d.:* „Report of Commission F." – Frankfurt a. M. 1964, 50 pages with 7 tables and 9 annexes.

2 *Neumaier, K.:* „Essais d'interprétation de »Bedford« et de »Waterbury«. Rapport commun établi par les Centres de la Commission E de l'OEEPE ayant participé aux tests" – „The Interpretation Tests of »Bedford« and »Waterbury«. Common Report Established by all Participating Centres of Commission E of OEEPE" – „Essais de restitution »Bloc Suisse«. Rapport commun établi par les Centres de la Commission E de l'OEEPE ayant participé aux tests" – „Test »Schweizer Block«. Joint Report of all Centres of Commission E of OEEPE." – Frankfurt a. M. 1966, 60 pages with 44 annexes.

3 *Cunietti, M.:* „Emploi des blocs de bandes pour la cartographie à grande échelle – Résultats des recherches expérimentales organisées par la Commission B de l'O.E.E.P.E. au cours de la période 1959–1966" – „Use of Strips Connected to Blocks for Large Scale Mapping – Results of Experimental Research Organized by Commission B of the O.E.E.P.E. from 1959 through 1966." – Frankfurt a. M. 1968, 157 pages with 50 figures and 24 tables.

4 *Förstner, R.:* „Sur la précision de mesures photogrammétriques de coordonnées en terrain montagneux. Rapport sur les résultats de l'essai de Reichenbach de la Commission C de l'OEEPE" – „The Accuracy of Photogrammetric Co-ordinate Measurements in Mountainous Terrain. Report on the Results of the Reichenbach Test Commission C of the OEEPE." – Frankfurt a. M. 1968, Part I: 145 pages with 9 figures; Part II: 23 pages with 65 tables.

5 *Trombetti, C.:* „Les recherches expérimentales exécutées sur de longues bandes par la Commission A de l'OEEPE." – Frankfurt a. M. 1972, 41 pages with 1 figure, 2 tables, 96 annexes and 19 plates.

6 *Neumaier, K.:* „Essai d'interprétation. Rapports des Centres de la Commission E de l'OEEPE." – Frankfurt a. M. 1972, 38 pages with 12 tables and 5 annexes.

7 *Wiser, P.:* „Etude expérimentale de l'aérotriangulation semi-analytique. Rapport sur l'essai »Gramastetten«." – Frankfurt a. M. 1972, 36 pages with 6 figures and 8 tables.

8 „Proceedings of the OEEPE Symposium on Experimental Research on Accuracy of Aerial Triangulation (Results of Oberschwaben Tests)" *Ackermann, F.:* „On Statistical Investigation into the Accuracy of Aerial Triangulation. The Test Project Oberschwaben" – „Recherches statistiques sur la précision de l'aérotriangulation. Le champ d'essai Oberschwaben"– *Belzner, H.:* „The Planning. Establishing and Flying of the Test Field Oberschwaben" – *Stark, E.:* Testblock Oberschwaben, Programme I. Results of Strip Adjustments" – *Ackermann, F.:* „Testblock Oberschwaben, Program I. Results of Block-Adjustment by Independent Models" – *Ebner, H.:* Comparison of Different Methods of Block Adjustment" – *Wiser, P.:* „Propositions pour le traitement des erreurs non-accidentelles"– *Camps, F.:* „Résultats obtenus dans le cadre du project Oberschwaben 2A" – *Cunietti, M.; Vanossi, A.:* „Etude statistique expérimentale des erreurs d'enchaînement des photogrammes"– *Kupfer, G.:* „Image Geometry as Obtained from Rheidt Test Area Photography" – *Förstner, R.:* „The Signal-Field of Baustetten. A Short Report" – *Visser, J.; Leberl, F.; Kure, J.:* „OEEPE Oberschwaben Reseau Investigations" – *Bauer, H.:* „Compensation of Systematic Errors by Analytical Block Adjustment with Common Image Deformation Parameters." – Frankfurt a. M. 1973, 350 pages with 119 figures, 68 tables and 1 annex.

9 *Beck, W.:* „The Production of Topographic Maps at 1 : 10,000 by Photogrammetric Methods. – With statistical evaluations, reproductions, style sheet and sample fragments by

Landesvermessungsamt Baden-Württemberg Stuttgart." – Frankfurt a. M. 1976, 89 pages with 10 figures, 20 tables and 20 annexes.

10 „Résultats complémentaires de l'essai d'«Oberriet» of the Commission C de l'OEEPE – Further Results of the Photogrammetric Tests of «Oberriet» of the Commission C of the OEEPE"
Hárry, H.: „Mesure de points de terrain non signalisés dans le champ d'essai d'«Oberriet» – Measurements of Non-Signalized Points in the Test Field «Oberriet» (Abstract)" – *Stickler, A.; Waldhäusl, P.:* „Restitution graphique des points et des lignes non signalisés et leur comparaison avec des résultats de mesures sur le terrain dans le champ d'essai d'«Oberriet» – Graphical Plotting of Non-Signalized Points and Lines, and Comparison with Terrestrial Surveys in the Test Field «Oberriet»" – *Förstner, R.:* „Résultats complémentaires des transformations de coordonnées de l'essai d'«Oberriet» de la Commission C de l'OEEPE – Further Results from Co-ordinate Transformations of the Test «Oberriet» of Commission C of the OEEPE" – *Schürer, K.:* „Comparaison des distances d'«Oberriet» – Comparison of Distances of «Oberriet» (Abstract)." – Frankfurt a. M. 1975, 158 pages with 22 figures and 26 tables.

11 „25 années de l'OEEPE"
Verlaine, R.: „25 années d'activité de l'OEEPE" – „25 Years of OEEPE (Summary)" – *Baarda, W.:* „Mathematical Models." – Frankfurt a. M. 1979, 104 pages with 22 figures.

12 *Spiess, E.:* „Revision of 1 : 25,000 Topographic Maps by Photogrammetric Methods." – Frankfurt a. M. 1985, 228 pages with 102 figures and 30 tables.

13 *Timmerman, J.; Roos, P. A.; Schürer, K.; Förstner, R.:* On the Accuracy of Photogrammetric Measurements of Buildings – Report on the Results of the Test "Dordrecht", Carried out by Commission C of the OEEPE. – Frankfurt a. M. 1982, 144 pages with 14 figures and 36 tables.

14 *Thompson C. N.:* Test of Digitising Methods. – Frankfurt a. M. 1984, 120 pages with 38 figures and 18 tables.

15 *Jaakkola, M.; Brindöpke, W.; Kölbl, O.; Noukka, P.:* Optimal Emulsions for Large-Scale Mapping – Test of "Steinwedel" – Commission C of the OEEPE 1981–84. – Frankfurt a. M. 1985, 102 pages with 53 figures.

16 *Waldhäusl, P.:* Results of the Vienna Test of OEEPE Commission C. – *Kölbl, O.:* Photogrammetric Versus Terrestrial Town Survey. – Frankfurt a. M. 1986, 57 pages with 16 figures, 10 tables and 7 annexes.

17 *Commission E of the OEEPE:* Influences of Reproduction Techniques on the Identification of Topographic Details on Orthophotomaps. – Frankfurt a. M. 1986, 138 pages with 51 figures, 25 tables and 6 appendices.

18 *Förstner, W.:* Final Report on the Joint Test on Gross Error Detection of OEEPE and ISP WG III/1. – Frankfurt a. M. 1986, 97 pages with 27 tables and 20 figures.

19 *Dowman, I. J.; Ducher, G.:* Spacelab Metric Camera Experiment – Test of Image Accuracy. – Frankfurt a. M. 1987, 112 pages with 13 figures, 25 tables and 7 appendices.

20 *Eichhorn, G.:* Summary of Replies to Questionnaire on Land Information Systems – Commission V – Land Information Systems. – Frankfurt a. M. 1988, 129 pages with 49 tables and 1 annex.

21 *Kölbl, O.:* Proceedings of the Workshop on Cadastral Renovation – Ecole polytechnique fédérale, Lausanne, 9–11 September, 1987. – Frankfurt a. M. 1988, 337 pages with figures, tables and appendices.

22 *Rollin, J.; Dowman, I. J.:* Map Compilation and Revision in Developing Areas – Test of Large Format Camera Imagery. – Frankfurt a. M. 1988, 35 pages with 3 figures, 9 tables and 3 appendices.

23 *Drummond, J.* (ed.): Automatic Digitizing – A Report Submitted by a Working Group of Commission D (Photogrammetry and Cartography). – Frankfurt a. M. 1990, 224 pages with 85 figures, 6 tables and 6 appendices.

24 *Ahokas, E.; Jaakkola, J.; Sotkas, P.:* Interpretability of SPOT data for General Mapping. – Frankfurt a. M. 1990, 120 pages with 11 figures, 7 tables and 10 appendices.

25 *Ducher, G.:* Test on Orthophoto and Stereo-Orthophoto Accuracy. – Frankfurt a. M. 1991, 227 pages with 16 figures and 44 tables.

26 *Dowman, I. J.* (ed.): Test of Triangulation of SPOT Data – Frankfurt a. M. 1991, 206 pages with 67 figures, 52 tables and 3 appendices.

27 *Newby, P. R. T.; Thompson, C. N.* (ed.): Proceedings of the ISPRS and OEEPE Joint Workshop on Updating Digital Data by Photogrammetric Methods. – Frankfurt a. M. 1992, 278 pages with 79 figures, 10 tables and 2 appendices.

28 *Koen, L. A.; Kölbl, O.* (ed.): Proceedings of the OEEPE-Workshop on Data Quality in Land Information Systems, Apeldoorn, Netherlands, 4–6 September 1991. – Frankfurt a. M. 1992, 243 pages with 62 figures, 14 tables and 2 appendices.

29 *Burman, H.; Torlegård, K.:* Empirical Results of GPS – Supported Block Triangulation. – Frankfurt a. M. 1994, 86 pages with 5 figures, 3 tables and 8 appendices.

30 *Gray, S.* (ed.): Updating of Complex Topographic Databases. – Frankfurt a. M. 1995, 133 pages with 2 figures and 12 appendices.

31 *Jaakkola, J.; Sarjakoski, T.*: Experimental Test on Digital Aerial Triangulation. – Frankfurt a. M. 1996, 155 pages with 24 figures, 7 tables and 2 appendices.

32 *Dowman, I. J.*: The OEEPE GEOSAR Test of Geocoding ERS-1 SAR Data. – Frankfurt a. M. 1996, 126 pages with 5 figures, 2 tables and 2 appendices.

33 *Kölbl, O.*: Proceedings of the OEEPE-Workshop on Application of Digital Photogrammetric Workstations. – Frankfurt a. M. 1996, 453 pages with numerous figures and tables.

34 *Blau, E.; Boochs, F.; Schulz, B.-S.*: Digital Landscape Model for Europe (DLME). – Frankfurt a. M. 1997, 72 pages with 21 figures, 9 tables, 4 diagrams and 15 appendices.

35 *Fuchs, C.; Gülch, E.; Förstner, W.*: OEEPE Survey on 3D-City Models.
Heipke, C.; Eder, K.: Performance of Tie-Point Extraction in Automatic Aerial Triangulation. – Frankfurt a. M. 1998, 185 pages with 42 figures, 27 tables and 15 appendices.

36 *Kirby, R. P.*: Revision Measurement of Large Scale Topographic Data.
Höhle, J.: Automatic Orientation of Aerial Images on Database Information.
Dequal, S.; Koen, L. A.; Rinaudo, F.: Comparison of National Guidelines for Technical and Cadastral Mapping in Europe ("Ferrara Test") – Frankfurt a. M. 1999, 273 pages with 26 figures, 42 tables, 7 special contributions and 9 appendices.

37 *Koelbl, O.* (ed.): Proceedings of the OEEPE – Workshop on Automation in Digital Photogrammetric Production. – Frankfurt a. M. 1999, 475 pages with numerous figures and tables.

38 *Gower, R.*: Workshop on National Mapping Agencies and the Internet. *Flotron, A.; Koelbl, O.*: Precision Terrain Model for Civil Engineering. – Frankfurt a. M. 2000, 140 pages with numerous figures, tables and a CD.

39 *Ruas, A.*: Automatic Generalisation Project: Learning Process from Interactive Generalisation. – Frankfurt a. M. 2001, 98 pages with 43 figures, 46 tables and 1 appendix.

40 *Torlegård, K.; Jonas, N.*: OEEPE workshop on Airborne Laserscanning and Interferometric SAR for Detailed Digital Elevation Models. – Frankfurt a. M. 2001, CD: 299 pages with 132 figures, 26 tables, 5 presentations and 2 videos.

41 *Radwan, M.; Onchaga, R.; Morales, J.*: A Structural Approach to the Management and Optimization of Geoinformation Processes. – Frankfurt a. M. 2001, 174 pages with 74 figures, 63 tables and 1 CD.

42 *Heipke, C.; Sester, M.; Willrich, F.* (eds.): Joint OEEPE/ISPRS Workshop – From 2D to 3D – Establishment and maintenance of national core geospatial databases. *Woodsford, P.* (ed.): OEEPE Commission 5 Workshop: Use of XML/GML. – Frankfurt a. M. 2002, CD.

43 *Heipke, C.; Jacobsen, K.; Wegmann, H.*: Integrated Sensor Orientation – Test Report and Workshop Proceedings. – Frankfurt a. M. 2002, 302 pages with 215 figures, 139 tables and 2 appendices.

44 *Holland, D.; Guilford, B.; Murray, K.*: Topographic Mapping from High Resolution Space Sensors. – Frankfurt a. M. 2002, 155 pages with numerous figures, tables and 7 appendices.

45 *Murray, K.* (ed.): OEEPE Workshop on Next Generation Spatial Database – 2005. *Altan, M. O.; Tastan, H.* (eds.): OEEPE/ISPRS Joint Workshop on Spatial Data Quality Management. 2003, CD.

46 *Heipke, C.; Kuittinen, R.; Nagel, G.* (eds.): From OEEPE to EuroSDR: 50 years of European Spatial Data Research and beyond – Seminar of Honour. 2003, 103 pages and CD.

47 *Woodsford, P.; Kraak, M.; Murray, K.; Chapman, D.* (eds.): Visualisation and Rendering – Proceedings EuroSDR Commission 5 Workshop. 2003, CD.

48 *Woodsford, P.* (ed.): Ontologies & Schema Translation – 2004. *Bray, C.* (ed.): Positional Accuracy Improvement – 2004. *Woodsford, P.* (ed.): E-delivery – 2005. Workshops. 2005, CD.

49 *Bray, C.; Rönsdorf, C.* (eds.): Achieving Geometric Interoperability of Spatial Data, Workshop – 2005. *Kolbe, T. H.; Gröger, G.* (eds.): International Workshop on Next Generation 3D City Models – 2005. *Woodsford, P.* (ed.): Workshop on Feature/Object Data Models. 2006, CD.

50 *Kaartinen, H.; Hyyppä J.*: Evaluation of Building Extraction. *Steinnocher, K.; Kressler, F.*: Change Detection. *Bellmann, A.; Hellwich, O.*: Sensor and Data Fusion Contest: Information for Mapping from Airborne SAR and Optical Imagery (Phase I). *Mayer, H.; Baltsavias, E.; Bacher, U.*: Automated Extraction, Refinement, and Update of Road Databases from Imagery and Other Data. 2006, 280 pages.

51 *Höhle, J.; Potuckova J.*: The EuroSDR Test "Checking and Improving of Digital Terrain Models". *Skaloud, J.*: Reliability of Direct Georeferencing, Phase 1: An Overview of the Current Approaches and Possibilities. *Legat, K.; Skaloud, J.; Schmidt, R.*: Reliability of Direct Georeferencing, Phase 2: A Case Study on Practical Problems and Solutions. 2006, 184 pages.

52 *Murray, K.* (ed.): Proceedings of the International Workshop on Land and Marine Information Integration. 2007, CD.

53 *Kaartinen, H., Hyyppä, J.*: Tree Extraction. 2008, 56 pages.

54 *Patrucco, R., Murray, K.*. (eds.): Production Partnership Management Workshop – 2007. Ismael *Colomina, I,. Hernández, E.* (eds.): International Calibration and Orientation Workshop, EuroCOW 2008. *Heipke, C., Sester, M.* (eds.): Geosensor Networks Workshop. *Kolbe, T. H.;* (ed.): Final Report on the EuroSDR CityGML Project. 2008, CD.

55 *Cramer, M.*: Digital Camera Calibration. 2009, 257 pages.

The publications can be ordered using the electronic order form of the EuroSDR website
www.eurosdr.net